REGULATION OF $CD4^+$ T CELL POLARISATION AND FUNCTION BY PYRUVATE KINASE M2 (PKM2)

Dissertation

zur Erlangung des akademischen Grades einer
Doktorin der Medizin (Dr. med.)
an der
Medizinischen Fakultät der Universität Hamburg

vorgelegt von

Katharina Johanna Moll

aus

Hamburg

2025

Betreuer:in / Gutachter:in der Dissertation: PD Dr. Andrea Kristina Horst
Gutachter:in der Dissertation: Prof. Dr. Johannes Herkel

Vorsitz der Prüfungskommission: Prof. Dr. Johannes Herkel
Mitglied der Prüfungskommission: Prof. Dr. Eva Tolosa
Mitglied der Prüfungskommission: Prof. Dr. Friedrich Koch-Nolte

Datum der mündlichen Prüfung: 25.11.2025

Contents

1. Introduction

1.1. $CD4^+$ T cells

T cell precursors (thymocytes) derive from progenitor cells in the bone marrow and, initially, the fetal liver and mature in the thymus, where they differentiate into functional $CD4^+$ and $CD8^+$ cells. This process involves T cell receptor (TCR) gene rearrangement to ensure T cells recognize multiple different antigens (Germain, 2002). Furthermore, thymocyte selection takes place and is characterized by the thymocytes T cell receptors affinity towards a peptide-MHC complex on thymic antigen presenting cells (APCs). Thymocytes with a very high affinity are destroyed while those with low to medium affinity undergo further differentiation into mature T cells (Germain, 2002). From these cells both $CD4^+$ and $CD8^+$ T cells derive, depending on whether the MCH binding property of their TCR is matched by their CD4 or CD8 receptors binding property (Germain, 2002). All $CD4^+$ T cells are T helper cells, which play a role in coordinating a successful immune response among other immune cells by releasing cytokines.

Following antigen recognition, naïve $CD4^+$ T cells are activated and further differentiate into different effector cell subsets depending on the cytokine environment. T helper 1 (Th1) cells promote the cellular immune response and further activate other immune cells such as cytotoxic T cells and macrophages. Th2 cell are promotors of the humoral immune response, mainly activating B cells for class switch, expansion and antibody production. Th17 cells are primarily known for supporting mucosal clearance and thereby maintaining barriers. In addition to $CD4^+$ T cells with effector cell function, T regulatory cells help prevent overshooting immune reactions. The following section focuses on Th1, Th17 and T cells.

1.1.1. Th1 and Th17 cells

The frequency of $CD4^+$ T cells specific for one particular antigen in homeostasis is very low. Therefore, once activated by binding of an antigen-MHC (major histocompatibility complex) -II complex with their TCR, $CD4^+$ T cells undergo clonal expansion and proliferation. This process of activation is enhanced by co-stimulatory signals, predominantly by CD28 binding to CD80 or CD86 on APCs. The differentiation into T helper cell types with unique profiles is influenced by the cytokine environment, the type of presenting APC and the concentration of antigens and is mediated by their master transcription factors. Yet, these transcription factors are expressed at different levels in Th1, Th17 or T regulatory cells (Luckheeram et al. 2012). This leads to the assumption, that it is

the relative level of expression of transcription factors and possible interaction with other transcription factors which determines T cell differentiation and thereby distinctive function. It may further be possible, that this simultaneous expression of different transcription factors allows for plasticity among T helper subsets (Luckheeram et al. 2012).

Th1 cell polarization is initiated by IL-12 secreted by APCs and Interferone γ (IFNγ) secreted by natural killer (NK) cells, which activate signal transducer and activator of transcription 1 (STAT1) and 4 (STAT4) (Thieu et al, 2008). STAT1 then induces the expression of T-box transcription factor (T-bet) which acts as master transcription factors for the differentiation of naïve $CD4^+$ helper cells into Th1 cells. STAT4, together with the Runt related transcription factors Runx1 (Runt related transcription factor 1) and Runx3 (runt related transcription factor 3), suppresses Th2 and Th17 differentiation by inhibition of their respective master transcription factors (Kohu et al. 2009, Lazarevic et al. 2011). STAT4 also induces IFNγ production, which is secreted by Th1 cells, thereby generating a positive feedback loop of Th1 cell induction (Luckheeram et al. 2012).
Once activated, Th1 cells secrete IL-2, IFNγ and TNFα (tumor necrosis factor α) and play a key role in eliminating intracellular pathogens. IL-2 production auto-stimulates Th1 cells besides playing a key role for T regulatory cell induction and survival and promoting a cytotoxic phenotype in $CD8^+$ cells. (Luckheeram et al. 2012). IFNγ activates macrophages, enhancing their phagocytic activity (Murray et al. 1985). TNFα promotes the inflammatory response by enhancing the production of cytokines such as IL-1 and IL-6, is involved in the production of acute phase molecules, and plays a role in autoimmunity (Suen et al. 1997, Chiang et al. 2009). Cytokine secretion is auto-regulated, for example IFNγ expression is repressed by the T helper cell repressor gene Bcl-6 in later stages of activation (Oestreich et al. 2011). This mechanism avoids overproduction in pro-inflammatory cytokines and thereby prevents hyperinflammation.

Th17 cells derive from naïve $CD4^+$ T cells and are induced by TGFβ (tumor growth factor β), IL-6, IL-21 and IL-23 in mice as well as humans (Luckheeram et al. 2012). Low concentrations of TGFβ in combination with IL-6 result in the activation of Th17 cells' lineage defining transcription factor retinoic acid receptor-related orphan receptor gamma-T (RORγT, Veldhoen et al. 2006, Mangan et al. 2006, Batelli et al. 2006). STAT3 and RORγT drive the expression of their signature cytokine IL-17 A and IL-17F (Yang et al. 2008). Following activation, self-amplification and stabilization of the Th17 populations are

achieved by IL-21, produced by Th17 cells themselves, and IL-23 produced by APCs (Ghoreschi et al. 2010).

Th17 cells are characterised by a special functional flexibility as they further differentiate into either pro-inflammatory Th17 cells or anti-inflammatory Treg17 cells, which play a role in regulating immune responses and are further discussed in chapter 2.1.2.

Pro-inflammatory Th17 cells exhibit their effector function in inflammation through their signature cytokines IL-17A and F (Korn et al. 2009). The receptor for IL-17A is expressed in several tissues, such as epithelial and endothelial cells, and keratinocytes which upon binding produce antimicrobial peptides. Furthermore, IL17A results in the indirect recruitment of neutrophils mediated by acting on epithelial or stromal cells, which then produce chemokines such as CXCL (C-X-C motif chemokine ligand) 1 and 2 attracting the neutrophils. By shaping the inflammatory environment, IL17A can also act on other immune cells such as macrophages, dendritic cells and B cells (Luckheeram et al. 2012, Leonard and Spolski, 2005).

Th17 cells are abundant in the intestine and play a special role in mucosal barriers and in response to extracellular bacteria, for instance by secreting IL-22 (Aujla et al. 2008). Furthermore, IL-22 is involved in providing protection to hepatocytes during acute liver inflammation (Zenewicz et al. 2007). However, when dysregulated, Th17 cells may drive chronic inflammation in autoimmune processes such as multiple sclerosis or inflammatory bowel disease (Korn et al. 2009).

Naïve as well as effector $CD4^+$ T cells may undergo the differentiation into a broad spectrum of memory cells after activation by their cognate antigen. Memory $CD4^+$ T cells have a long lifespan, therefore during the life of an individual, their percentage among $CD4^+$ T cells steadily increases. Once re-exposed to their antigen, they are activated and expand to larger numbers of effector cells, allowing for a stronger and faster immune response. Activated antigen specific $CD4^+$ T cells, which don't become memory cells, die once the immune response comes to an end (Luckheeram et al. 2012).

1.1.2. T regulatory cells

Finally, T regulatory cells make for a special subset of $CD4^+$ T cells as they play a key role in role in regulating immune reactions and mediating tolerance. Thereby they prevent an overshooting effector cell reaction or collateral tissue damage and pave the way for a efficient yet controlled immune reaction.

Natural T regulatory cells (nTregs) are selected in the thymus and are important for tolerance against autoantigens. These T regulatory cells continuously express their master transcription factor forkhead box protein 3 (FoxP3, Fontenot et al. 2003). On the other hand, like $CD4^+$ T effector cells, induced T regulatory cells (iTregs) derive from naïve $CD4^+$ T cells under the influence of IL-2 and TGFβ and express FoxP3 only upon TCR activation and downstream TGFβ signaling (Chen et al. 2003, Davidson et al. 2007). In addition, Smad 2, Smad 3 and STAT5 signaling, activated by TGFβ and IL-2 respectively, are involved in theinduction of T regulatory cells by enhancing FoxP3 expression (Takimoto et al. 2010, Burchill et al. 2007). They play an important role in preventing overshooting inflammation either in the context of autoimmune disease or in response to foreign antigens. $CD4^+$ T regulatory cells are generally defined as $CD25^{high}$ $FoxP3^+$ cells.

Th17 and T regulatory cell development are tightly connected, since both rely on TGFβ to differentiate. It has been shown that FoxP3 positive T regulatory cells can acquire a Th17 phenotype in the presence of IL-6 or when embedded into a hypoxic and inflammatory (micro-) environment. Here, HIF1α (hypoxia inducible factor 1 α) can promote Th17 differentiation by inducing RORγT and IL-17, promoting glycolysis and inducing FoxP3 degratation in the proteasome. (Yang et al. 2008, Dang et al. 2011).
Th17 cells which display regulatory characteristics are called Treg17 cells. These cells may co-express not only RORγT and FoxP3, but also IL10 and IL-17 (Yang et al 2008). Xu et al. (2020) found that Th17 plasticity to acquire Treg function is required to induce immunological tolerance and tissue protection and is achieved via Smad 2 and 4-dependent IL-10 production. This phenomenon was observed in the intestinal barrier. Gagliani et al. (2015) also showed that Th17 cells differentiate into T regulatory cells in the course of intestinal bacterial infections and contribute to the resolution of intestinal inflammation. These findings suggest a high degree of plasticity of Th17 cells and highlight an additional important mechanism of immune adaption.

T regulatory cells exert their regulatory function by different mechanisms influencing not only $CD4^+$ T cells, but a wide range of other immune cells. By producing inhibitory cytokines such as TGFβ and IL-10, they suppress inflammation and thereby overshooting tissue damage beyond pathogen clearance. (Li et al. 2007, Asseman et al. 1999)
Immune suppression additionally takes place by a feedback loop centered around the cytokine IL-2. Activated $CD4^+$ T cells, such as Th1 cells, produce IL-2, which in turn senses

high effector and therefore inflammatory activity to T regulatory cells and stimulates them. In addition, it was shown that the uptake of IL-2 by T regulatory cells may as a side effect deprive T effector cells of it and induce apoptosis (Pandiyan et al. 2007).
In addition, several other mechanisms by which T regulatory cells suppress other immune cells are investigated but not yet well understood. Comparably much is known about the expression of ectonucleotides by T regulatory cells, also known as the purinergic system.

1.1.3. The purinergic system (CD39 and CD73)

The cellular environment at the site of inflammation plays a crucial role for the function and activity of different immune cell subsets. Therefore, several mechanisms exist to maintain immune homeostasis and prevent overshooting immune reactions either in the context of autoimmune disease or inflammation induced by factors like pathogens or tissue damage. One method of fine-tuning is the purinergic system with its two key mediators ATP and adenosine.
While in healthy cells, adenosine triphosphate (ATP) is the main unit of energy, extracellular ATP is a danger signal released for example by cell lysis, vesicle exocytosis, channels permeable for nucleotides or lysosomes (Elliott et al. 2009). The ectonucleotidase CD39 phosphohydrolyses ATP to adenosine monophosphate (AMP), thereby clearing the cellular environment from ATP (Bono et al. 2015). CD73, the second of two sequential ecto-enzymes, further dephosphorylates 5'adenosine monophosphate to adenosine (Bono et al. 2015).
The immunomodulatory effects are mediated by different receptors for either ATP or adenosine respectively. ATP induces pro-inflammatory responses through binding on P2X receptors on T cells and P2X as well as P2Y receptors on a variety of other immune cells (Cekic et al. 2016). T effector cells express $P2X_1R$, $P2X_4R$ and P2X12R which all act by activating a pro-inflammatory NF-κB (Nuclear Factor kappa-light-chain-enhancer of activated B cells) and NFAT (Nuclear factor of activated T cells) response, thereby stimulating IL-2 secretion and the ongoing production of pannexin-1 channels upholding pro-inflammatory ATP-P2X signaling (Cekic et al. 2016).
Extracellular adenosine levels are influenced by bidirectional processes of secretion and uptake as well as the production through CD73 from AMP. Adenosine can bind to different G-protein coupled receptors, A1, A2A, A2B and A3. Upon activation $CD4^+$ T cells express A2A, which, when stimulated, mediates immunosuppressive effects through cAMP production, protein kinase A activation and thereby finally the inhibition of NF-κB and

NFAT dependent gene expression (Bono et al. 2015). Accordingly, it was shown that adenosine had anti-inflammatory effects suppressing $CD4^+$ effector cell proliferation (Kobie et al. 2006, Deaglio et al. 2007). It suppresses Th1 and Th2 differentiation and effectively downregulates cytokine secretion, such as of IFNγ in Th1 and Th2 cells and IL-2 production in naïve and Th1 cells (Csoka et al. 2008). Furthermore, it was shown to reduce Th17 differentiation (Zarek et al. 2008). Accordingly, CD73 deficiency and thereby the inability to produce adenosine from extracellular AMP resulted in an autoimmune inflammatory phenotype in mice (Blume et al. 2012, Bynoe et al. 2009). CD39 deletion, respectively, was associated with an increase in susceptibility towards DCC-colitis in mice and a genetic polymorphism mediating reduced CD39 expression was discovered in patients with Crohns disease (Friedmann et al. 2009).

Ectonucleotidases are expressed on a variety of tissues and immune cells, including neutrophils, M2 macrophages, dendritic cells and $CD8^+$ T cells (Antonioli et al. 2013). Yet, they appear to be of special importance to $CD4^+$ T regulatory cells, as they help to reduce pro-inflammatory ATP from the cellular environment and replace it with adenosine.
Murine Tregs express both CD39 and CD73 on their surface and use it as a suppressional pathway (Deaglio et al. 2007). Tregs are very sensitive to necrosis by P2X7 signaling and thereby high extracellular ATP levels (Aswad et al. 2005). CD39 may therefore be helpful for them to survive in ATP rich environments as it supports ATP clearance. (Borsellino et al. 2007).
This may also be a reason why Th1 and Th17 cells express CD39. Kobie et al. (2006) demonstrated that $CD4^+$ T precursor cells and Th1 cells expressed both CD39 and CD73, yet to lower amounts as shown for CD73 expression in $CD25^-$ uncommitted primed $CD4^+$ T cells. Additionally, CD73 and CD39 expression was shown in Th17 cells (Chalmin et al. 2012, Hernandez-Mir, 2017)
Despite the role of ectonucleotidases not being fully understood, it can be stated, that the purinergic system consisting of CD39 and CD73 makes for a distinct suppressional pathway of T regulatory cells by catalysing the shift from a pro-inflammatory ATP containing cellular environment to an anti-inflammatory adenosine containing cellular environment (Antonioli et al. 2013).

1.2. Immunometabolism in CD4$^+$ T cells

Once activated, T cells have specific metabolic demands to proliferate and fulfil their respective immunological functions. To meet these demands, they undergo different adaptations in glycolysis, oxidative phosphorylation and other metabolic pathways depending on their role in inflammation. Figure 2 (page 12) gives an overview of metabolic changes during T cell activation.

1.2.1. The Warburg Effect

Differentiated tissue cells classically metabolise glucose depending on the availability of oxygen either by oxidative phosphorylation or anaerobic glycolysis. Supplied with enough oxygen, pyruvate from the glycolytic breakdown of glycose is transferred to the mitochondrion and undergoes the formation of acetyl-CoA. During the reactions in the tricarboxylic acid cycle (TCA) cycle and electron transport chain the Coenzymes nicotinamide adenine dinucleotide (NAD^+) and flavine adenine dinucleotide (FAD) are reduced to $NADH+H^+$ and $FADH_2$. Both are used for oxidative phosphorylation resulting in the formation of CO_2 from O_2 and to fuel ATP synthesis in the mitochondrion. This process allows for the phosphorylation of up to 36 mol ATP per 1 mol glucose.

When lacking oxygen for this process 2 mol ATP can be generated in the process of glycolysis by transferring inorganic phosphate from a donor molecule such as fructose-1,6-bisphosphate, to an ADP molecule. Glycolysis consumes NAD^+ molecules and produced $NADH+H^+$. To ensure continuous glycolytic activity, NAD^+ can be regenerated by the reduction of pyruvate to lactate.

In 1924 Otto Warburg first described the reduction of pyruvate to lactate instead of performing oxidative phosphorylation despite sufficient oxygen supply to support oxidative phosphorylation in proliferating sarcoma cells (Warburg et al. 1924) – a phenomenon which he named “aerobic glycolysis” and hypothesized to be caused by impaired mitochondrial function. However, soon after, this hypothesis was proved wrong and the actual advantages which this change in cellular metabolism has for cell proliferation was discovered (Racker, 1972). This effect was later named “Warburg Effect” in honor of Otto Warburg.

A reason for the Warburg effect lies in the metabolic requirements for cell proliferation, including ATP as energy source, but also metabolic intermediates for cell division (Vander Heiden et al., 2009). Yet, sufficient ATP production is not the limiting factor for proliferation in human cells as glycolysis alone continuously generates 2 mol ATP per 1 mol glucose and does so comparably fast. For each cell to divide, all cellular components must be duplicated,

including the nucleotides, but also cellular membranes or enzymes. These processes require for example amino acids for protein biosynthesis or carbon atoms from Acetyl-CoA for lipid synthesis, which are generated during metabolic breakdown of glucose. The problem of asymmetry between the energy requirements and the need of intermediates to produce biomass for cell division can be solved by performing aerobic glycolysis as it balances the ratio of ATP production and the generation of cellular building blocks (Vander Heiden et al., 2009). The elimination of excess carbon atoms can be achieved by lactate secretion. Lactate as a waste product during an immune response may be regenerated in the liver – a process called Cori cycle (Cori and Cori, 1946). This process may further solve the problem of high ATP concentrations inhibiting glycolysis, as the generation of lactate contributes to consumption (Vander Heiden et al. 2009).

Aerobic glycolysis was first described in leukocytes by Bakker et al. (1927). While resting $CD4^+$ T cells engage in oxidative metabolism, upon activation they fuel by aerobic glycolysis (Geltink et al. 2018).

1.2.2. The Glycolytic Switch in $CD4^+$ T Cells

Upon activation, T effector cells need to proliferate and to produce cytokines, for which they need energy and cellular building blocks. These requirements of activated $CD4^+$ T cells are met by undergoing a metabolic switch following distinctive signals of stimulation. Resting $CD4^+$ T cells show a balanced metabolism, relying on glycolysis and oxidative phosphorylation as fuel sources (Maclver et al. 2013). Upon activation via their T cell receptor and CD28, growth and metabolic programming are regulated by identical signaling pathways mediating the glycolytic switch, which results in the preferential use of glucose as fuel.

In Th1 cells mechanistic target of rapamycin complex 1 (mTORC1) was found to modulate for example the transcription factors cellular myelocytomatosis oncogene (cMyc) and HIF1a (Ray et al. 2015). cMyc regulates the expression of different glycolytic genes as does HIF1α, which can induce glucose transporter 1 (GLUT1), hexokinase-2, aldolase A, enolase-1, PKM2 and Lactate dehydrogenase A (LDH A), but also glutamine transporters (Wang et al. 2011, Semenza et al. 1996, 31, 23, 33). HIF1α and c-Myc have been shown to regulate glucose metabolism specifically during Th1 and Th17 differentiation (Shi et al. 2011, Dang et al. 2011, Shehade et al. 2015, 34, 35, 36). In Th1 cells, interferon regulatory factor 4 (IRF4) is involved in metabolic reprogramming as well (Mahnke et al. 2016).

The glycolytic switch allows T effector cells to sport proliferation and cytokine production. Central to this switch are adaptations in performing glycolysis allowing for glycolytic intermediates to be used in other metabolic pathways. The pentose phosphate way uses glucose-6-phosphate, fructose-6-phosphate and glyceraldehyde-3-phosphate to produce ribose-5-phosphate, which is especially important to produce ribonucleic acid and therefore directly involved in facilitating proliferation. Furthermore, transferring glycolytic intermediate into other metabolic pathways to produce amino acids or fatty acids may help uphold the demands of proliferating cells. Fructose-6-phosphate can be metabolized to dihydroxyacetone phosphate (DHAP) and further to glycerol 3-phosphate, which can be used in fatty acid metabolism (Bantug et al. 2018). 3-phosphoglycerate may contribute to ensuring a continuous supply with amino acids via the serin biosynthesis pathway (de Koning et al. 2003). Additionally, a benefit of the metabolic switch lies in the glycolytic enzymes non-enzymatic functions.

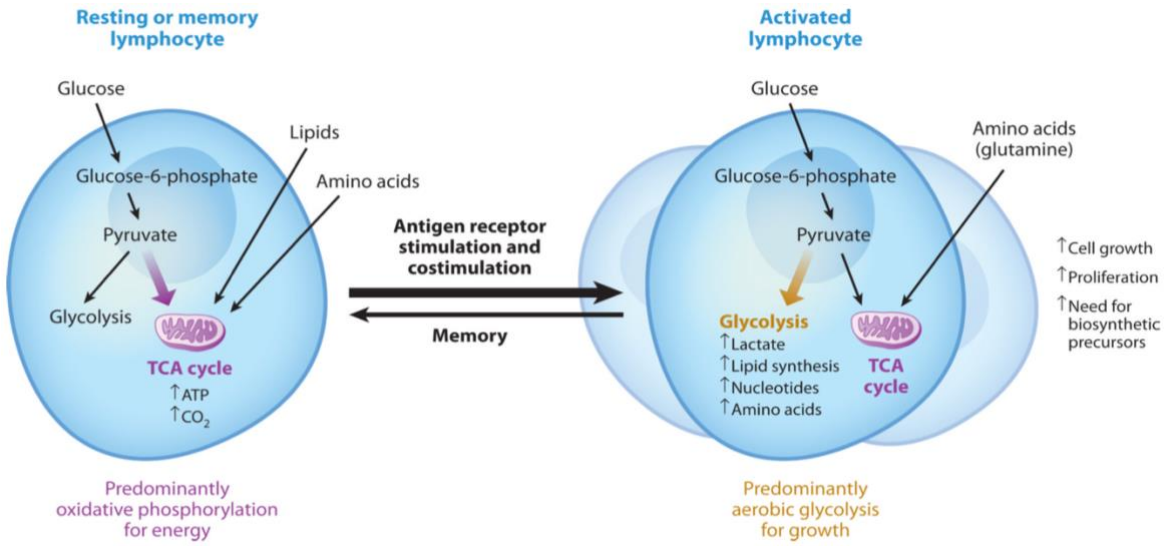

Figure 1: The glycolytic switch in CD4$^+$ T cells. When activated by antigen receptor stimulation, lymphocytes such as CD4$^+$ T cells undergoe a metabolic switch from predominately metabolizing pyruvate, lipids and amino acids to perform oxidative phosphorylation towards performing aerobic glycolysis. This process produces lactate and allows for the synthesis of lipids, amino acids and nucleotides from intermediates. From Maclver et al. Metabolic regulation of T lymphocytes Annu Rev Immunol 2013 Vol. 31 Pages 259-83

1.2.3. Non-metabolic functions of glycolytic enzymes in CD4$^+$ T cells

Some glycolytic enzymes have additional functions apart from catalyzing metabolic reactions, such as modifying the expression of genes (Seki et Gaultier. 2017).

Hexokinase catalyzes the first step of glycolysis by phosphorylating glucose and thereby producing glucose-6-phosphate (G6P). It can do so most efficiently when located at the outer

mitochondrial membrane (OMM) where ATP for glucose phosphorylation is available. G6P then induces dissociation from the OMM. Yet, in its OMM location, hexokinase may undergoe posttranslational modification and may acquire an anti-apoptotic function (Seki et Gaultier, 2017).

Chang et al. (2013) suggested that Glyceraldehyde-3-phosphate dehydrogenase (GAPDH) could influence IFNγ translation by binding the 3' untranslated region of IFNγ messenger RNA (mRNA) at the ribosome and thereby blocking translation. Hence, the authors hypothesized that high glycolytic activity was associated with elevated IFNγ expression, as GAPDH would fulfil its role as glycolytic enzyme instead of blocking IFNγ translation. Accordingly, the addition of glyceroladehyde-3-phosphate, the substate of GAPDH, restored IFNγ production in cell culture experiments.

α-Enolase usually converts 2-phosphoglycerate to phosphoenolpyruvate (PEP), if transcribed to a full length protein of 48 kDa. In case of transcription initiation at a different site, a 37 kDa α-enolase protein may form, which in its role as Myc promotor binding protein 1 (MPB-1) has been shown to influence gene expression (Feo et al. 2000). C-Myc inhibition by MPB-1 binding has anti-proliferative effects (Wang et al. 2011). Specifically in T regulatory cells, MBP-1 binds FoxP3 regulatory regions initiating the transcription of FoxP3 (De Rosa et al. 2015). Yet, the regulation of differential translation of enolase in T cells to date is not fully understood.

Lactate dehydrogenase (LDH) converts pyruvate to lactate either in case of anaerobic or aerobic glycolysis and thereby offers a possibility to regenerate NAD^+ for further glycolytic activity. By reducing Acetyl CoA consumption, LDH-A ensures proper histone acetylation, thereby allowing for IFNγ transcription (Peng et al. 2016) Accordingly, LDH-A has been shown to be strongly expressed in activated T cells. (Peng et al. 2016). Furthermore, it may be possible that LDH-A in a manner comparable with GAPDH could influence Granulocyte-Macrophage Colony-Stimulating Factor (GM-CFS) translation (Seki et Gaultier, 2017).

Lastly, the PKM2 dimer has been shown to translocate to the cell's nucleus, where it may interact with transcriptional regulation of other glycolytic enzymes as well as signaling molecules such as HIF1α (Luo et al. 2011, see chapter 2.3.1.).

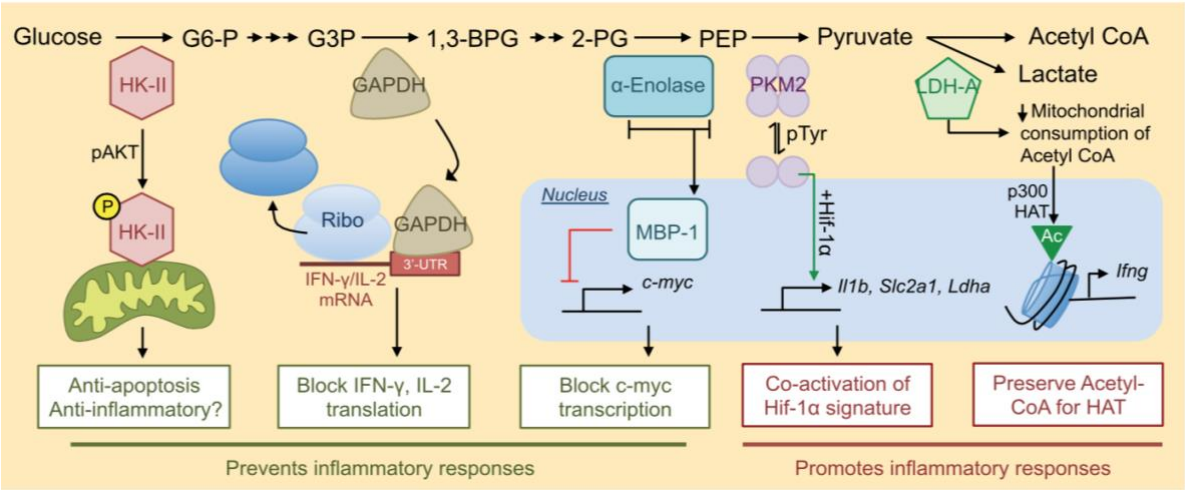

Figure 2: Non-metabolic functions of glycolytic enzymes in CD4⁺ T cells. This graphic gives an overview about non-glycolytic functions of glycolytic enzymes, such as influencing transcription and translation of cytokines and transcription factors. From Seki SM and Gaultier A (2017) Exploring Non-Metabolic Functions of Glycolytic Enzymes in Immunity. Front. Immunol. 8:1549.

1.2.4. Metabolic requirements of different CD4⁺ T cell subsets

CD4⁺ T cells act as coordinators of immunity and therefore differ in their specific function and role during inflammation. Their metabolic requirements are associated with their function as either effector, regulatory or memory cells.

When activated, T effector cells become hypermetabolic and undergo a metabolic switch, as they require aerobic glycolysis to ensure fast proliferation and cytokine production upon activation. For instance, in low-glucose environments impaired T effector function was observed (Chang et al 2013). It was shown that CD4⁺ T cells upon activation upregulate GLUT1. An elevated glucose uptake via GLUT1 expression was associated with an increase in IL-2 and IFNγ production in T cells. Accordingly, GLUT1 deletion resulted in a decrease in disease severity in autoimmune disease models such as experimental colitis (Macintyre et al. 2014).

Aerobic glycolysis in CD4⁺ T cells was also found to be associated with elevated lactate production. Pyruvate can either be metabolized to lactate by lactate dehydrogenase A (LDHA) or alternatively to actetyl-CoA by pyruvate dehydrogenase (PDH). PDH can be inhibited by pyruvate dehydrogenase kinase 1 (PDK1), which is upregulated in Th17 cells. Th17 metabolism appears to favor the conversion of pyruvate into lactate as inhibition of PDK1 block Th17 yet enhances Th1 differentiation (Gerriets et al. 2015). Yet, the high amounts of produced lactate were found to impair effector function, which may be explained by an environment deprived in glucose but also as a mechanism of self-regulation (Calcinotto et al. 2012, Fischer et al. 2007).

T regulatory cells, on the contrary, rely primarily on oxidative phosphorylation to fulfill their suppressive functions (Gerrits et al. 2015, Michalek et al. 2011). For instance, electron transport chain (ETC) complex I has been shown to be essential for their functioning (Angelin et al 2017). Angelin et al. (2017) have further shown that FoxP3, the main transcription factor of T regulatory cells, suppresses glycolysis by binding to the Myc promotor while enhancing oxidative phosphorylation. Thereby, contrary to T effector cells which rely on glucose for fueling, T regulatory cells can persist in low glucose, high lactate environments and promote immune tolerance at the site of inflammation. Tregs further produce less lactate as FoxP3 influences the direction of the LDH reaction depending on the cellular environment (Angelin et al. 2017).

Although induced T cells rely mainly on oxidative phosphorylation for maintenance, they require glycolysis for activation and Treg induction. On reason for this could be that Enolase-1 controls FoxP3 splicing variants, such as FoxP3-E2, which was shown to be associated with suppressive ability of T regulatory cells and to be impaired in autoimmune disease (De Rosa et al. 2015). While in resting T cells with little glycolytic demand, enolase is recruited to the FoxP3 regulatory region and inhibits transcription, in activated T regulatory cells it is enzymatically active allowing for adequate FoxP3 expression. Consequently, the glycolytic inhibitor 2-DG affected T regulatory cells induction and function negatively (De Rosa et al. 2015).

Even though they may rely on a high glycolytic activity for activation, oxidative metabolism has been at the center of T regulatory cell metabolism ensuring metabolic flexibility and functioning in nutrient rich or deprived sites of inflammation (Bantug et al. 2018). Similarly, $CD4^+$ T memory cells engage in oxidative metabolism (Maclver et al. 2013).

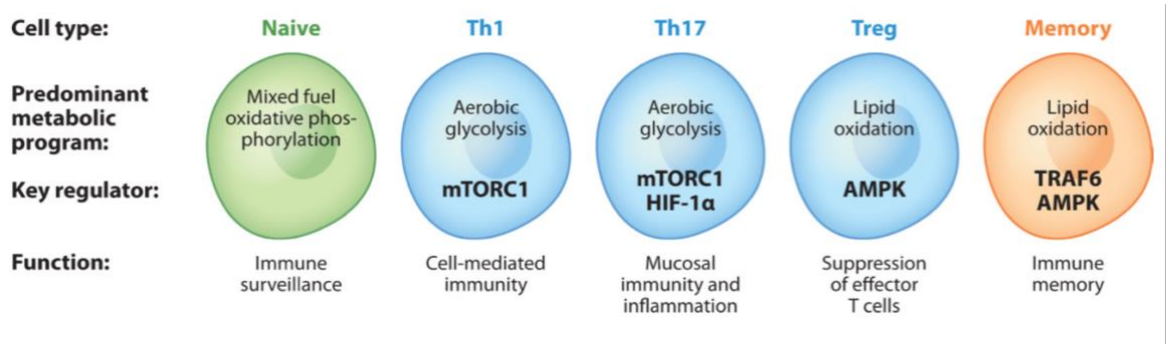

Figure 3: Metabolic requirements of different subsets of $CD4^+$ T cells. $CD4^+$ T cells subsets differ in their metabolic requirements to fulfil their function in mediating or regulating immunity. Mediated by transcription factors such as mTORC1 or AMPK, effector $CD4^+$ T cells mainly rely on aerobic glycolysis while T regulatory and memory cells thrive on oxidative phosphorylation. From Maclver et al. Metabolic regulation of T lymphocytes Annu Rev Immunol 2013 Vol. 31 Pages 259-83

1.3. Pyruvate Kinase

The last and rate limiting step (Jurica et al. 1998) of glycolysis is catalyzed by an enzyme called pyruvate kinase and consists in the transformation of phosphoenolpyruvate (PEP) to pyruvate by transferring a phosphate group from PEP to ADP generating ATP. Pyruvate then undergoes further TCA cycle metabolism being the cells main source of protons and carbon.

1.3.1. Pyruvate Kinase Isoforms

In mammals, 2 different genes for pyruvate kinases exist from which 4 different isoforms of the enzyme are synthesized. The *Pklr* gene encodes for 2 isoforms of pyruvate kinase. The PKL protein has a molecular weight of 59kDa. It is expressed in tissues able to perform gluconeogenesis, like liver or kidney (Domingo et al. 1992). PKR (62 kDa) is expressed in red blood cells only (Rodriguez-Horche et al. 1987). The *Pkm* gene is expressed ubiquitously and encodes for PKM1 and PKM2, which both have a molecular weight of 58kDa. They are generated by the process of alternative slicing and differ only by one exon (Noguchi et al 1986). PKM1 or PKM2 transcription is favored by splicing regulators such as heterogenous nuclear ribonucleoproteins (hnRNPs) A1 and A2 which bind to exon 9 or 10 in a dose dependent manner (Spellman et al. 2007, Clower et al. 2010).

PKM1, including exon 9, is expressed in differential tissue, such as myocytes or neurons (Imamura and Tanaka, 1972). Furthermore, PKM1 only occurs in the state of a tetramer with high affinity towards PEP. Most non-proliferating tissues rely on PKM1 to meet their metabolic demands as it ensures continuous oxidative metabolism (Christofk et al. 2008). PKM2, including exon 10, is expressed during embryogenesis, but its expression was also observed in cancer and immune cells (Dayton et al. 2016). While PKM1 does not appear to influence tumor cell proliferation, PKM2 plays a crucial role in cancer cells metabolism (Bluemlein et al. 2011). This may be due to its occurrence in either the form of a tetramer or a dimer, which in a dynamic balance control cellular metabolism.

Each the tetramer and the dimer consist of monomers with different domains. PKM2 dimers are formed by the interaction of two A-domains. The formation of tetramers depends on the C-domains. PKM2 monomers do not possess enzymatic function.

The tetramer is known to be enzymatically active and to have a high affinity towards PEP, thereby showing similarities with PKM1. According to its metabolic functions, the tetramer is primarily located in the cytosol (Gao et al 2012).

Contrarily, the dimer is rather inactive resulting in the accumulation of glycolytic intermediates. Only the PKM2 dimer may translocate to the cell's nucleus, where it influences gene expression of inflammatory molecules such as HIF1α, Arylhydrocarbon receptor (AhR) and STAT3 (Yang et al. 2011, Gao et al. 2012, Luo et al. 2011). Seki and Gaultier (2017) hypothesize that due to its association with HIF1α, PKM2 may especially be relevant as a regulator of Th17 differentiation.

1.3.2. Regulation of PKM2 activity

PKM2 is a metabolic control point for aerobic glycolysis and a regulated step in in proliferating cells metabolism (Vander Heiden 2009).

PKM2 reacts to many nutrients, such as fructose-1,6-bisphosphate (FBP) and serine. PKM2 but not PKM1 has been shown to be allosterically activated by the glycolytic intermediate FBP (Dombrauckas et al. 2005, Morita et al., 2018, Liu et al., 2020). C-domains of PKM2 contain a binding site for fructose-1,6-bisphosphate (FBP), which is known to stabilize the PKM2 tetramer. Influenced by activators like FBP the PKM2 tetramer can further alter its symmetry and occur in the form of an active R-state or a T-state with reduced activity.

The amino acid serine, like FBP, promotes tetramerization and thereby enzymatic activity of PKM2 (Ashizawa et al. 1991, Chaneton et al. 2012, Keller et al. 2012, Morgan et al. 2013). Contrarily, succinate may in high concentrations succinylate PKM2, favoring dimer formation (Wang et al. 2017).

Furthermore, PKM2 may undergo posttranslational modifications such as phosphorylation or acetylation (Prakasam et al. 2018). For example, phosphorylation at position Y105 was found to lead to dimerization of PKM2, a process which was primarily observed in tumor cells and mediated by kinases such as Breakpoint Cluster Region - Abelson (BRC-ABL) and Janus kinase 2 (JAK2, Hitosugi et al. 2009). Acetylation reduces PKM2 activity as well and may even induce lysosomatic digestion of PKM2 (Lv et al. 2011). Another possible modification is hydroxylation. Hydroxylated PKM2 may enhance a HIF1α transcriptional program thereby supporting glycolytic metabolism (Luo et al. 2011). Post translational modification processes may at least partly be limited to the PKM2 dimer, as for instance serine phosphorylation does not occur in the PKM2 tetramer thereby preventing nuclear translocation (Yang et al. 2012).

An isoform switch from tetramer to dimer is known from cancer cell proliferative metabolism yet has also been observed during the activation of immune cells. Angiari et al.

(2020) described how the PKM2 dimer can translocate to $CD4^+$ T cell's nuclei and induce hyperglycolysis as well as an elevated expression of cytokines such as TNFα.
As for its role in proliferation, PKM2 has become an interesting target for pharmacological modification aiming to reduce the growth of tumor cells or regulate the expansion and function of immune cells. Its complex regulatory mechanisms offer a multitude of strategies to modify its activity.

1.3.4. Pharmacological targeting of PKM2

Investigations in the possibilities of modifying cell proliferation by targeting PKM2 have long been conducted in the field of oncology, and it has been shown that it's inhibition may inhibit glycolysis and proliferation of tumor cells (Christofk et al. 2008, Anastasiou et al. 2012).
TEPP-46, a small molecule activator stabilizing the PKM2 tetramer, has been broadly studied in this context. It activates PKM2 and increases its enzymatic activity by stabilizing the tetramer (Jiang et al. 2010, Boxer et al. 2010, Anastasiou et al. 2012). IN macrophages 50 to 100mM of TEPP-46 were shown to inhibit macrophage activation (Palson-McDermott et al. 2015). In $CD4^+$ T cells, TEPP-46 was shown to block nuclear translocation of the PKM2 dimer by inducing tetramer formation, thereby reducing the secretion of cytokines such as IL-2 and TNFα, inhibiting glycolysis and ameliorating experimental autoimmune encephalomyelitis (EAE, Angiari et al. 2020). In this context, TEPP-46 inhibited Th1 as well as Th17 cell formation, by downregulating the expression of key proliferative transcription factors such as Myc, mammalian target of rapamycin (mTOR) and HIF1α (Angiari et al. 2020).

Shikonin is a naphtoquinone derived from the plant *Alkanna tinctoria* inhibiting PKM2 enzymatic activity in general (Chen et al. 2012). Inhibition therefore occurs in a dose dependent manner. Shikonin was shown to inhibit cancer cell glycolysis by inhibiting tumor cell PKM2, inducing a necroptotic death in cancer cells depending on aerobic glycolysis (Chen et al. 20011, Han et al. 2007).
Furthermore, shikonin has been shown to reduce glycolysis and glycolytic capacity in Th1 and Th17 cells in a comparable manner. At doses of 0.05μM and 0.1μM the number of IFNγ and IL-17 positive cells respectively was lowered in flow cytometric analysis in vitro. (Kono et al. 2019). Kono et al. (2019) further associated PKM2 inhibition by shikonin with a reduced disease severity and cytokine expression in EAE. Additional evidence hints at a T

regulatory cell promoting effect by Shikonin dependent inhibition of the AKT/MTOR pathway (Zhang et al. 2019). Favoring T regulatory cell development, it may also prolong allograft survival of skin allografts in mice (Zeng et al. 2019).

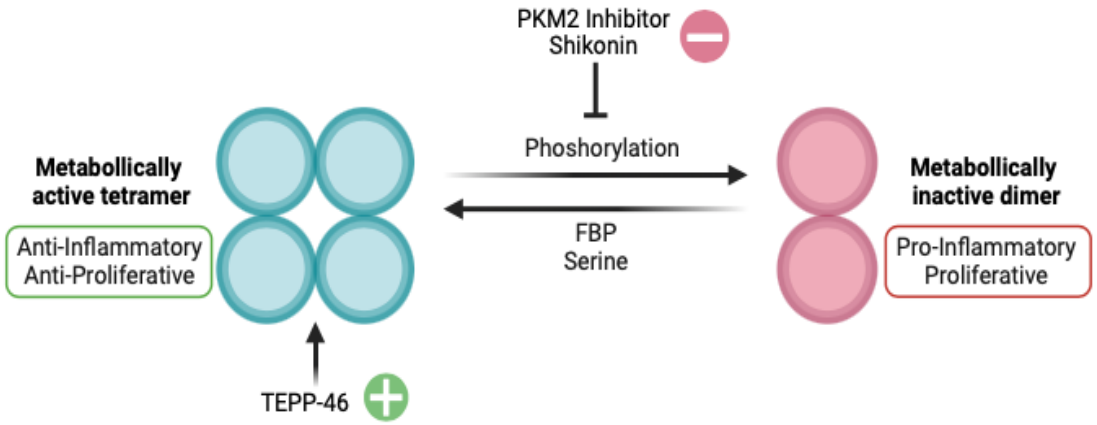

Figure 4: Effects of TEPP-46 and Shikonin on PKM2. PKM2 exists in the form of either a metabolically active tetramer, as which is it present in the cells` cytoplasm, or an inactive dimer. While the tetramer's role is solely one of a glycolytic enzyme, the dimer transfers to the cells' nucleus, where it enfolds a proliferative effect in effector cells. The small molecule TEPP-46 stabilizes the tetrameric form of PKM2. The naphtoquinone Shikonin inhibits both forms of PKM2. Image created in BioRender.com

1.4. Autoimmunity and acute autoimmune hepatitis

1.4.1. $CD4^+$ T cells in autoimmunity and autoimmune hepatitis

Autoimmunity displays a vast group of different diseases. Yet, a common feature of is the generation of pathogenic T cells accompanied by insufficient immune regulation, as it is for example in systemic lupus erythematosus (SLE), rheumatoid arthritis (RA), multiple sclerosis (MS), inflammatory bowel disease (IBD) and autoimmune hepatitis (AIH).

AIH is a comparably rare autoimmune disease with an incidence of 25/100.000, often occurring in middle aged women and first described in the 1950's (Manns 2011). To date, it's pathogenesis is not entirely elucidated, yet several contributing factors are being discussed, among them autoantigens such as CYP P450 members in hepatocytes or genetic predisposition in terms of major histocompatibility complex (MHC) also known as human leukocyte antigen (HLA) variants (Treichel et al. 1994, Donaldson, 2004). Triggers such as virus hepatitis or pharmacological stressors may contribute to disease manifestation (Vento et al 1991, Alla et al 2006). An exogenous antigen presented via MHC may show similarities with hepatocytes thereby stimulating autoreactive T cells, which under impaired T regulatory cell function and therefore immune control, trigger inflammation and AIH

(Longhi et al. 2006). Consequently, myeloid immune cells, such as macrophages, are recruited to the site of inflammation which contribute to liver damage (Czaja, 2019).
To date no causal treatment for autoimmune hepatitis is known. Common therapeutic options include corticosteroids - which were already known to be effectful in the 1950's - which reduces inflammatory activity but also has broad side effects, in combination with azathioprine. Another treatment option in case of insufficient disease control may be the TNFα inhibitor Infliximab, although side effects such as infections occur frequently (Weiler-Norman et al. 2013). After discontinuation of the immunosuppressive medication relapses are frequent. In cases with fulminant disease progression or cirrhosis due to non-responding to the treatment liver transplantation becomes the final therapeutic option.

$CD4^+$ T cells are key players in multiple autoimmune disorders. Th1 and Th17 cells have been shown to play a special role in the development of autoimmune diseases, for example SLE, rheumatoid arthritis, MS, inflammatory bowel disease, AIH and their respective animal models. By producing pro-inflammatory cytokines such as IFNγ Th1 cells promote inflammation and tissue destruction, for instance demyelination of neurons in multiple sclerosis. Similarly, Th17 cells are a main driver in mediating inflammation and recruiting other immune cells in diseases such as inflammatory bowel disease or psoriasis, where the main mediators of inflammation are cytokines such as IL-17, IL-21 or IL-22 (DiCesare et al. 2009, Luckheeram et al. 2012).
Specifically in colitis, a dysregulation between Th17 cells and microbiota dependent RORγT positive T regulatory cells were described (Yang et al. 2016), resulting in overactivity of proinflammatory compartments. Similarly for most other autoimmune diseases, T regulatory cells are of high relevance as they control homeostasis and under physiological circumstances avoid overshooting immune reactions.

Autoimmune hepatitis is one example for an autoimmune disease influenced mainly by $CD4^+$ T cells. Autoimmune hepatitis (AIH) is a medical condition caused by a T cell mediated immune response against hepatic antigens, potentially leading to either acute hepatic failure or a chronic state with fibrotic and cirrhotic remodeling. Cases of autoimmune hepatitis have, like other immune diseases, a functional imbalance between immune effector cells targeting hepatic antigens and regulatory cells in common, which leads to overshooting tissue damage (Horst et al. 2021). In an interplay with other immune cells, such as macrophages and neutrophilic granulocytes, $CD4^+$ T cells play an important role in

mediating inflammation and therefore their activation influences the outcome and severity of the disease.

1.4.2. The Concanavalin A model of acute autoimmune hepatitis

The Concanavalin A model simulates autoimmune hepatitis in mice by intravenous application of the plant lectin Concanavalin A (ConA), derived from *Canavalia ensiformis*, to activate immune cells (Tiegs et al. 1992).

Injected Concanavalin A accumulates in the liver where it binds to liver sinusoidal endothelial cells (LSEC) and is presented via MHC-II on Kupffer cells. Both processes activate $CD4^+$ T cells via TCR and induce differentiation into IFNγ, TNFα and IL-2 secreting Th1 cells thereby leading to inflammation and tissue damage (Gartner et al. 1995). Subsequently, macrophages are activated by Th1 cells, which contribute to tissue damage. Additionally, $CD4^+$ T cells regulatory become activated by IL-2, which play a role in resolving the reaction to Concanavalin A. Typically, the Concanavalin A reaction is specific to the liver and does not affect other organs. Depending on animal and dose, the overshooting immune reaction comes to an end leaving areas of damaged liver tissue or in extreme cases leading to liver failure.

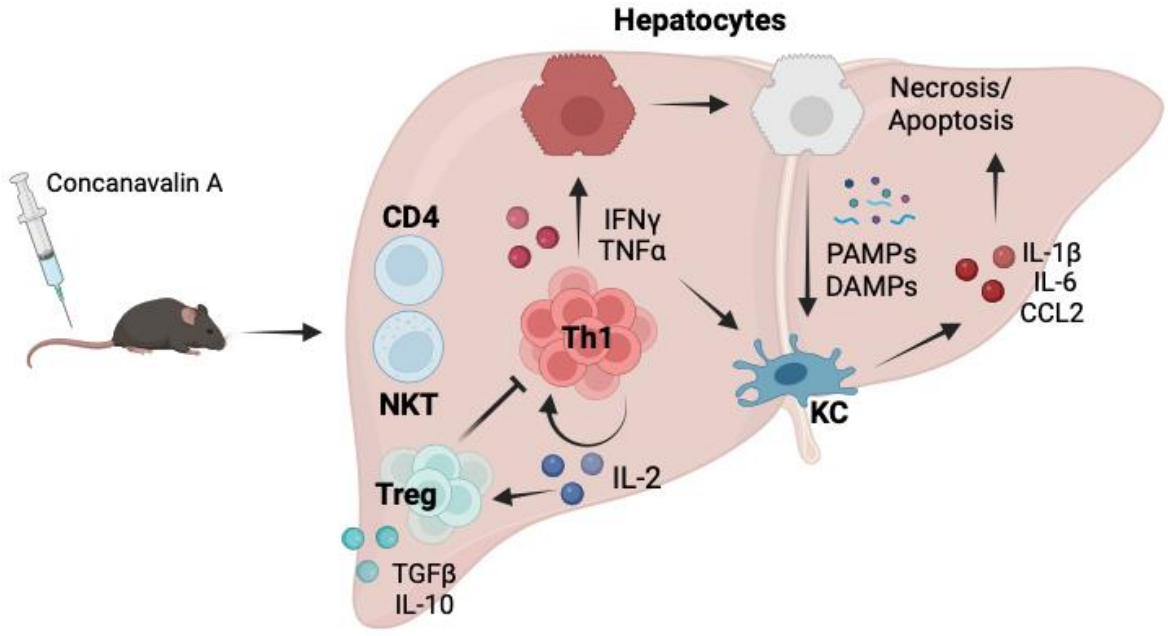

Figure 5: The Concanavalin A model of acute autoimmune hepatitis. Mice receive an intravenous dose of 5-7 mg/g of Concanavalin A. Once Concanavalin A reaches the liver, it binds to LSEC and is presented by Kupffer cells. $CD4^+$ T cell activation and Th1 polarisation result in the production of cytokines such as IL-2, IFNγ and TNFα. IL-2 acts as a restimulator of Th1 cells yet additionally induces T regulatory cell polarisation. IFNγ and TNFα meanwhile activate other immune cell subsets, such as Kupffer cells and mediate cellular damage in hepatocytes. Figure created in BioRender.com

1.5. Hypothesis

Although much is already known about metabolism in $CD4^+$ T cells, the role of PKM2, especially in the context of autoimmunity and AIH, remains rather unclear. The focus of this study is to examine the effects of a $CD4^+$ T cell specific cre-recombinase mediated knockout of PKM2 in vivo and primarily in vitro and elucidate how it may influence the cells metabolism, proliferation and function.

A knockout of PKM2 alters $CD4^+$ T effector cells metabolism.
Activated $CD4^+$ T effector cells rely on aerobic glycolysis to fuel expansion and cytokine production. PKM2 plays a crucial role in achieving this metabolic shift as it not only is rate limiting for glycolysis but also influences the expression of other glycolytic enzymes or glucose transporters.

A $CD4^+$ T cell specific knockout of PKM2 affects T effector and T regulatory cell proliferation in vitro.
PKM2 is a key enzyme allowing for the metabolic shift in activated T effector cells, thereby providing metabolic intermediates to be used as building blocks for proliferation. Contrarily to effector T cells, which rely on aerobic glycolysis for fueling, T regulatory cells thrive on oxidative phosphorylation. Therefore, PKM2 deletion may affect $CD4^+$ T cell proliferation differently.

A $CD4^+$ T cell specific knockout of PKM2 reduces T effector cells function in vitro.
Glycolytic enzymes are known to influence the expression of different inflammatory cytokines. PKM2 may possibly alter cytokine expression and thereby $CD4^+$ T cells function either by influencing $CD4^+$ T cell metabolism and thereby the availability of building blocks or affecting intracellular signaling and transcription regulation.

A $CD4^+$ T cell specific knockout of PKM2 influences T regulatory cells function in vitro.
T regulatory cells mainly rely on oxidative phosphorylation for fueling, yet their activation also depends on glycolysis. We therefore hypothesized that altering T regulatory cell metabolism may influence their activation or suppressive ability.

A $CD4^+$ T cell specific knockout of PKM2 reduces inflammation in vivo.

As activated T effector cells rely in glycolysis and PKM2 is a key regulator of the metabolic shift we hypothesized that a knockout of PKM2 would ameliorate $CD4^+$ T cell dependent models of autoimmune disease, such as the severity of a Concanavalin A hepatitis in mice.

PKM2 activity and therefore CD4+ T cell proliferation and function can be influenced by pharmacologic activators or inhibitors in vitro.

PKM2 has long been an interesting target for pharmacological interventions in the field of tumor biology as it plays a key role in enabling the Warburg effect. It was recently shown that Shikonin and Tepp-46 may alter immune cell function and reduce $CD4^+$ T cell effector activity (Zhang et al. 2019, Angiari et al. 2020).

2. Materials and Methods

2.1. Materials

2.1.1. List of technical equipment

Technical equipment	Manufacturer
BD FACSAria™ III	Becton Dickinson, Franklin Lakes, NJ
BD FACSCanto™ II	Becton Dickinson, Franklin Lakes, NJ
BD LSRFortessa™	Becton Dickinson, Franklin Lakes, NJ
C1000 Thermal Cycler	Bio-Rad, Hercules, CA
Cell SureLock™ Electrophoresis System	Thermo Fisher Scientific, Waltham, MA
Centrifuge 5417	Eppendorf, Hamburg
Centrifuge 5810 R	Eppendorf, Hamburg
CFX96TM Real-Time PCR Detection System	Bio-Rad, Hercules, CA
CK40 Microscope	Olympus, Hamburg, Germany
Cobas Integra 400	Roche, Basel
Eppendorf Research® plus Single-channel pipettes (0.1-2.5 l, 0.5-10 l, 2-20 l, 10-100 l, 20-200 l, 100-1000 l)	Eppendorf, Hamburg, Germany
Eppendorf Research® plus 8-channel pipette (10-100 l)	Eppendorf, Hamburg, Germany
Eppendorf Research® Plus Pipettes	Eppendorf, Hamburg
Galaxy® 48R CO2 Incubator	Eppendorf, Hamburg, Germany
HandyStep®	BRAND Gmbh, Wertheim
HERAcell® 240 CO2 Incubator	Thermo Fisher Scientific, Waltham, MA, USA
KL2 Shaker	Edmund Bühler GmbH, Bodelshausen, Germany
MACS® MultiStand	Milteny BioTech Inc. Auburn, CA
Nano-Drop ND-1000	PEQLAB, Erlangen
Neubauer Improved Hemocytometer	Carl Roth GmbH & Co.KG, Karlsruhe, Germany
Pipetboy® Acu 2	Integra Biosciences AG, Biebertal, Germany
PowerPac® HC Power Supply	Bio-Rad, Hercules, CA, USA
QuadroMACS® cell separator	Milteny BioTech Inc. Auburn, CA
Seahorse XFe96 Analyzer	Agilent Technologies Inc., Santa Clara, CA
Tecan Infinite M200 Plate Reader	Tecan, Crailsheim, Germany
Thermoleader Dry Block Heat Bath	UniEquip, Planegg, Germany
Thermoleader Dry Block Heat Bath	UniEquip, Planegg, Germany
TissueLyser II®	Qiagen, Venlo, Netherlands
VersaDoc™ 4000 MP Imaging System	BioRad, Hercules, CA
Vortex Mixer	Heidolph, Schwabach, Germany
XCell SureLock™ Electrophoresis System	Thermo Fischer Scientific, Waltham, MA

Table 1: List of technical equipment

2.1.2. List of consumables

Consumable	Manufacturer
1 µm, 0,2 µm filters, stericup	Merck, Darmstadt, Germany
6, 24 and 96-well culture plates	Sarstedt, Nümbrecht
Cell culture dishes (60mm, 100mm)	Sarstedt, Nümbrecht, Germany
Cell strainer 30µm, 100µm	Corning, CA, USA
Cover slips, 21 26mm	Gerhard Menzel GmbH, Braunschweig, Germany
Flow cytometer tubes, 5 ml	Sarstedt, Nümbrecht, Germany
MACS® columns for magnetic cell sorting	Miltenyi BioTech Inc. Auburn, CA
Microscope slides	Glaswarenfabrik Karl Hecht GmbH & Co.KG, Sondheim, Germany
NuPAGE Bis-Tris Gradient Gels, 4-12%, 15-well	Thermo Fisher Scientific, Waltham, MA, USA
Parafilm M	Pechiney Plastic Packaging Inc., Chicago, IL, USA
PCR Tubes	Abgene, ThermoFisher, Hamburg
Pipette tips (10µl, 200µl, 1000µl)	Sarstedt, Nümbrecht, Germany
Pipette tips, sterile and RNAse free (10µl, 200µl, 1000µl)	Sarstedt, Nümbrecht, Germany
Pipettes (2ml, 5ml, 10ml, 25ml 50ml)	Sarstedt, Nümbrecht, Germany
Reaction tubes (1.5ml, 2ml)	Sarstedt, Nümbrecht, Germany
Reaction tubes, conical/non-conical (15ml, 50ml)	Sarstedt, Nümbrecht, Germany
Reaction tubes, sterile, RNAse free (1.5ml, 2ml)	Sarstedt, Nümbrecht, Germany
SafeSeal® reaction tubes (1.5 ml, 2ml)	Sarstedt, Nümbrecht, Germany
XF 96 well culture plate	Agilent Technologies Inc., Santa Clara, CA

Table 2: List of consumables

2.1.3. List of kits and reagents

Kit/Reagent	Manufacturer
ABgene DNA Synthesis Kit	Thermo Fisher Scientific, Waltham, NY
Antibody Diluent for Immunohistochemistry	Agilent/DAKO, Glostrup, Denmark
Bradford Protein Assay	Bio-Rad, Hercules, CA, USA
Concanavalin A from Canavalia ensiformis	Sigma-Aldrich, St. Louis, MO, USA
Crystal Mount™ Aqueous Mounting Medium	Sigma-Aldrich, St. Louis, MO, USA
CSFE Cell Division Tracker Kit	BioLegend, San Diego, CA
Liqiod DAB+ (Diaminobenzidine)	Agilent/DAKO, Glostrup, Denmark
D-Glucose, 100x	Thermo Fisher Scientific, Waltham, MA, USA
Dimethyl Sulfoxide (DMSO)	Sigma-Aldrich, St. Louis, MO, USA
ELISA diluent	Becton Dickinson, Franklin Lakes, NJ
Ethanol 100%	Th. Geyer GmbH & Co.KG, Renningen, Germany
Ethanol 70%	Th. Geyer GmbH & Co.KG, Renningen, Germany
Foxp3 Transcription Factor Staining Set	eBioscience™ Inc., San Diego, CA, USA
Glucose Uptake Cell-Based Assay Kit	Cayman Chemical, Ann Arbor, MI
Hydrogen Chloride (HCl)	Carl Roth GmbH & Co.KG, Karlsruhe, Germany
Hydrogen Peroxide (H2O2)	Carl Roth GmbH & Co. KG, Karlsruhe, Germany
Invitrogen™ DNA-free™ Kit	Thermo Fisher Scientific, Waltham, NY
L-Glutamin, 100x	Thermo Fisher Scientific, Waltham, MA, USA
Liberase™	Roche, Basel
Luminol Sodium Salt	Sigma-Aldrich, St. Louis, MO, USA
Lyophilized standard for ELISA	Becton Dickinson, Franklin Lakes, NJ
MACS CD4+ T cell isolation kit	Milteny BioTech Inc. Auburn, CA, USA
Maxima SYBR Green	Thermo Fisher Scientific, Waltham, MA, USA
Mercaptoethanol	Carl Roth GmbH & Co.KG, Karlsruhe, Germany
NucleoSpin RNA II Kit®	Macherey&Nagel, Düren, Germany
NucleoSpin RNA Kit®	Macherey&Nagel, Düren, Germany
NuPAGE™ LDS Sample Buffer	Thermo Fisher Scientific, Waltham, MA, USA
NuPAGE™ MES SDS Running Buffer	Thermo Fisher Scientific, Waltham, MA, USA
NuPAGE™ Sample Reducing Agent	Thermo Fisher Scientific, Waltham, MA, USA
Para-hydroxy Coumaric Acid	Sigma-Aldrich, St. Louis, MO, USA
Percoll	GE Healthcare, Glattbrugg, Zurich
Precision Plus Protein™ WesternC™ Standard	BioRad, Hercules, CA
Pyruvate, 100x	Thermo Fisher Scientific, Waltham, MA, USA
Roswell Park Memorial Institute Medium (RPMI) 1640	Thermo Fisher Scientific, Waltham, MA, USA
Shikonin (5,8-dihydroxy-2-[(1R)-1-hydroxy-4-methyl-3-penten-1-yl]-1,4-naphthalenedione)	Cayman Chemical, Ann Arbor, MI, USA
Sodium Hydroxide (NaOH)	Carl Roth GmbH & Co.KG, Karlsruhe, Germany
Sodium Orthovanadate (NaVO4)	Sigma-Aldrich, St. Louis, MO, USA
Strep-Tactin® HRP	IBA Lifesciences, Göttingen, Germany
Swine Serum	Agilent/DAKO, Glostrup, Denmark
Target Retrieval Solution	Agilent/DAKO, Glostrup, Denmark

TEPP-46 (6-[(3-aminophenyl)methyl]-4,6-dihydro-4-methyl-2-(methylsulfinyl)-5H thieno[2',3':4,5]pyrrolo [2,3-d]pyridazin-5-one)	Cayman Chemical, Ann Arbor, MI, USA
Tetramethylbenzidine	Becton Dickinson, Franklin Lakes, NJ
Tris Hydrochloride (HCl)	Carl Roth GmbH & Co.KG, Karlsruhe, Germany
Tween® 20 (Polysorbat)	ThermoFisher Scientific, Waltham, MA, USA
Vectastain Elite ABC HRP Kit	Vectorlabs, Burlingame, CA, USA
Williams E Medium + GlutaMAX™	Gibco, Waltham, MA, USA
XF Seahorse Base Medium (used for glycolysis stress test)	Agilent Technologies Inc., Santa Clara, CA
XF Seahorse calibrant	Agilent Technologies Inc., Santa Clara, CA
XF Seahorse DMEM Medium (used for glycolytic rate assay)	Agilent Technologies Inc., Santa Clara, CA
XF Seahorse e96 FluxPak	Agilent Technologies Inc., Santa Clara, CA
XF Seahorse Glycolysis stress test kit	Agilent Technologies Inc., Santa Clara, CA
XF Seahorse Glycolytic rate assay kit	Agilent Technologies Inc., Santa Clara, CA
X-Vivo™ 20 Medium	Lonza, Basel, Switzerland
Xylene Substitute (HS200-5 XEM)	DiaTec, Bamberg, Germany

Table 3: List of kits and reagents

2.1.4. List of solutions and buffers

Buffer/Solution	Composition
Phosphate Buffer Saline (PBS, 10x)	137 mM NaCl 2,7 mM KCl 8,1 mM Na_2HPO_4 1,5 mM KH_2PO_4
BD-Diluent Buffer	0,1% BSA 0,05% Tween 20 20 mM Tris Base 150 mM NaCl
BL-Blocking Solution	1% BSA in 1x PBS
BD-Blocking Solution	1% BSA 5% Sucrose 0,05% NaN_3 in 1x PBS
BD-Coating Buffer	0,1 M Na_2HPO_4 0,1 M NaH_2HPO_4
Lysis buffer for protein lysates	12.5ml Tris (25mM) 75ml NaCl (150mM) 5ml EDTA (5mM) 100ml Glycerol (10%) 50ml TritonTM X-100 (1%) 12.5ml Sodium Pyrophosphate (10mM) 10ml Sodium Orthovanadate (1mM) 5ml Glycerophosphate (10mM) ad 500ml Milli-Q® ultrapure H2O
FACS Buffer (1 l)	978ml PBS 2ml NaN3 (0.02% w/v) 20ml FCS
Hank's Balanced Salt Solution (HBSS)	5.4mM KCl 0.3mM Na2HPO4 7 H2O 4.2mM NaHCO3 1.3mM CaCl2 0.5mM MgCl2 6 H2O 0.6mM MgSO4 7 H2O 137mM NaCl 5.6mM D-Glucose ad 1l Milli-Q® ultrapure H2O
Ammoniumchloride (NH4CL) (1 l)	19 mM Tris-HCL 140 mM NH4CL ad to 1 L H2O, pH 7.2
Percoll/HBSS	38% Percoll Working Solution 60% HBSS 2% Heparin (100IU/ml)
10x Transfer buffer for western blot	250mM TRIS 2M Glycin ad 2l Milli-Q® ultrapure H2O Transfer buffer (1): 200ml Transfer buffer (10) 400ml Methanol ad 2l Milli-Q® ultrapure H2O
RNAse A Buffer	RNAse A Buffer 121mg Tris (10mM) 29mg EDTA (1mM)

	20 RNAse A (100mg/ml) Sodium Orthovanadate Solution Sodium Orthovanadate (10mM)
5% milk solution	TBS-T 5 % dry milk powder
Sodium Pervanadate Solution	100 µl Sodium Orthovanadate Solution 16 µl H2O2
Sodium Orthovanadate Solution	Sodium Orthovanadate (10mM) 150ml Milli-Q® ultrapure H2O
Tris buffer saline (TBS, 10x)	100mM Tris 1.5M NaCl ad 2l Milli-Q® ultrapure H2O
Tris buffer saline with Tween 20 (TBS-T)	200ml TBS 2ml Tween® ad 2l Milli-Q® ultrapure H2O
PPML Medium	5,36 mM KCl 0,44 mM KH_2PO_4 4,17 mM $NaHCO_3$ 138 mM NaCl 0,38 mM Na_2HPO_4 x2 H_2O 5 mM Glucose 0,5 mM EGTA 50 mM Hepes
PM Medium (1l)	400 mg KCl 190 mg $MgSO_4$ x 7 H_2O 190 mg $MgCl_2$ x 6 H_2O 60 mg Na_2HPO4 x 2 H_2O 2,38 mg Hepes 8g NaCl 60 mg KH_2PO4 2 g Glucose 220 mg $CaCl_2$ 2 g BSA

Table 4: List of solutions and buffers

2.1.5. List of antibodies

2.1.5.1. List of antibodies used in western blotting

Target	Host	Clone	Conjugate	Dilution	Distributor
Primary					
PKM1	Rabbit	D30G6	---	1:1000	Cell Signaling Technology, Cambridge UK
PKM2	Rabbit	D78A4	HRP	1:1000	Cell Signaling Technology, Cambridge UK
Enolase	Rabbit	polyclonal	---	1:1000	Cell Signaling Technology, Cambridge UK
PKM2	Rabbit	D78A4	---	1:1000	Cell Signaling Technology, Cambridge UK
β-Actin	Goat	polyclonal	HRP	1:1000	Santa Cruz Biotechnology Inc., Dallas, TX, USA
Secondary					
Anti-rabbit IgG	Goat	Polyclonal	HRP	1:5000	Cell Signaling Technology, Cambridge UK

Table 5: List of antibodies used in western blotting

2.1.5.2. List of antibodies used in immunohistochemistry

Target	Host	Clone	Conjugate	Dilution	Distributor
Primary					
MPO	Goat	polyclonal	---	1:40	R&D Systems Inc., Minneapolis, MN, USA
Secondary					
Anti-Rabbit IgG	Goat	polyclonal	Biotin	1:200	Jackson Laboratories, Inc., West Grove, PA, USA

Table 6: List of antibodies used in immunohistochemistry

2.1.5.3. List of antibodies used for flow cytometry

Target	Clone	Fluorophore	Dilution	Distributor
Zombie NIR	---	APC/Cy7	1:500	BioLegend Inc, San Diego, CA
CD4	RM4-5	BV711	1:200	BioLegend Inc, San Diego, CA
CD4	RM4-5	FITC	1:200	BioLegend Inc, San Diego, CA
CD25	PC61	BV421	1:200	BioLegend Inc, San Diego, CA
CD25	PC61	PE/Cy7	1:200	BioLegend Inc, San Diego, CA
CD73	TY/11.8	BV605	1:200	BioLegend Inc, San Diego, CA
CD39	24DMS1	PE	1:200	eBioscience™ Inc, San Diego, CA
CD39	Duha59	PE/Cy7	1:200	BioLegend Inc, San Diego, CA
CD39	Duha59	AF674	1:200	BioLegend Inc, San Diego, CA
FoxP3	MF-14	AF647	1:100	BioLegend Inc, San Diego, CA
FoxP3	FJK-16s	FITC	1:100	eBioscience™ Inc, San Diego, CA
PD-1	J43	PE/Cy7	1:100	eBioscience™ Inc, San Diego, CA
RORγT	AFKJS-9	PE	1:100	eBioscience™ Inc, San Diego, CA
Bcl2	BCL/10C4	PE	1:100	BioLegend Inc, San Diego, CA
Bcl2	BCL/10C4	PE/Cy7	1:100	BioLegend Inc, San Diego, CA
Ki67	REA183	FITC	1:100	Miltenyi BioTech Inc. Auburn, CA
Tbet	4B10	BV711	1:100	BioLegend Inc, San Diego, CA
IL-17A	TC111-18H10	AF647	1:100	BD Pharmingen, Franklin Lakes, NJ
IL-17A	BL168	BV605	1:100	BioLegend Inc, San Diego, CA
IFNγ	XMG1.2	BV711	1:100	BioLegend Inc, San Diego, CA
IFNγ	XMG1.2	FITC	1:100	BioLegend Inc, San Diego, CA
Galectin 9	RG9-35	PerCP/Cy5.5	1:100	BioLegend Inc, San Diego, CA
pStat5	C71E5	AF647	1:100	Cell Signaling Technology, Cambridge
Bcl-6				

Table 7: List of antibodies used for flow cytometry

2.1.5.4 List of antibodies used in enzyme linked immunosorbent assay (ELISA)

Target	Host	Clone	Conjugate	Dilution	Distributor
Primary					
IL-2	rat	JES6-1A12	---	1:10	BioLegend Inc, San Diego, CA
IFNγ	rat	37801/37875	---	1:200	R&D Systems, Minneapolis, Minnesota, USA
Secondary					
IL-2	rat	JES6-5H4	Biotin	1:40	BioLegend Inc, San Diego, CA
IFNγ	goat	polyclonal	Biotin	1:200	R&D Systems, Minneapolis, Minnesota, USA

Table 8: List of antibodies used in ELISA

2.1.6. List of oligonucleotide sequences used in RT-qPCR.

All primers were obtained from Metabion International AG, Planegg, Germany.

Target	Forward primer sequence Reverse primer sequence	Annealing Temperature (°C)	Extension time (sec)
ß-Actin	TATTGGCAACGAGCGTTCC GGCATAGAGGTCTTTACGCATGTC	60	20
Pkm1	TCGCATGCAGCAGCACCTGATAG CCATGAGGTCTGTGGAGTGAC	60	20
Pkm2	CATTACCAGCGACCCCACAG CACTCCTGCCAGACTTGGTG	60	20
IFNγ	ACAGCAAGGCGAAAAAGGATG TCTTCCCCACCCCGAATCA	60	20
TNFα	GATCGGTCCCCAAAGGGATG GCTACAGGCTTGTCACTCGAA	60	20
Enolase	CATGGGGAAGGGTGTCTCAC CACTTTCTTGCTAACCAGAGCA	60	20
Hif1α	CTTGACAAGCTAGCCGGAGG CGACGTTCAGAACTCATCCTATTTT	60	20

Table 9: List of oligonucleotide sequences in RT-qPCR

2.1.7. Laboratory animals

C57BL6 Pkm2 fl/fl mice (kindly provided by Matthew G. Vander Heiden) were crossed with CD4-cre transgenic mice (Christopher B. Wilson, 2001) resulting in animals carrying a cre recombinase downstream the CD4 promotor ($CD4^{\Delta PKM2}$ mice). As controls either wildtype mice (WT) or CD4-cre transgenic mice were used ($CD4^{cre}$). All animal experiments were approved (ORG950, Behörde für Verbraucherschutz, Hamburg, Germany) and conducted according to the German Animal Protection Law. For the experimental work male mice aged 8-14 weeks were used, for the removal or organs male mice aged 8-18 weeks were used. Mice were held in groups of up to six animals in individually ventilated cages, received food and water ad libitum and standard care in the animal facility.

2.1.8. Software

Software and Databases	Distributor
Microsoft Office 2016	Microsoft Corporation, Redmont, WA
GraphPad Prism Version v9	GraphPad Software Inc., San Diego, CA
Tbase V16	4D Germany, Eching
BD FACS Diva™	Becton Dickinson, Franklin James, NJ
FlowJo™ 10.5.3	FlowJo LCC, Ashland, OR
Seahorse Wave Desktop Software	Agilent Technologies Inc., SantaClara, CA
Cytobank	Beckman Coulter, Brea, CA
EndNote 21	Clarivate Analytics, Philadelphia, PA
ImageLab™ 2.0	BioRad, Hercules, CA
Tecan Magellan™ v6	Tecan, Crailsheim
LEGENDplex™ Data Analysis Software v8	BioLegend Inc., San Diego, CA
Quantity One® Software	BioRad, Hercules, CA

Table 10: List of used software

2.2. Methods

2.2.1. Experimental animal treatment with Concanavalin A

$CD4^{cre}$ and $CD4^{\Delta PKM2}$ mice (8-12 weeks old) were treated with a dose of 5-7 mg/kg Concanavalin A dissolved in Dulbecco's phosphate buffered saline (DPBS). After 2, 8 and 24 hours, blood was taken and analysed for liver transaminases (3.2.3). Mice were sacrificed after 24 hours, and liver samples were analysed for necrotic area, neutrophil invasion and inflammatory markers.

2.2.2. Extraction of biological samples

Mice were anesthetized and sacrificed by cervical dislocation. Then, a blood sample was taken by cardiac puncture. Blood samples were centrifuged at 20000 x g and 4 °C for 5 minutes and plasma was stored at -20 °C or analysed directly.
Spleens were completely removed and stored in sterile HBSS on ice until further processing to isolate $CD4^+$ T cells (see 3.2.4). Livers were removed and stored either in HBSS (in case of isolation of hepatocytes for co-culture, see 3.2.6.) or in liquid nitrogen for mRNA or protein isolation. Samples for histology or immunohistochemistry were placed in 4% paraformaldehyde until further processing (see 3.2.8).

2.2.3. Measurement of liver enzymes, cholesterol and triglycerides

Liver enzyme activity as well as the concentrations of cholesterol and triglycerides was measured using a Cobas Integra 400. Prior to measurement plasma samples were diluted 1:5 with Milli-Q® ultrapure H_2O.

2.2.4. Isolation of $CD4^+$ T cells from spleens by MACS® Sorting

$CD4^+$ T cells were isolated by using a MACS® $CD4^+$ T cell isolation kit (Milteny BioTech Inc. Auburn, CA, USA) from mouse spleens following the manufacturer's manual.
Briefly, sterile removal of mice spleens was conducted, and spleens were kept in sterile HBSS on ice. Next, they were transferred to 50ml reaction tubes using 30 µm sterile filters and centrifugated at 500 x g and 4 ° C for 5 minutes. The supernatant was discarded, and cells were washed again, as described, in 30 ml HBSS. Cells were then resuspended in 15ml MACS buffer and counted.
Cells were once more centrifugated and the supernatant discarded, before the cells were resuspended in 40µl MACS buffer and 10µl Biotin antibody per $1x10^7$ cells and incubated for 5 minutes at 4° in the dark. The following steps were conducted with minimal light

influence. Following incubation, an additional 30µl MACS buffer and 20µl anti-biotin-beads per $1x10^7$ cells were added. Incubation was continued for 10 minutes.
Next, cells were applied to MACS sorting columns (Milteny BioTech Inc. Auburn, CA) and collected in 15 ml reaction tubes on ice. To each column $1x10^8$ cells were applied and columns were washed with MACS buffer. The sorted cells were pooled and centrifugated as described prior and, following the removal of the supernatant, resuspended in RPMI medium at a concentration of $1x10^6$ cells per ml for further use in cell culture.

2.2.5. Isolation of non-parenchymal liver cells

To identify certain groups of immune cells in the liver FACS analysis (see 3.2.15) of liver NPCs was performed. For this purpose, liver tissue from mice was crushed in a petri dish, diluted with 15 ml HBSS and transferred to a 50 ml reaction tube through a 100 µm cell strainer. Cells were centrifugated at 500 x g for 5 minutes at RT.
The supernatant was then carefully discarded, and the cell pellet was resuspended in 10 ml 36% Percoll in HBSS containing Heparin and centrifugated at 800 x g for 20 minutes at RT (brake: 7). Cell debris in the supernatant was carefully removed and the remaining supernatant poured off. The remaining cells were resuspended in 5 ml ACK lysis buffer (ammonium chloride (140 mM) with Tris/HCl (19 mM)), transferred to a fresh reaction tube and incubated for 3 minutes at RT. Next, lysis was stopped with 15 ml HBSS, and the suspension was centrifugated at 500 x g for 5 minutes at 4°C. The supernatant was discarded, and cells were stored in 1 mL FACS puffer until staining.

2.2.6. Isolation of hepatocytes

For co-cultures with $CD4^+$ T cells hepatocytes were isolated from liver tissue of wild type as well as $CD4^{cre}$ and $CD4^{\Delta PKM2}$ mice. To achieve this, mice were sacrificed, and their vena cava superior was tied off. A cannula and tube were prefilled with PPML medium and inserted into the vena porta of the mouse. Next, PM medium was injected into the liver tissue while holding the vena cava inferior closed. After letting the Liberase™ work, pressure on the vena cava inferior was released. Livers were transferred to a petri dish with PM medium and the liver capsule was opened to wash out the hepatocytes. The cell suspension was then transferred to a reaction tube through a 100µm cell strainer and 20 ml of HBSS were added. While waiting for formation of a cell sediment, 21,6 ml Percoll and 2,4 ml DPBS (+$MgCl_2$ and $CaCl_2$) were mixed. Subsequently, 25 ml of the cell supernatant was discarded and the rest mixed with Percoll and inverted. The suspension was then

centrifuged at 600rpm and 5°C for 10 minutes, the supernatant was discarded. The remaining hepatocytes were kept in Williams E Medium at $1x10^5$ cells per ml until further usage.

2.2.7. Cell culture

For all cell cultures either 6-, 24- or 48- well plates were used, which were coated with anti-CD3 one day prior to harvesting and culturing cells. Wells prepared by washing them with 250 µl sterile PBS and coating them with 250µl of anti-CD3 diluted 1:200 in PBS. Plates were then sealed with parafilm and kept at 4 °C overnight. Before being used wells were washed with 250µl sterile PBS each and directly refilled with cell suspension.

Induction of Th1, Th17 and T regulatory $CD4^+$ T cells

Naive mouse $CD4^+$ T cells isolated from spleenocytes (see 3.2.4) were used for the induction of Th1 and Th17 as well as T regulatory cells. Cells for T cell polarisation were cultured in 1 ml complete RPMI medium per $0,5x10^6$ cells. Reagents for polarisation were added to the cell suspension as described in Table 10 and described by Flaherty et al (2015). T regulatory cell induction was performed as described by Fantini et al. (2007) using $1x10^6$ cells per ml of X-Vivo™ medium. For Treg induction 4ng/ml TGFβ was added per ml of medium. Cells were incubated for 3 days at 5% O_2 and 37 °C.

Reagent	Assay concentration	Clone	Host	Distributor
T cells				
Anti-CD3	5 µg/ml	145-2C11	hamster	BioLegend Inc, San Diego, CA
Anti-CD28	2 µg/ml	37.51	hamster	BioLegend Inc, San Diego, CA
Th1 cells				
Anti-CD3	5 µg/ml	145-2C11	hamster	BioLegend Inc, San Diego, CA
Anti-CD28	2 µg/ml	37.51	hamster	BioLegend Inc, San Diego, CA
Anti-IL-4	10 µg/ml	QA19A66	mouse	BioLegend Inc, San Diego, CA
IL-2	100 U/ml	---	E. coli	R&D Systems, Minneapolis, Minnesota, USA
IL-12	10 ng/ml	---	Spodoptera frugiperda	R&D Systems, Minneapolis, Minnesota, USA
Th17 cells				
Anti-CD3	5 µg/ml	145-2C11	hamster	BioLegend Inc, San Diego, CA

Anti-CD28	2 µg/ml	37.51	hamster	BioLegend Inc, San Diego, CA
Anti-IL-4	2 µg/ml	QA19A66	mouse	BioLegend Inc, San Diego, CA
Anti-IFNγ	12 µg/ml	R4-6A2	rat	BioXCell, Lebanon, New Hampshire, USA
IL-1β	10 ng/ml	---	E. coli	BioLegend Inc, San Diego, CA
IL-6	10 ng/ml	---		
IL-23	20 ng/ml	---	Insect cells	BioLegend Inc, San Diego, CA
TGFβ	0,5 ng/ml	---	Hamster ovary cell line	R&D Systems, Minneapolis, Minnesota, USA
T regulatory cells				
Anti-CD3	5 µg/ml	145-2C11	hamster	BioLegend Inc, San Diego, CA
TGFβ	4 ng/ml	---	Hamster ovary cell line	R&D Systems, Minneapolis, Minnesota, USA

Table 10: Cytokines and Antibodies used for $CD4^+$ T cell culture

Co-culture of $CD4^+$ T cells and hepatocytes

Hepatocytes were isolated from livers as described in 3.2.6 and stored in Williams E medium. Also, $CD4^+$ T cells were isolated as described (3.2.4.) and kept as a cell suspension of $1x10^6$ cells per ml in Williams E medium on ice. For the co-culture 0,5 ml of each cell suspension was transferred to a prepared 24 well plate. Furthermore, half of the co-cultured were treated with 4ng/ml of TGFβ to induce the formation of T regulatory cells. Cells were cultured for 3 days at 5 % O_2 and 37 °C before being analysed by flow cytometry for T regulatory cell formation.

Treatment of cells with Tepp46 and Shikonin

To examine whether PKM2 can be a pharmacological target, cultured cells were treated with either TEPP-46 (6-[(3-aminophenyl)methyl]-4,6-dihydro-4-methyl-2(methyl)-sulfinyl-5H-thieno [2',3':4,5]-pyrrolo-[2,3-d]-pyri-dazin-5-one) or Shikonin (5,8-dihydroxy-2-[(1R)-1-hydroxy-4-methyl-3-penten-1-yl]-1,4-naphthalenedione).

TEPP-46 is a small molecule activator inducing PKM2 tetramerisation (Jiang et al. 2010, Boxer et al. 2010). Stocks were obtained from Cayman Chemical, Ann Arbor, MI, USA, diluted to 100µM in DMSO and added to cell culture medium (1 µl per 1ml).

Shikonin is a naphthoquinine, which can be isolated from L. erythrorhizon roots and is known for its effect as a small molecule inhibitor on PKM2 and thereby glycolysis (Chen et

al. 2012). Shikonin was obtained from Cayman Chemical, Ann Arbor, MI, USA and dissolved in DMSO (20mg/ml in DMSO) to be added to cell culture medium (1 µl per 1 ml). Both were used in $CD4^+$ T cells of wildtype mice, primarily, yet also added to $CD4^{cre}$ and $CD4^{\Delta PKM2}$ cells to examine effects unspecific to PKM2. As a control 1µl DMSO per ml medium was used.

Suppression assay and CSFE labeling of cells

T regulatory cells were induced as described prior and cultivated for 2 days. They were then sorted for $CD4^+$ CD25 high cells using fluorescence activated cell sorting as described prior (see 3.2.15 Fluorescence Activated cell sort). A small part of the cells was stained intracellularly for FoxP3 using the Foxp3 Transcription Factor Staining Buffer Kit (eBioscience™) to confirm successful Treg induction.

Splenocytes were labeled using a CSFE cell division tracker kit (BioLegend, ORT). CSFE working solution was prepared following the manufacturer's instructions. Briefly by reconstituting CSFE in DMSO and further diluting a stock solution in PBS.

Splenocytes were centrifuged, resuspended at $1x10^7$ cells/ml in 50mL PBS and 50µl CSFE working solution was added (5µM). Cells were incubated for 20 minutes at room temperature protected from light. For further processing CSFE labeled cells were diluted in a ration of 1:5 in RPMI. Then CD4+ T cells were isolated from CSFE labeled splenocytes by MACS sorting (as described in 3.2.3). CSFE labeled CD4+ T cells were cultured with CD4+ CD25 high cells in ratios from 1:1 up to 16:1 for two days before being analysed for CSFE distribution among cells by flow cytometry.

Restimulation of T cells

To examine cytokine production $CD4^+$ T cells were restimulated after polarisation. First, cells were centrifuged at 300 x g and 4 °C for 5 minutes and the supernatant was discarded. Meanwhile, 20 ng/ml PMA and 1 µg/ml ionomycin were dissolved in RPMI and 1ml was added to each well of the 24-well plate containing the T cell base layer. After 1 hour, 1µg/ml Brefeldin A and Monensin (2µM final concentration) were added and cells were incubated for another 4 to 6 hours at 37 °C. Afterwards, 100 µl of the supernatant was stored for ELISA analysis. 150µl of PBS were added per well and the plate was centrifuged at 300 x g and 4 °C for 5 minutes to then proceed with the FACS staining of the cells.

2.2.8. Histological stainings

All liver samples were fixed in 4% paraformaldehyde and dehydrated in ascending ethanols before being embedded in paraffin.

Hematoxylin Eosin (H.E.) staining

To identify histological features such as necrosis area and invasion of lymphocytes in livers of mice treated with Concanavalin Hematoxylin Eosin staining was conducted according to standard H.E. staining procedures. Images and quantification of the necrotic area were kindly conducted by Sören Weidemann (Institute of pathology, University Medical Center Hamburg Eppendorf).

Immunohistochemical stainings

For all immunohistochemical stainings liver sections were first deparaffinized using xylene substitute medium for 20 minutes. Next, sections were rehydrated in descending ethanols of 100%, 90%, 70% and 50% for 5 minutes each and washed in H_2O.

Next, sections retrieved using citrate-based retrieval solution diluted 1:10 in dH_2O at 750 °C in a microwave for 10 minutes. If necessary, citate-based retrieval buffer or dH_2O were refilled. After 20 minutes of cooling at room temperature sections were washed 5 minutes in TBS pH 7,4. To avoid unspecific antibody binding, sections were then incubated for 30 minutes at room temperature with swine serum diluted in 1:10 in Dako Antibody Diluent (50 µl per section). Primary antibody (see Table 6) was diluted in Antibody Diluent, applied and sections were incubated overnight at 4°C in the dark.

The next day, sections were washed 15 minutes in total in TBS (pH 7,4) and incubated with secondary antibody (see Table 6), diluted in Dako antibody diluent, for 30 minutes. Following incubation, sections were washed as described and incubated with horseradish Peroxidase (HRP) conjugated Streptavidin (Vectastain Elite ABC HRP kit, 50 µl of reagent A and 50 µl of reagent B mixed in 5 ml TBS pH 7,4) for 30 minutes and washed as described. Next, 3,3'-diaminobenzidine (Dako Liquid DAB+) was applied to the sections. Following incubation for 2 to 5 minutes and checking for a successful staining under a light microscope, sections were washed with dH_2O. Crystal Mount™ was applied to the sections and let dry for 1 hour. Finally, sections were covered with Entellan® and cover slips.

2.2.9. Extraction of protein lysates from T cells and liver tissue

To perform western blot analysis of proteins from whole liver tissue as well as T cells cell lysis was carried out. Lysis buffer was prepared as described in Table 4 from KLB buffer, 0,1 M PMSF, Aprotinin solution, 1 M sodiumflouride and sodiumpervanadat solution. A sample of lysis buffer was kept for the Bradford assay. Cultured cells were resuspended twice in cold PBS, transferred to Eppendorf reaction tubes and stored on ice whenever not used. To each sample 40µl lysis buffer was added and pellets were dissolved by manual pipetting. Samples were then kept 10 seconds in an ultrasound bath and incubated 30 minutes on ice. Protein lysates from liver were produced combining chemical lysis by adding 500µl of lysis buffer and mechanical lysis using metal beads and a TissueLyser II® for 2 minutes at 30Hz. Following mechanical lysis samples were transferred to Eppendorf tubes and incubated for 30 minutes on ice. Both sample types were lastly centrifuged 10 minutes at 14000 RPM and 4 °C. Supernatants with protein lysates were transferred to new tubes and stored on ice. Lysates were stored at -80°C until being further processed.

2.2.10. Gel electrophoresis and Western Blot

First, a Bradford assay was conducted to determine protein concentration. Bradford day reagent was diluted 1:5 with Milli-Q® ultrapure H_2O. Next, 198µl of the solution was pipetted in a 96-well plate and 2µl of each protein lysate was added. In case of high expected protein density, lysates were diluted 1:5 or 1:10 with H_2O. As a blank 198 µl Bradford solution and 2 µl stored lysis buffer were used. Measurement was conducted with a TECAN Infinite® 200 PRO multi reader. The protein concentration and thereby the exact amounts of sample to be loaded on the gels were calculated.

For gel electrophoresis 30µg of protein was used per sample and loaded next to 4µl of Precision Plus Protein Western Standard™ on NuPAGE® 15-cell 4-12% Bis-Tris Mini Gels. Cells were loaded with 5-10µl NuPAGE® LDS Sample Buffer, 2-2,5µl NuPAGE® Reducing Agent and the respective amount of protein lysate up to a total volume of 20-25µl depending on the experiment. Gels were run at 200V for 35-60 minutes depending on the experiment in SDS Running Buffer.

The western blotting procedure was conducted using a wet blot method (350 mA 70 min on ice) on a nitrocellulose membrane and western blotting transfer buffer. The membrane was then treated with Ponceau red color on a shaker for 2 minutes and washed with Tris-buffered saline with Tween® 20 (TBS-T). The marker was then cut from the membrane and treated separately. To prevent unspecific binding of antibodies, membrane and marker were then

incubated for an hour in 5% BSA/nonfat dry milk powder (Bio-Rad) in TBS-T. The membrane was then incubated overnight at 4 °C on a shaker in a 50 mL reaction tube containing primary antibody solution (see table 5 for western blot antibodies). Thereafter, the membrane was washed three times 10 min each in TBS-T. Secondary antibody (see table 5) was added and the membrane was incubated or 1 hour at room temperature on a shaker. Meanwhile StrepTactin® HRP diluted 1:10000 in TBS-T was applied to the marker and incubated for 1 hour. The membrane was then washed again three times as described previously. For visualization electrochemiluminescence solution was prepared from 3 ml 0.00025% Luminol in 0.1M Tris/HCl and 30µl 0.0011% para-hydroxy coumaric acid in dimethyl sulfoxide (DMSO) and applied to the membrane. The Molecular Imager® Versa Doc™ MP Imaging System was using to detect the protein bands and ImageLab 2.0 Software was used for quantification.

2.2.11. Enzyme linked immunosorbent assay (ELISA)

128 well high binding plates were coated with 100 µl primary antibody (see table 6) per well the day before measurement and incubated at 4 °C. For IL-2 ELISA 6 µl/ml diluted in 100µl BD coating buffer was used while IFNγ was diluted 1:120 in PBS. Plates were washed 4 times with 200µl 0,5%Tween/PBS per well and blocked for 1 and 2 hours at room temperature using 200µl per well of BD or BL blocking solution. Plates were washed and 200µl cell culture supernatant was filled in the wells.

Standard was applied according to standard dilution protocols with increasing concentration. After 2 hours of incubation at room temperature plates were washed and secondary antibody (see table 6) was diluted in BD diluent according to the manufacturers instruction and applied. Following incubation and washing, 100µl streptavidin-horseradish peroxidase (IL-2 1:200, IFNγ 1:40) was applied and plates were incubated for 30 minutes and washed. Finally, 100µl tetramethylbenzidine substrate (Beckton Dickinson) was applied and plates were incubated in the dark for 5-30 minutes. Measurement was conducted at 450 nm to 570 nm.

2.2.12. RNA isolation and transcription to cDNA

For isolation of RNA from liver tissue or T cells a NucleoSpin RNA II Kit® was used. Whole liver tissue was put in 2 ml Eppendorf rection tubes and metal beads as well as lysis buffer consisting of 3,5µl mercaptoethanol and 350µl RA1 buffer per reaction tube was added.

Tissue was fragmented using a TissueLyser II® for 2 min at 30 Hz. Samples were then filtered into 1.5 ml collection tubes using a NucleoSpin® filter and centrifuged 1min at 11000 x g. Next, 350µl of 70% ethanol were added mixed using a Vortexer. Samples were then loaded on NucleoSpin® RNA columns and centrifuged at 11000 x g for 30sek at room temperature. 350 µl membrane dissolving buffer (MDB) were added and probes were centrifuged again at 11000 x g for 1 min. RNA concentration of samples was measured using a spectrophotometer NanoDrop ND-1000.

To eliminate DNA contamination a DNA-free™ kit (Invitrogen) was used according to the manufacturer's instructions. For samples containing 1-200µg/mL RNA the routine procedure was chosen. Per sample of 50µl 0,1 Vol. 10x DNase I buffer were added, and samples were carefully vortexed. Then, 0,5µl rDNase I was added, and samples incubated in a MyCycler™ thermal cycler at 37°C for 30 minutes. This step was repeated once. Next 0,1 Vol. of DNase inactivation reagent were added, and samples were incubated at RT for 2 min while carefully being vortexed twice in between. Lastly, samples were centrifuged at 10000 x g for 90 second and the supernatant was carefully transferred to a new 1,5 ml reaction tube, while leaving the pellet untouched. Afterwards, RNA concentration was measured again. In case of concentrations above 500 µl/ml samples were diluted to concentrations between 200 and 300 µl/ml. Samples were stored at -80 °C until being used.

For cDNA synthesis the ABGENE kit and a the MyCycler™ system were used. RNA samples were diluted to a concentration of 1µg/µl. Then 1µl RNA sample was mixed with 1µl of anchored oligo-dT nucleotides and made up to a total of 11µl with RNase free water. The mix was resuspended and kept in a thermal cycler at 70 ° C for 10minutes. Samples were then stored on ice before being processed further. A mastermix of 4µl 5x cDNA buffer, 2µl deoxynucleotide triphosphates (dNTP) mix, 1µl reverse transcriptase enhancer and 1 µl verso enzyme per sample was produced. Of this mastermix 8µl were added to each tube. Lastly tubes were kept in the thermal cycler for an additional hour at 42 °C and 5 min at 95 °C. Samples were stored at -20 °C until being used or at 4°C for immediate analysis.

2.2.13. Quantitative real-time PCR

cDNA produced as described in 3.2.11 was diluted 1:10 in RNase free H_2O. Next, 9 µl of master mix per sample was prepared by mixing 5µl Maxima™ SYBR Green qPCR, 0,7 µl of each primer and 2,6µl RNase free H_2O. 9 µl were transferred to each well of a 96-well plate and 1 µl of each cDNA sample was added.

To exclude plate contamination H_2O was used as a control. Before analysis the plate was sealed and centrifuged at 1000 x g and 4 ° C for 30 seconds. The running conditions of the CFX 96 Real-Time System were adjusted to primer sets listed in Table 8. mRNA data are demonstrated using the ΔΔCT method.

2.2.14. Flow cytometry and fluorescence activated cell sorting (FACS)

To identify subpopulations and certain characteristics of T cells and hepatic non-parenchymal cells (NPCs) flow cytometric analysis was performed. $CD4^+$ T cells as well as hepatic NPCs were stained and analyzed according to standard protocols. Gates were set using unstained controls and in some cases fluorescence minus one (FMO) samples. For each panel compensation controls were used. Samples were measured using a LSR Canto II and a LSR Fortessa™ flow cytometer and BD FACSDiva™ software for data collection. Files were analysed using FlowJoTM software.

Staining and analysis of $CD4^+$ T cells

$CD4^+$ T cells were cultured and stimulated as described in 3.2.1. and transferred to FACS tubes. In case cells were co-cultured with hepatocytes 30µm filters were used to collect the latter ones. Next, they were centrifuged for 5 min at 500 x g and supernatants were collected for ELISA. Cells were washed twice in PBS and centrifuged for 5 min at 500 x g and 4 °C. Cells were then pre-treated for 20 minutes with an anti-CD16/32 antibody to block unspecific F_c receptor binding. Cells were washed in FACS buffer as described previously and incubated for 30 minutes at 4 °C in the dark with an antibody mastermix (for antibodies and panels used see Table 7). Cells were washed again, and fixation was performed by adding 200µl FixPerm (Fixation/Permeabilization Concentrate in Permeabilization Diluent, 1:4) from a Foxp3 Transcription Factor Staining Buffer Kit (eBioscience™) per sample and incubating samples for 35 minutes dark at 4 °C. Cells were centrifuged and supernatant was discarded and washed twice using 200µl PermWash (Permeabilization Buffer, 1:10 in Milli-Q® ultrapure H2O) each. Next, cells were incubated with antibody mastermix for intracellular staining and incubated for 30 min at 4 ° C in the dark and washed twice as described in PermWash. Until FACS analysis, cells were stored in 150µl FACS buffer dark at 4°C. Whenever stored cells were covered with Parafilm M®.

Flow cytometric data were processed using FlowJo software and gating was performed as demonstrated in Figure 4. Cells were first analysed for cell size (FSC-A) and granularity (SSC-A). Aggregates were excluded and single cells were included by analysing further for

height (FSC-H) against size (FSC-A). Next, dead cells were excluded by gating for viability dye. Subsequently, gating for $CD4^+$ T cells was performed ($CD4^+$). Within the $CD4^+$ T cells $CD25^+$ were gated and considered activated T effector cells. Th1 and Th17 cells were identified by their respective master transcription factors Tbet and RORγT.
Additionally, within the $CD4^+$ population $CD25^{high}$ cells were gated, and $FoxP3^+$ T regulatory cells were identified within this group.
The identified T regulatory cell, T cells, Th1 cells and Th17 cells were then analysed for their expression of ectonucleotidases (CD73 and CD39), PD-1, Ki67, Bcl-2, Bcl-6 and IFNγ.

Staining and analysis of hepatic NPCs

Following isolation of liver NPCs cells were transferred to FACS tubes, centrifuged at 500 xg and 4 ° C for 5 min and resuspended in 500µl FACS buffer. Staining was further performed as described for $CD4^+$ T cells above.
Cells were gated as described prior for size, granularity, single and vital cells. CD4 positive T cells were identified and further gated for their levels of CD25 expression. Additionally, the $FoxP3^+$ population was identified and defined as T regulatory cells and the RORγT positive population as Th17 cells respectively. Within $CD4^+$ T cells and $FoxP3^+$ T regulatory cells the expression of CD39 and CD73 was analysed.

Fluorescence activated cell sorting of $CD4^+$ CD25high cells

To obtain T regulatory cells for suppression assays fluorescence activated cell sorting for $CD4^+$ CD25high cells was performed. $CD4^+$ T cells from cell culture were stained with an antibody cocktail including anti-CD4 and anti-CD25 antibodies by first washing the cells, then incubating them with antibody cocktail and washing again in FACS buffer. Cells were sorted using a BD FACS Aria™ III. Cells were gated as mentioned above for size, granularity, single and vital cells. Then, $CD4^+$ cells were identified and $CD25^{hi}$ cells were sorted (see Figure 6). Sorted cells were collected in RPMI medium and directly used for suppression assays.

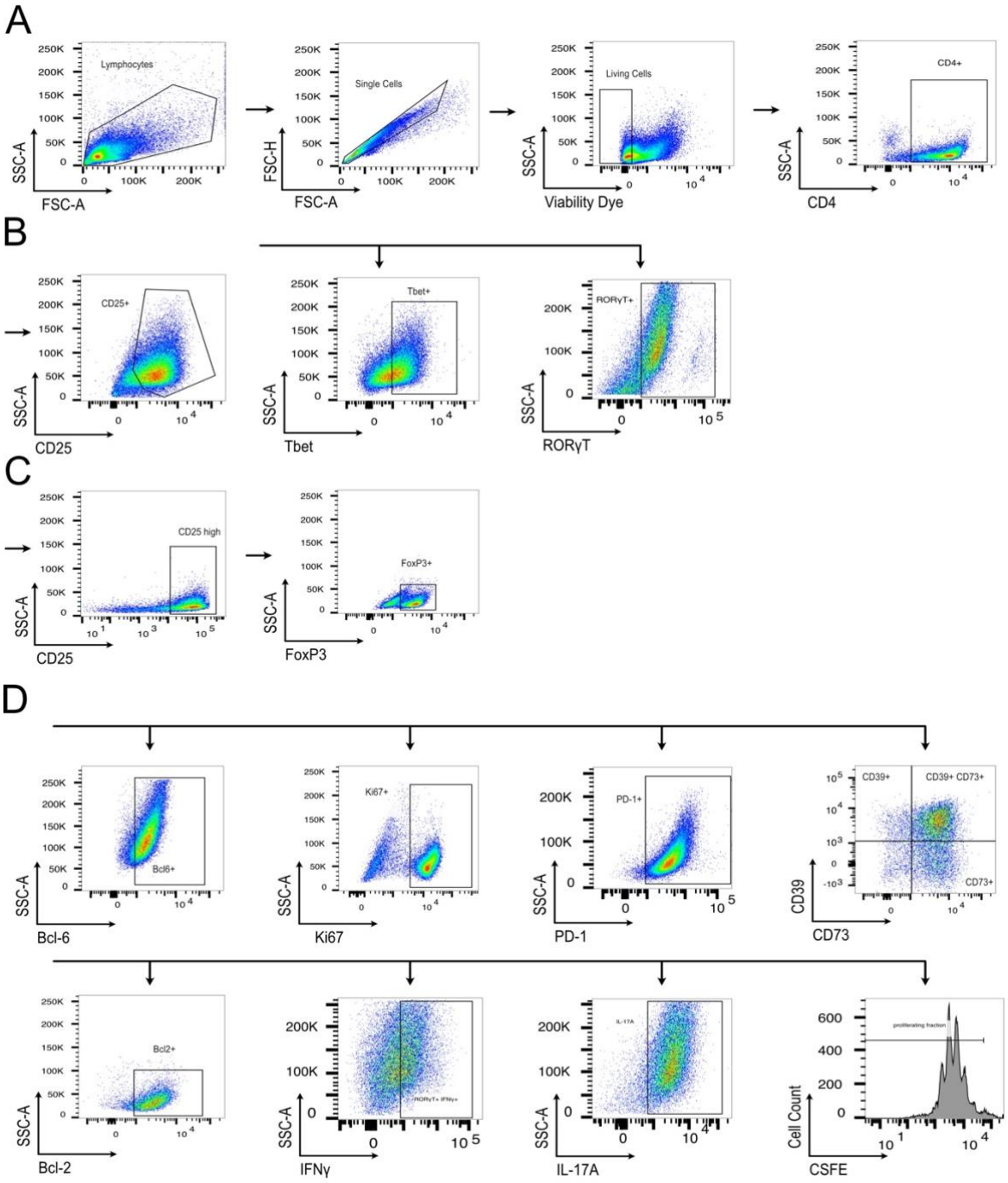

Figure 6: Representative gating strategy for flow cytometric analysis of CD4$^+$ T cell subsets. (A) Gating strategy to identify CD4$^+$ T cells. (B) Gating strategy within the CD4$^+$ subset to identify CD25$^+$ cells and Tbet$^+$ Th1 cells as well as RORγT$^+$ Th17 cells. (C) Gating strategy within the CD4$^+$ subset to identify CD25^{high} FoxP3$^+$ T regulatory cells. (D) Gating strategy to characterize each cell type including CD73, CD39, Ki67, PD-1, IFNγ, Bcl-2 and Bcl-6 expression.

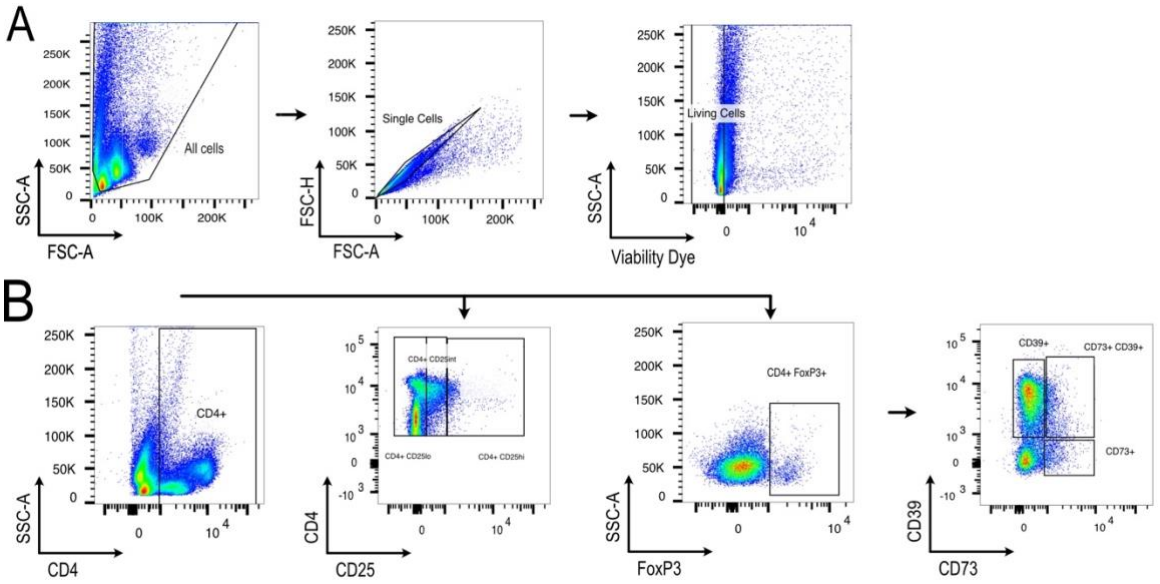

Figure 7: Gating strategy for flow cytometric analysis of liver CD4$^+$ cells (from NPCs) (A) Gating strategy to identify all living liver NPCs. (B) Gating strategy within the subset of living cells to identify CD4$^+$ cells, among them subsets of different CD25 expression and the FoxP3$^+$ cells in the CD25high subset. These were further characterized for the expression of ectonucleotidases CD73 and CD39.

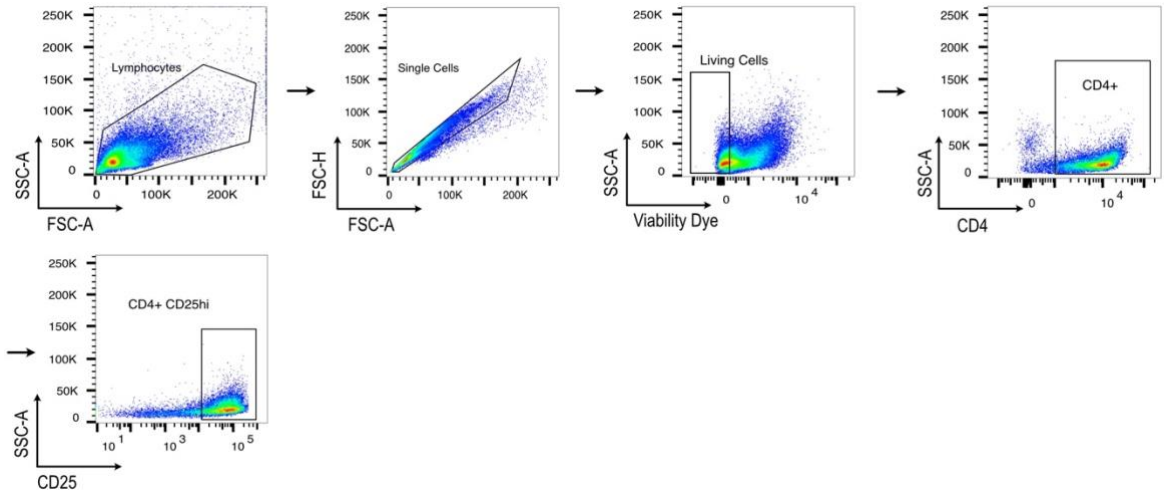

Figure 8: Gating strategy for fluorescent activated cell sorting of T regulatory cells according to CD4 and CD25 expression. Gating strategy of cells polarised under T regulatory cell induction conditions to identify living cells and among them CD4$^+$ cells. Among these CD25h^{igh} cells were sorted and considered to be T regulatory cells.

2.2.15. Metabolic rate assays

To measure the rate at which T cells perform glycolysis Agilent Seahorse glycolytic rate assays were conducted. It gives information about metabolic pathways in cells by real-time proton generation in extracellular fluids. Changes in the extracellular acidification rate (ECAR, mph/min) can be explained for instance by lactate generation after glycolysis.

The assay was performed using polarized $CD4^+$ T cells isolated from mouse spleens and cultured in 24-well plates as described previously. Wave Seahorse Desktop Software was used for template design.

Glycolysis rate assay was used to measure basal glycolytic rate and compensation for inhibition of mitochondrial function which is achieved by adding Rotenon/AA before glycolytic flux is reduced by adding 2-Desoxyglucose. The cartridge for the assay was hydrated one day prior to the assay with 200µl ddH2O per well together with 25mL of calibrant at 37°C.

On the day of the assay, 97 ml XF Medium was warmed to 37°C in a warming bath and 1 ml of 200 mM L-glutamine (final concentration 2mM), 1 ml of glucose solution (1M, 100x) and 1 ml of pyruvate (100mM 100x) were added. Next, the medium was adjusted to a pH value of 7.4 +/- 0,01 using 1 N NaOH if necessary and kept at 37 °C. PH was checked again and the medium sterilized by filtering through a 0,2 µm filter afterwards and kept at 27°C in a water bath. Subsequently the companion plate was prepared by coating with 20 µl poly-D-lysine solution (from 10x stock diluted with ddH_2O) and incubated for 2 hours at 37°C in an incubator. Wells were then washed with water and air-dried.

Cells for analysis were pooled for either genotype or treatment method if necessary and adjusted to $5x10^6$ cells per ml. $2x10^5$ cells were added to each well and the plate was centrifuged at 400 x g for 5 minutes. Next, 140µl of medium were added to each well while not disrupting the monolayer of cells on the bottom of each well.

1 hour prior to the assay cells were incubated in a non-CO_2 incubator at 37 °C. ddH2O was discarded from the cartridge, replaced with 200 µl of pre-equilibrated calibrant and the sensor plate was inserted into the wells with calibrant avoiding the formation of air bubbles. The plate then was incubated for 1 hour in a non-CO_2 incubator at 37 °C.

Rotenone/AA and 2-desoxyglucose were resuspended with assay medium to stock concentrations of 0,5µM and 50mM until dissolved completely and loaded onto the sensor cartridge using port applicator lids provided with the kit.

All ports were inspected for equal loading and the sensor cartridge as well as the utility plate were inserted into the pre-heated Seahorse XFe96 Analyzer for calibration. Next the cell culture microplate was loaded and a pre-designed WAVE template for the glycolytic rate assay was run.

2.2.16. Glucose Uptake Assay

Prior to the assay $CD4^+$ T cell polarization (Th0, Th1, Th17, see 3.2.6) was performed. The Glucose uptake assay was conducted according to the manufacturer's instructions. It shows the 2-NBDG, a fluorescent labeled desoxyglucose analog, which can be depicted by FACS analyses if taken up by cells. As a negative control apigenin, an inhibitor of glucose uptake, is used. Briefly, reagents were prepared according to the instructions, then cells were treated with glucose-free medium. 10 minutes before the end of treatment different doses of 2-NBDG were added in a final concentration of 100µg/ml in glucose free medium. Cells were incubated for 2 hours. At the end of the treatment cells were washed in cell-based assay buffer, then analyzed in 100µl assay buffer using FACS. For analysis a regular gating on living aka positive cells was performed.

2.2.17. Statistical analysis

Data was analysed using GraphPad Prism 9 (GraphPad Software, San Diego, CA, USA). All data is presented as arithmetic mean ± standard error of the mean (SEM). Statistical comparison of two groups was performed using Mann-Whitney test. Comparison of multiple groups were analyzed by a one-way ANOVA. Outliers were identified by using the ROUT method. P values <0.05 were considered statistically significant (*p<0.05, **p<0.01, ***p<0.001, ****p<0.0001).

3. Results

3.1. Validation of a CD4$^+$ T cell specific knockout of PKM2

To ensure a complete knockout of Pyruvate kinase M2 in CD4$^+$ T cells of CD4$^{\Delta PKM2}$ mice, CD4$^+$ T cells were isolated from mouse spleens and a western blot for PKM2 was performed from protein lysates. While PKM2 was detectable in CD4cre cells, it was not detectable in CD4$^{\Delta PKM2}$ cells, indicating the absence of PKM2 protein in these cells. To confirm the result, a western blot for actin was performed on the identical material, showing comparable amounts of actin protein in both CD4^{cre} and CD4$^{\Delta PKM2}$ cells (Figure 8).

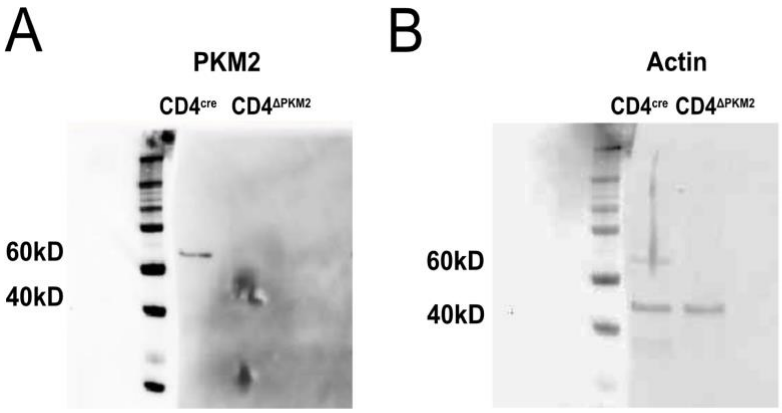

Figure 9: PKM2 knockout in CD4$^+$ T cells. (A) PKM2 western blot in CD4^{cre} and CD4$^{\Delta PKM2}$ cells. (B) Western blot for actin in CD4^{cre} and CD4$^{\Delta PKM2}$ cells on the same membrane.

3.2. Liver damage in Concanavalin A mediated hepatitis persists in CD4$^{\Delta PKM2}$ mice.

Mice with deletion of PKM2 in CD4$^+$ T cells (CD4$^{\Delta PKM2}$ mice) received a dose of 5-7 mg/kg Concanavalin A and were sacrificed after 2,5 or 24 hours*. Concanavalin A is known to lead to Th1 cell activation resulting in cellular damage in hepatocytes. In H.E. stainings of liver tissue comparable amounts of necrotic areas* of 10-60 % as well as lymphocyte invasion from the blood vessels have been detected in CD4^{cre} as well as CD4$^{\Delta PKM2}$ mice. PBS controls neither showed lymphocyte invasion nor necrotic areas within livers. Therefore, infiltration with lymphocytes persist in CD4$^{\Delta PKM2}$ mice. In addition, CD4$^{\Delta PKM2}$ mice showed a higher elevation of liver transaminases (ALT) and were hypersensible, showing higher lethality (Figure 9).

To examine further markers of inflammatory regulators, quantitative real-time PCR of whole liver tissue of Concanavalin A treated mice was conducted. Expression of HIF1α was higher 2,5 hours after Concanavalin A injection in both genotypes compared to PBS injection in CD4$^{\Delta PKM2}$ mice. Yet, no significant difference could be observed between CD4^{cre} and CD4$^{\Delta PKM2}$ mice challenged to Concanavalin A. In CD4^{cre} mice no HIF1α m RNA was

* Concanavalin A experiments were conducted by A. K. Horst (Institute of Experimental Immunology and Hepatology, Hamburg)
* Quantification of the necrotic area was conducted by S. Weidemann (Institute of Pathology, Hamburg)

detectable after PBS injection, yet higher amounts were expressed in both $CD4^{cre}$ (p=0,0022) and $CD4^{\Delta PKM2}$ (p=0,0012) mice after Concanavalin A challenge. No significant difference was detected within these groups. Similarly, IFNγ mRNA was expressed in very little amounts in whole liver tissue of mice receiving PBS treatment, while 2,5 hours after Concanavalin A treatment $CD4^{\Delta PKM2}$ mice had significantly lower levels of IFNγ mRNA than $CD4^{cre}$ mice (p=0,0426). On the contrary, IL-18 mRNA expression was significantly higher in $CD4^{\Delta PKM2}$ mice 2,5 hours after Concanavalin A challenge (p=0.0238). No expression of IL-18 mRNA could be detected in mice receiving PBS (Figure 10).

To assess whether other immune cell lines than $CD4^+$ T cells may have been influenced, MPO staining of liver sections of Concanavalin A treated mice was performed. There was no significant difference in neutrophil numbers per tissue or necrotic area in $CD4^{\Delta PKM2}$ mice compared to $CD4^{cre}$ mice, suggesting a persistence of invasion of neutrophils during Concanavalin A hepatitis (Figure 10).

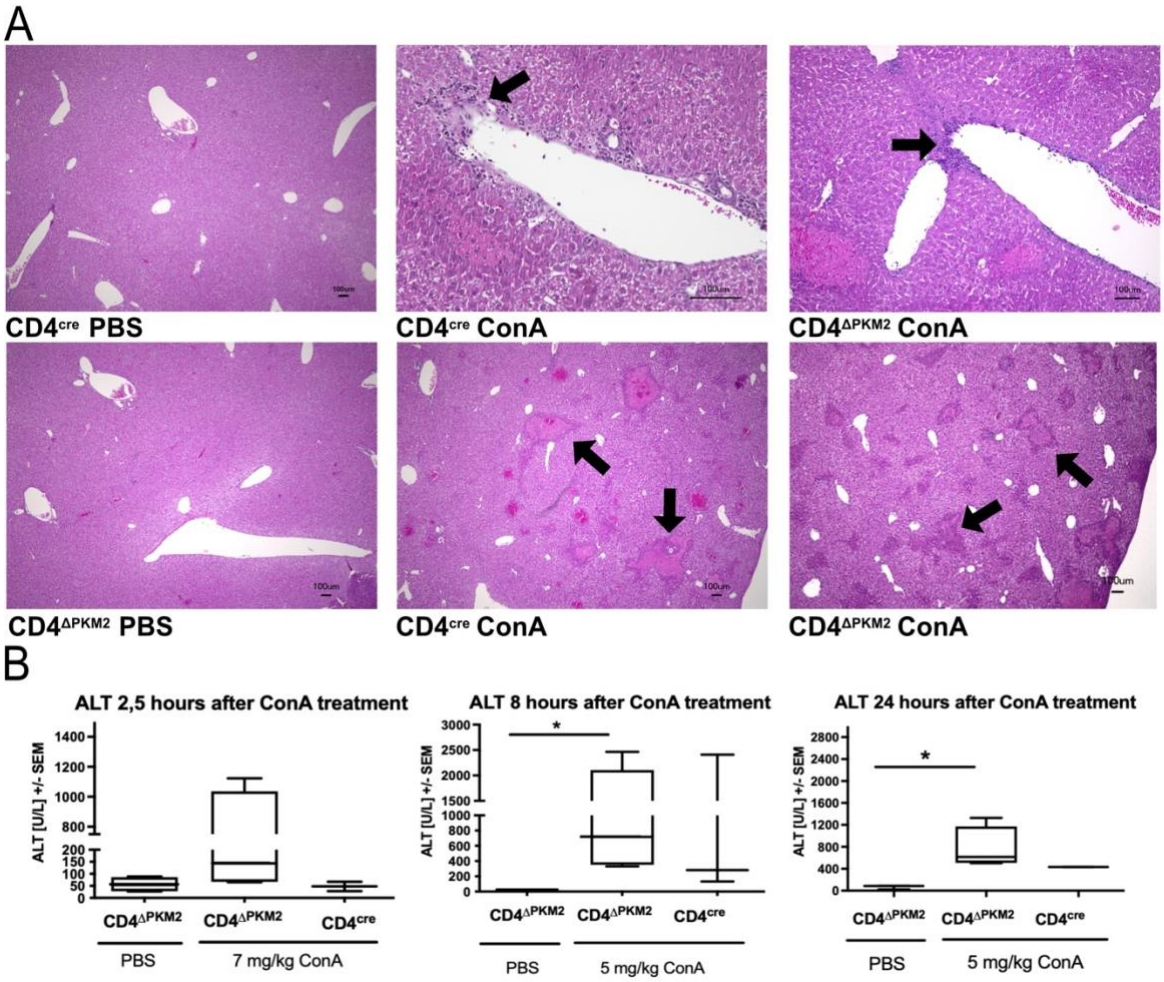

Figure 10: **Liver damage in $CD4^{cre}$ and $CD4^{\Delta PKM2}$ mice after Concanavalin A challenge**. (A) H.E. microscopy of liver tissue obtained from $CD4^{cre}$ and $CD4^{\Delta PKM2}$ mice treated with Concanavalin A (5-7mg/kg) (B) ALT measurements demonstrate elevated ALT in livers of $CD4^{\Delta PKM2}$ mice. (n=3 $CD4^{\Delta PKM2}$ PBS, n=4 $CD4^{\Delta PKM2}$ ConA, n=3 $CD4^{cre}$ ConA)

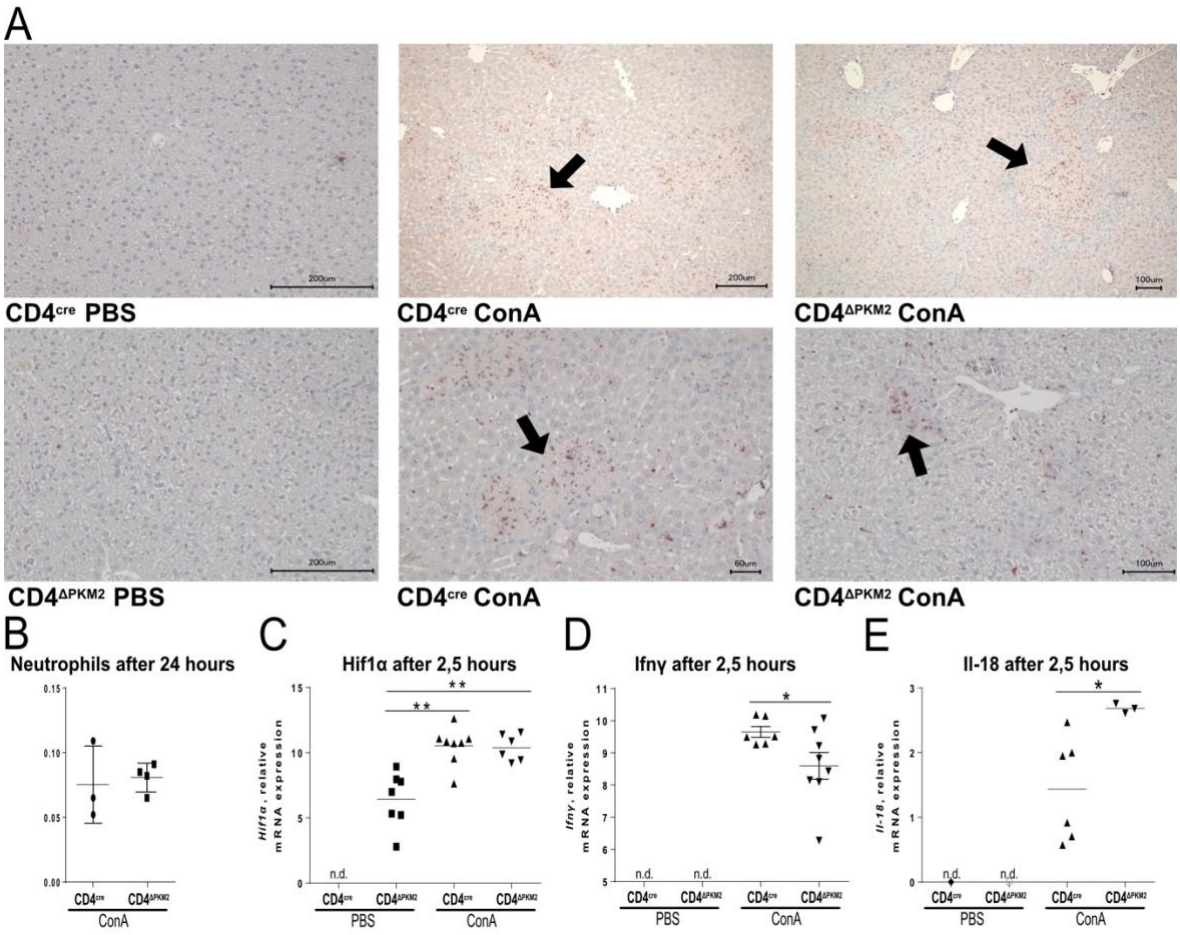

Figure 11: **Inflammation in CD4^{cre} and CD4$^{\Delta PKM2}$ mice after Concanavalin A challenge** (A) MPO staining of livers of mice challenged to either Concanavalin A or PBS control (B) Quantifications of neutrophils from the MPO staining (C) rtPCR for HIF1α expression (D) rtPCR for IFNγ expression (E) rtPCR for IL-18 expression. (n=3 CD4$^{\Delta PKM2}$ PBS, n=4 CD4$^{\Delta PKM2}$ ConA, n=3 CD4^{cre} ConA)

3.3. CD4$^{\Delta PKM2}$ mice show an altered composition of CD4^{+} T cells within the liver.

To better understand the effects of the Concanavalin A challenge to CD4$^{\Delta PKM2}$ mice and whether a CD4^{+} T cell specific knockout of PKM2 may influence other immune cell subsets, the immune cell composition within the livers of CD4$^{\Delta PKM2}$ and CD4^{cre} mice were assessed. Therefore, liver NPCs were isolated* and analyzed using flow cytometry.

Both genotypes had about similar numbers of CD4^{+} T cells. Within the CD4^{+} T cells subset the amount of CD25 high and intermediate cells appeared reduced, although not significantly (p=0,1) in CD4$^{\Delta PKM2}$ cells. Compared to CD4^{cre} cells CD4^{+} T cells had more FoxP3 positive cells, yet not significantly. CD4$^{\Delta PKM2}$ T cells were further characterised by altered expression of CD39 (p=0.4) and significantly reduced CD73 (p=0,038). These results indicate that a CD4^{+} T cell specific knock out of PKM2 may affect immune cell composition in the liver with special regard to CD4^{+} T regulatory cells (Figure 11).

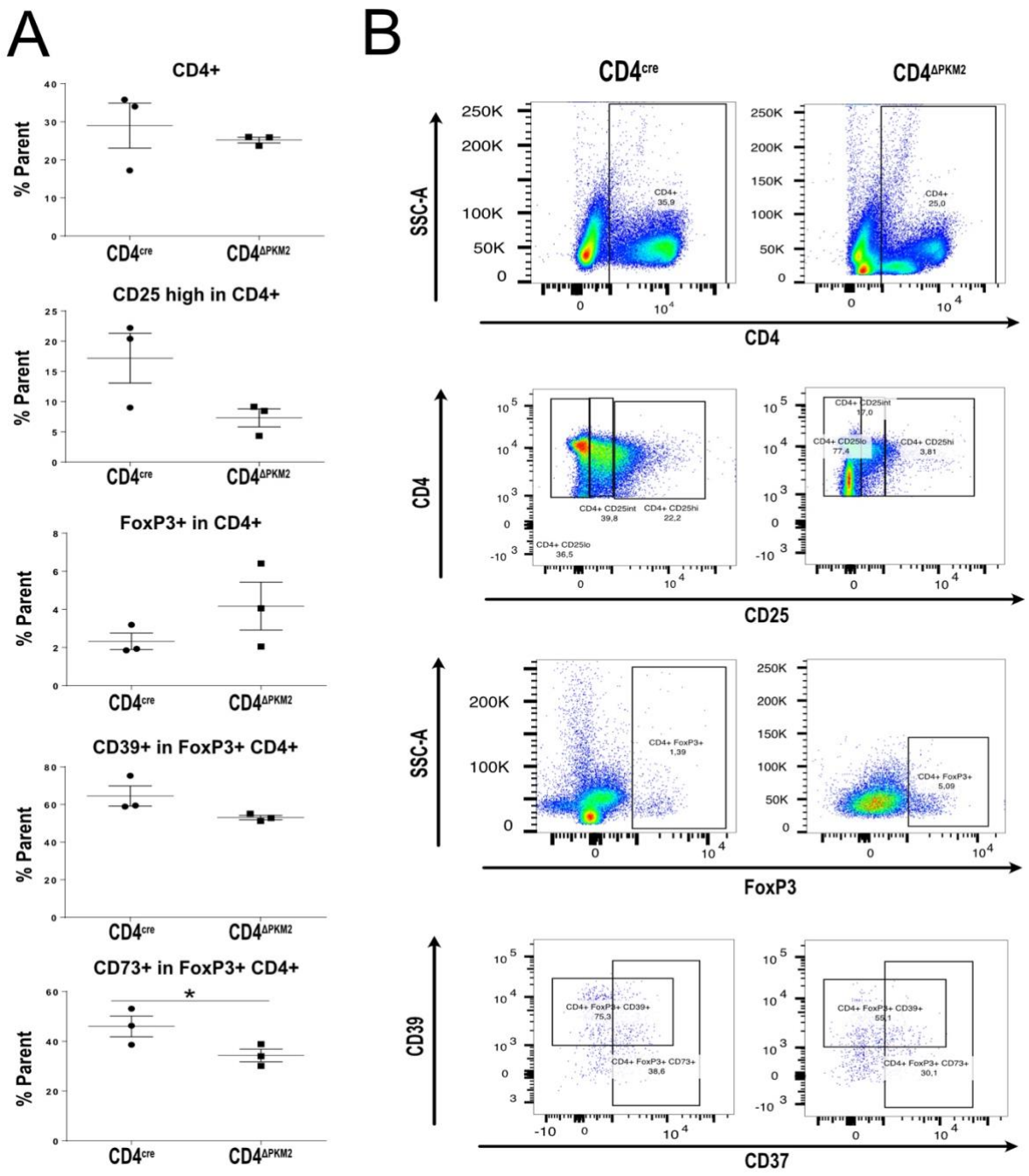

Figure 12: Immune cell composition in livers of CD4$^{\Delta PKM2}$ and CD4^{cre} mice. (A) Flow cytometric analysis of CD4$^+$ T cell subsets from liver NPCs of CD4$^{\Delta PKM2}$ and CD4^{cre} mice including CD4$^+$, CD25 high, FoxP3$^+$, CD39$^+$ and CD73$^+$ cells. (B) Respective dotplots in pseudocolor for CD4$^+$, CD25 high, FoxP3$^+$, CD39$^+$ and CD73$^+$ liver NPCs. (n=3 per genotype, replicated 2 times)

3.4. CD4$^{\Delta PKM2}$ T cells are characterized by altered glucose metabolism.

To examine whether PKM2 deletion had an impact on CD4$^+$ T cells overall glucose metabolism, a Seahorse glycolytic rate assay was performed. Cultured CD4$^+$ T cells as well as in vitro polarized Th1 and Th17 cells were used. First, basal metabolic activity consisting of basal glycolysis and mitochondrial activity was measured by proton efflux and indicated as extracellular acidification rate (ECAR). Next, Rotenone and Antimycin A (Rot/AA) were

used to inhibit the mitochondrial electron transport chain, resulting in compensatory glycolysis. Lastly, 2-desoxyglucose (2-DG), a glucose analog, was injected, inhibiting regular hexokinase function by competitive antagonism. A reduction of ECAR down to a minimum is meant to provide evidence for the rise in ECAR being a result of increased glycolytic activity.

ECAR data suggested a higher basal rate of glycolysis in $CD4^{\Delta PKM2}$ T cells as well as Th1 cells compared to $CD4^{cre}$ cells, with a stronger increase of ECAR upon Rotenon/AA and subsequently a stronger decrease of glycolytic activity upon 2-DG injection in $CD4^{\Delta PKM2}$ cells. To the contrary, in Th17 cells higher basal glycolytic was detected in $CD4^{cre}$ cells, followed by a comparable rise in glycolytic activity upon Rotenon/AA injection and a decrease of glycolytic activity upon 2-DG injection. Thereby, $CD4^{\Delta PKM2}$ are hypoglycolytic in comparison (Figure 12).

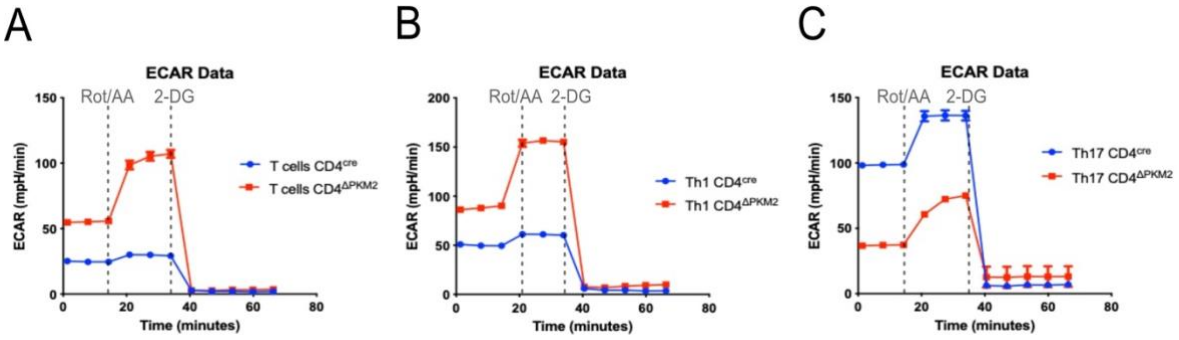

Figure 13: Detailed glycolytic rates of $CD4^{\Delta PKM2}$ and $CD4^{cre}$ T cells, Th1 and Th17 cells. (A) Glycolysis rate assay of CD4+ T cells (B) Glycolysis rate assay of Th1 cells (C) Glycolysis rate assay of Th17 cells (n=3 per genotype. Exemplary data chosen from 3 identical experiments with comparable outcomes.)

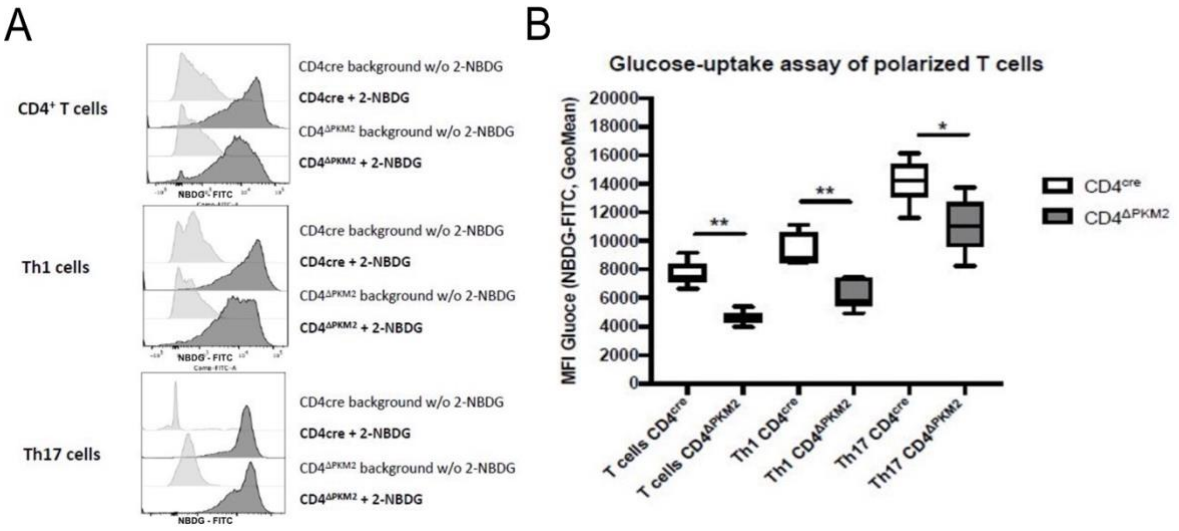

Figure 14: **Uptake of 2-NBD Glucose by $CD4^{\Delta PKM2}$ and $CD4^{cre}$ T cells, Th1 and Th17 cells.** (A) Uptake of 2-NDBG measured by flow cytometry and compared to background controls without 2-NDBG. (B) Comparison of mean fluorescent intensities (MFI) of NBDG-FITC fluorophore among $CD4^{cre}$ and $CD4^{\Delta PKM2}$ cells. (n= 3 per genotype)

Further, a glucose uptake assay* of Th1 and Th17 polarized $CD4^{\Delta PKM2}$ and $CD4^{cre}$ T cells was performed to assess the cells capacity for glucose transport into the cell. A significantly reduced uptake of 2- desoxy-1-D-glucose could be detected in all subsets of $CD4^{\Delta PKM2}$ cells (p (T cells) = 0.0022, p (Th1) = 0.0095, p (Th17) = 0.0152, Figure 13).

$CD4^+$ T cells perform basal glycolysis also by PKM1. To examine whether a complete deletion of PKM2 influences PKM1 expression, a western blot of the PKM1 protein was performed (A). $CD4^+$ T cells, Th1 and Th17 cells showed higher amounts of PKM1 protein, while Th17 cells appeared to express more PKM1 protein compered T cells and Th1 cells. Compensatory PKM1 upregulation is further indicated by higher levels of PKM1 mRNA measured in $CD4^{\Delta PKM2}$ Th1 cells.

Additionally, expression of the glycolytic enzyme enolase was assessed. In $CD4^{\Delta PKM2}$ Th1 cells significantly elevated relative mRNA expression of the enolase could be measured compared to $CD4^{cre}$ cells (p= 0,0238). Therefore, a western blot was performed to determine the amount of enolase protein in polarised $CD4^+$ T cells. In $CD4^{\Delta PKM2}$ Th17 cells, having shown lower glycolytic activity than $CD4^{cre}$ cells previously, a western blot for enolase indicated less Enolase protein (Figure 13).

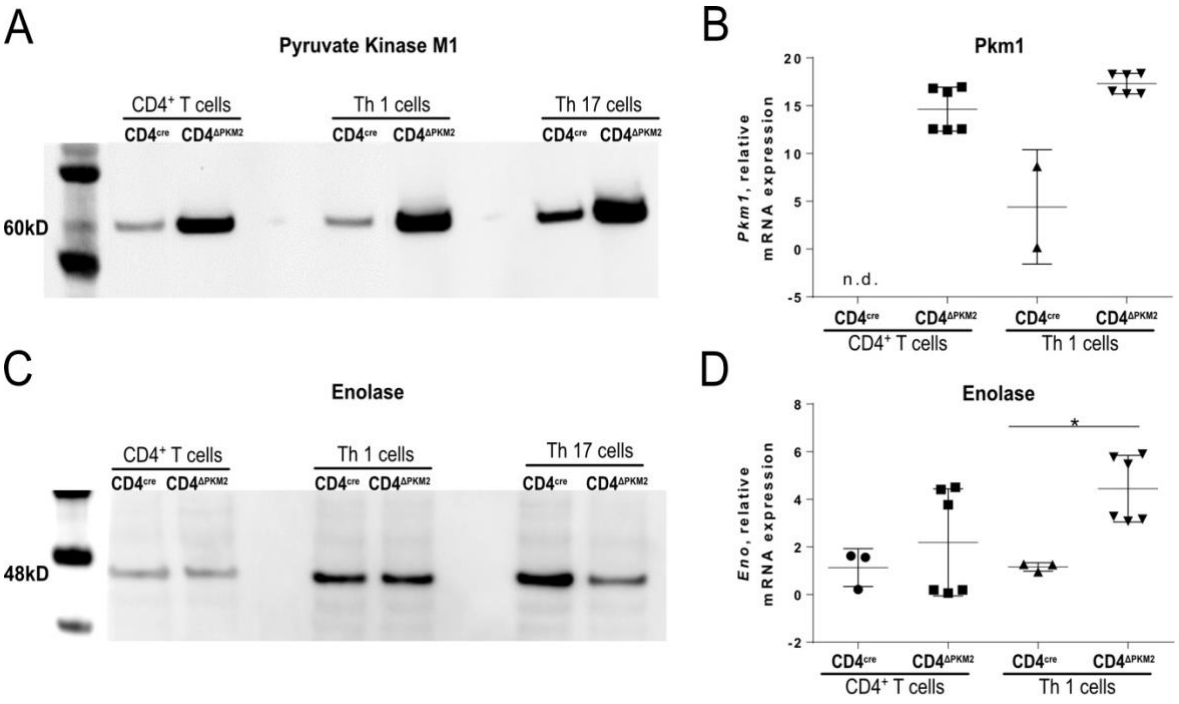

Figure 15: **Expression of glycolytic enzymes in $CD4^{\Delta PKM2}$ and $CD4^{cre}$ T cells, Th1 and Th17 cells.** (A) Western blot for PKM1 protein in polarised $CD4^+$ T cells (B) rtPCR of Pkm1 from $CD4^+$ T and Th1 cells (C) Western blot for Enolase protein in polarised $CD4^+$ T cells (D) rtPCR of enolase from $CD4^+$ T and Th1 cells. (n=3 per genotype)

* Flow cytometric measurement of the glucose uptake assay was conducted by A. K. Horst (Institute of Experimental Immunology and Hepatology, Hamburg)

3.5. CD4$^{\Delta PKM2}$ T cells show reduced IFNγ and IL-2 production

To assess whether an altered glucose metabolism had consequences for CD4^{+} T cell functioning, naïve CD4^{+} T cells were polarized in vitro, and their production of cytokines was measured. Therefore, culture supernatant was analysed for IL-2 and IFNγ using an enzyme linked immunosorbent assay (ELISA).

CD4$^{\Delta PKM2}$ T cells, Th1 as well as Th17 cells all (p= 0,0143) showed significantly reduced concentrations of IFNγ as well as lower levels of IL-2 in cell culture supernatant (p=0,0143).

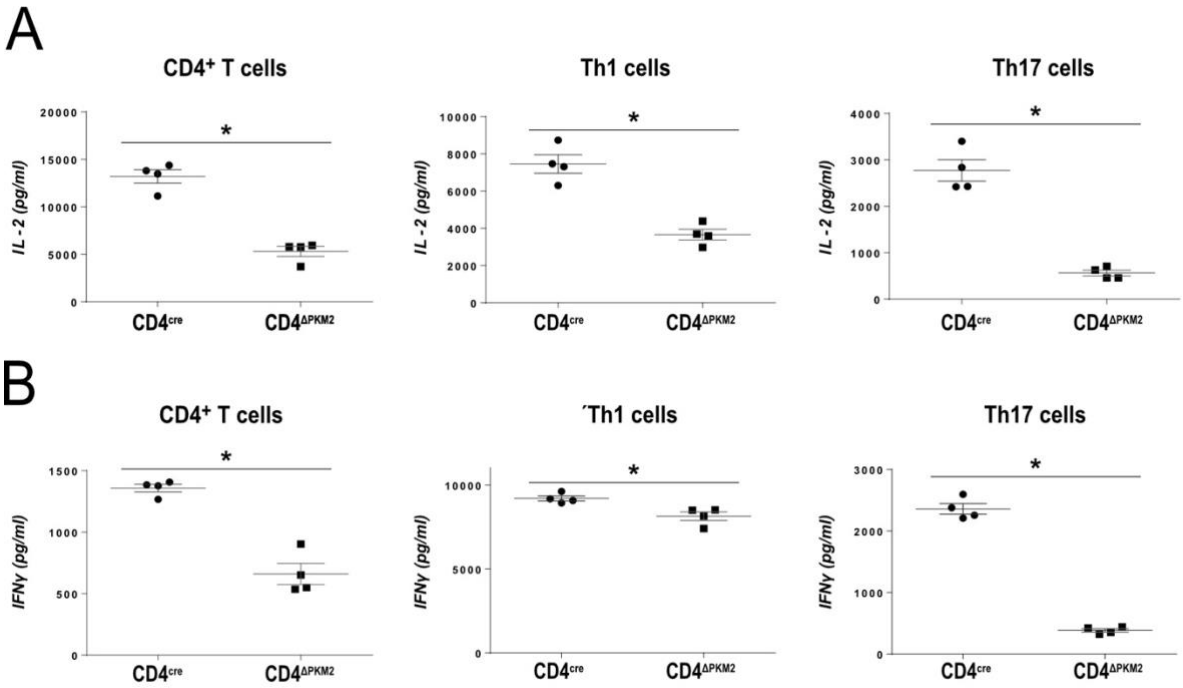

Figure 16: Production of IFNγ and IL-2 in CD4$^{\Delta PKM2}$ and CD4^{cre} T cells, Th1 and Th17 cells. (A) IL-2 in cell culture supernatant determined by ELISA. (B) IFNγ in cell culture supernatant determined by ELISA. (n=4 per genotype, replicated 4 times)

3.6. CD4$^{\Delta PKM2}$ T cells show impaired proliferation.

Glycolysis is known to fuel T cell polarisation and expansion. Naive CD4^{+} T cells were therefore polarized in vitro and stained for CD4, CD25, Tbet, RORγT to evaluate the success of the polarisation as well as for PD-1 and Galectin to examine whether a CD4^{+} T cell specific PKM2 knockout would impair their polarisation and proliferation.

To evaluate the size of a proliferating cell fraction cells were labeled with CSFE*. The proliferating fraction, defined a CSFE dilution <10^{4}, was significantly reduced in CD4$^{\Delta PKM2}$ Th1 and Th17 cells (both p=0,0022).

FACS data of polarised CD4^{+} T cells showed a high fraction of CD25 positive cells, indicating activation. There were no significant differences between genotypes. In Th1

polarised cells a non-significant reduction of Tbet^{+} cells could be observed. CD4$^{\Delta PKM2}$ T cells treated with a cytokine mix to induce Th17 differentiation displayed a significantly reduced number of RORγT^{+} cells (p=0,0143).

Th1 and Th17 cells were characterized as Tbet^{+} or RORγT^{+} cells for further analysis. To evaluate cell death, Galectin 9 was stained. While there were no significant differences between genotypes, a reduction of positive cells in Th1 and especially in Th17 could be observed. Staining of PD-1 revealed reduced expression in CD4$^{\Delta PKM2}$ Th17 cells compared to CD4^{cre} Th17 cells (p=0,0286), while no difference could be observed in other CD4^{+} T cell subsets (Figure 16).

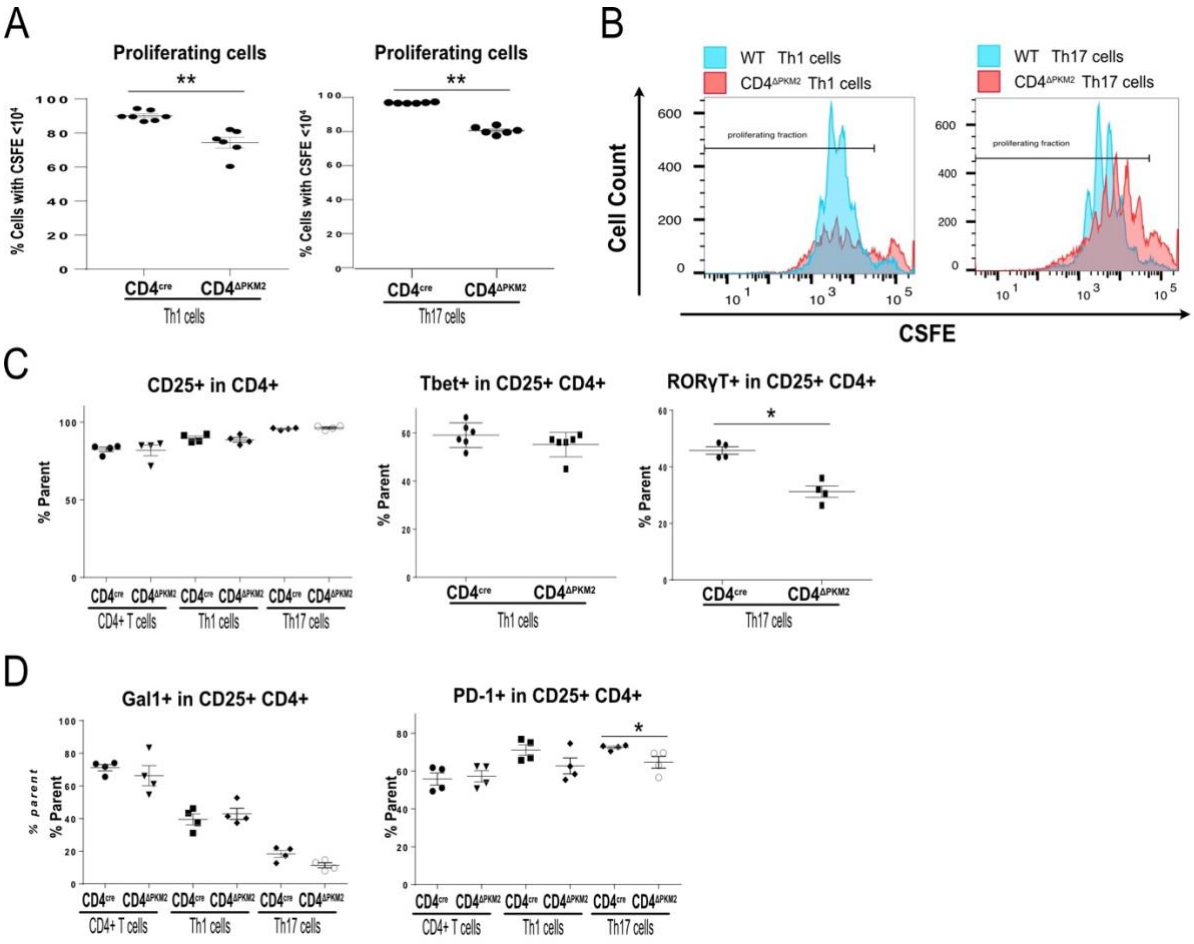

Figure 17: Markers of CD4^{+} T cell proliferation and polarisation in CD4$^{\Delta PKM2}$ and CD4^{cre} T cells, Th1 and Th17 cells. (A) Frequencies of proliferating Th1 and Th17 cells defined as cells with CSFE <10^{4} (B) Representative histograms of CSFE labeled Th1 and Th17 cells (C) Expression of CD25 in CD4^{+}, Th1 and Th17 cells as well as expression of Tbet in Th1 and RORγT in Th17 cells. (D) Expression of cell death markers Galectin 1 and PD-1 in CD4^{+}, Th1 and Th17 cells. (n=3 per genotype)

* Flow cytometric measurement of the CSFE labeled cells was conducted by A. K. Horst (Institute of Experimental Immunology and Hepatology, Hamburg)

3.7. Ectonucleotidase expression of $CD4^{\Delta PKM2}$ T cells

T cells activation and tissue damage in the context of inflammation leads to a rise in ATP levels in the extracellular environment, which has been shown to have proinflammatory effects (Elliott et al. 2009). CD39 and CD73 are ectonucleotidases expressed on the surface of $CD4^+$ T cell subsets and dephosphorylate extracellular ATP to anti-inflammatory adenosine (Bono et al. 2015).

Within the subset of $CD4^+$ $CD25^+$ T cells no significant difference in CD73 or CD39 expression could be observed between $CD4^{\Delta PKM2}$ and $CD4^{cre}$ cells. In $CD4^+$ $CD25^+$ $Tbet^+$ $CD4^{\Delta PKM2}$ Th1 cells the percentage of $CD39^+$ cells were significantly higher from $Tbet^+$ $CD4^{cre}$ Th1 cells (p=0,0076). Additionally, a significant difference in percentage of $CD73^+$ cells was detected, with $CD4^{\Delta PKM2}$ T cells expressing less CD73 than $CD4^{cre}$ cells (p=0,0011). $ROR\gamma T^+$ $CD4^{\Delta PKM2}$ Th17 cells expressed both lower CD73 (p=0,0095) and lower CD39 (p=0,0333) compared to $CD4^{cre}$ cells. These data indicate that a knockout of PKM2 in Th1 and Th17 $CD4^+$ T cells influences their expression of the ectonucleotidases CD39 and CD73 (Figure 17).

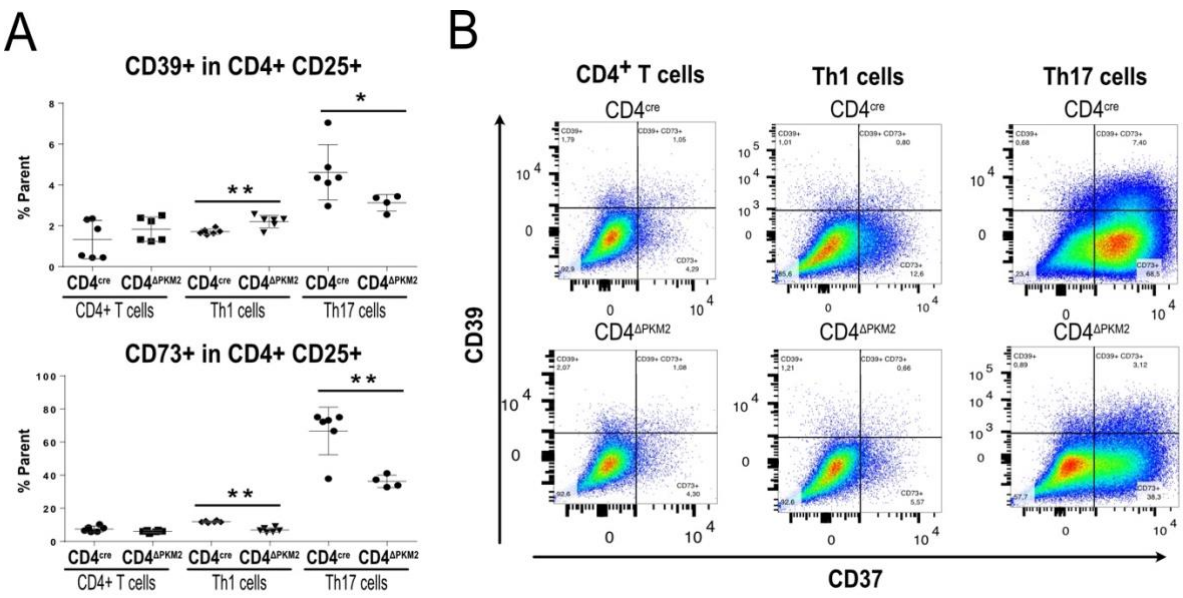

Figures 18: Expression of ectonucleotidases CD39 and CD73 in $CD4^{cre}$ and $CD4^{\Delta PKM2}$ T cells, Th1 and Th17 cells. (A) Frequencies of CD39 and CD73 expression in $CD4^+$ T cells, Th1 and Th17 cells following in vitro differentiation. (B) Representative dot plots of flow cytometric analysis of CD39 and CD73 expression.

3.8. Induction and suppressive ability of CD4$^{\Delta PKM2}$ T regulatory cells

Hepatocytes can induce hepatic Tregs and thereby support immunological tolerance. To see whether Treg induction in the presence of hepatocytes in CD4$^{\Delta PKM2}$ mice is altered, MACS-sorted CD4^{+} T cells from either CD4$^{\Delta PKM2}$ or CD4cre mice were cultivated with hepatocytes and stimulated with TGFβ.

FACS analysis shows a significant increase of FoxP3 positive cells within the population of CD4^{+} CD25 high cells in CD4$^{\Delta PKM2}$ cells (p=0,0022) in co-culture with CD4cre hepatocytes). To examine, whether this effect takes place also in absence of hepatocytes, naïve CD4^{+} T cells were stimulated with TGFβ and cultured over 3 days. Here, FACS analysis did not indicate altered numbers of FoxP3 positive T regulatory cells in CD4$^{\Delta PKM2}$ cells compared to CD4^{cre} T cells. Still, these experiments revealed a higher amount of Bcl-2 positive cells within the subset of FoxP3^{+} T regulatory cells (p=0,0317). Further, a lower percentage of CD4$^{\Delta PKM2}$ T regulatory cells was positive for PD-1 (p=0,0007) and higher expression of pSTAT5 was detected in restimulated CD4$^{\Delta PKM2}$ T regulatory cells (p=0,0079). In conclusion, these data indicate an overall positive effect on T regulatory cell induction characterized by higher numbers of FoxP3 cells and reduced signals of cell death.

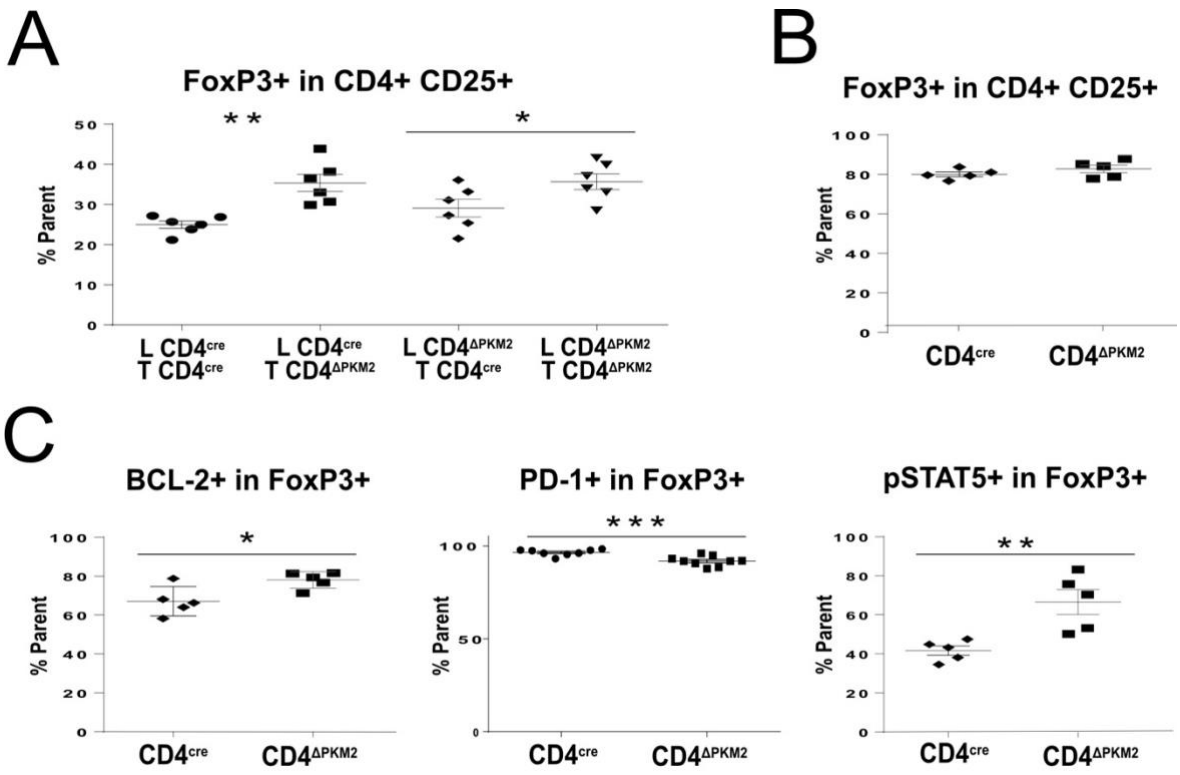

Figure 19: Markers of proliferation from co-culture with hepatocytes and T regulatory cell induction in CD4$^{\Delta PKM2}$ and CD4^{cre} cells. (A) Expression of FoxP3 in CD4^{+} CD25^{high} population from co-culture (B) Expression of FoxP3 in CD4^{+} CD25^{high} population from T regulatory cell induction (C) Expression of cell death markers Bcl-2 and PD-1 and pStat5 in CD4^{+} T regulatory cells. (n=3 per genotype)

The expression of CD39 and CD73 is of special importance to T regulatory cells, as they clear the cellular environment from pro-inflammatory ATP and convert it to anti-inflammatory adenosine (Deaglio et al. 2007). After co-culture with hepatocytes $CD4^{\Delta PKM2}$ T regulatory cells expressed significantly less CD73 (p=0,0011). Data from regular T regulatory cell induction in the absence of hepatocytes confirmed a significant decline in CD73 (p<0,0001) expression as well as CD39 (p=0,0003) expression in $CD4^{\Delta PKM2}$ T regulatory cells. These data indicate a reduced capacity of $CD4^{\Delta PKM2}$ T regulatory cells to produce anti-inflammatory adenosine at the site of inflammation.

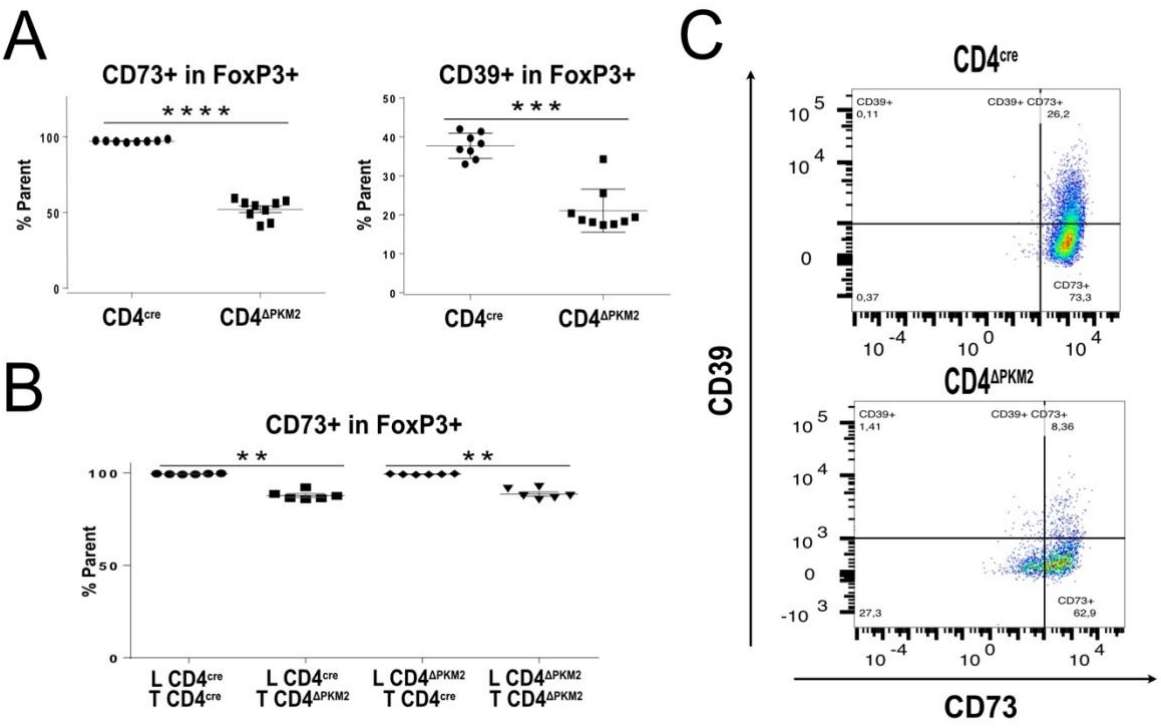

Figure 20: Expression of ectonucleotidases CD39 and CD73 in $CD4^{cre}$ and $CD4^{\Delta PKM2}$ by $CD4^+$ regulatory cells. (A) Frequencies of ectonucleotidase expression from $CD4^+$ T cell culture. (B) Frequencies of CD73 expression from co-culture of hepatocytes and $CD4^+$ T cells (C) Representative dot plots from $CD4^+$ T cell culture. (N=3 per genotype, both setups replicated twice)

T cells rely on IL-2 to be activated, yet they don't produce it themselves. An ELISA showed significantly less IL-2 in supernatant in $CD4^{\Delta PKM2}$ cells cultured with hepatocytes compared to $CD4^{cre}$ cells (p=0,004).

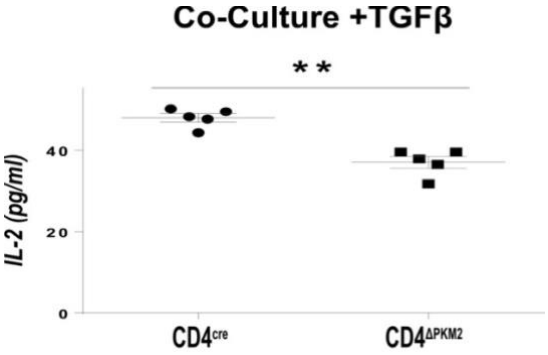

Figure 21: IL-2 Production in T cell hepatocyte co-culture. IL-2 ELISA of cell culture supernatant from co-cultures of hepatocytes (L) and $CD4^+$ T cells (T) with TGFβ.

Furthermore, a suppression assay was performed to better understand the suppressive ability of $CD4^{\Delta PKM2}$ T regulatory cells. Suppression was measured by using CFSE labeled wildtype $CD4^+$ T cells. During the process of cell division, the individual cells CSFE count is reduced by half per cell division. Thereby a high number of cells with low concentration of CSFE indicates that these cells have undergone several cell divisions. PKM2 knockout $CD4^+$ T cells appear to have slightly better suppressive ability when combined with wildtype CSFE labeled T cells in a 1:1 ratio. In all other ratios suppressive ability measured by the amount of CSFE in WT $CD4^+$ T cells was not significantly different.

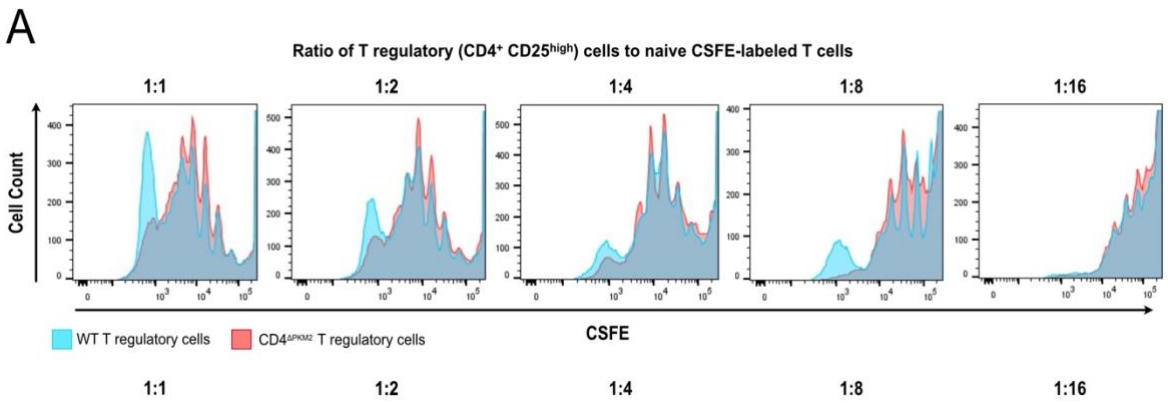

Figure 22: Suppression assay (A) Cell count of CSFE labeled naïve CD4+ T cells after cell culture with either $CD4^{cre}$ or $CD4^{\Delta PKM2}$ cells in ratios of 1:1 to 1:16.

3.9. Pharmacological targeting of PKM2 activity by Tepp 46 and Shikonin

To examine whether PKM2 can be modulated pharmacologically, the effect of TEPP-46 and Shikonin were tested in vitro. The small molecule activator TEPP-46 stabilizes the PKM2 tetramer and thereby enhances the enzymatic activity of PKM2 (Jiang et al. 2010, Boxer et al. 2010, Anastasiou et al. 2012). Shikonin, a plant derived naphthoquinone, acts as a general inhibitor of PKM2 (Chen et al. 2012).

3.9.1. Effects of Tepp 46 and Shikonin on $CD4^+$ T cell proliferation

$CD4^+$ T cells were isolated from spleens of C57/BL6 mice and polarized in vitro while treated with either TEPP-46, Shikonin or a DMSO control. They were then stained for flow cytometric analysis to examine the effects of modifying PKM2 activity on proliferation and differentiation. In $CD4^+$ T cells as well as Th17 cells treated with TEPP46 a significantly smaller number of cells was CD25 positive compared to DMSP treatment (both p=0,0011), while in Th1 cells no significant difference in treatments was observed. $CD4^+$ $CD25^+$ Th17 cells treated with Shikonin also were significantly reduced (p=0,0011). Expanded T cells, Th1 and Th17 cells treated with TEPP-46 further had a tendency of showing smaller percentages of cells positive for the proliferation marker Ki67. Cells treated with Shikonin did not show differences in Ki67 expression. In wildtype Th1 cells TEPP46 further lead to a significant reduction in $Tbet^+$ cells, in wildtype Th17 cells treated with TEPP-46 showed significantly lower numbers of $ROR\gamma T^+$ cells, respectively. Additionally, TEPP-46 lead to a reduced number of Bcl-6 positive cells (p=0,0011). A reduced effect was observed for Shikonin (p=0,0206). Hence the strong effect of TEPP-46 on $CD4^+$ T cell proliferation, $CD4^{\Delta PKM2}$ T cells were treated with TEPP to investigate the specificity of TEPP-46 and evaluate possible cell toxicity. No significant effects of TEPP-46 on Tbet and RORγT expression could be observed in $CD4^{\Delta PKM2}$ T cells. Taken together, while Shikonin appears to have little effect in $CD4^+$ T cells proliferation, TEPP-46 strongly affects proliferation and differentiation (Figure 21).

Again, ectonucleotidase expression was assessed in Th1 as well as Th17 cells treated with TEPP-46 or Shikonin. While Shikonin did not lead to changes in CD39 expression, TEPP-46 resulted in a significant increase in CD39 positive Th1 and Th17 cells (both p=0,0011). In Th1 Shikonin resulted with a significant increase of CD39 in Th1 cell (p=0,0325), while no effect could be observed in Th17 cells. In Th1 cells an increase in CD73 positive cells

was observed upon TEPP-46 application (p=0,0022). Contrarily, TEPP-46 resulted in a significant reduction of CD73 positive cells in Th17 cells (p=0,0011) (Figure 22).

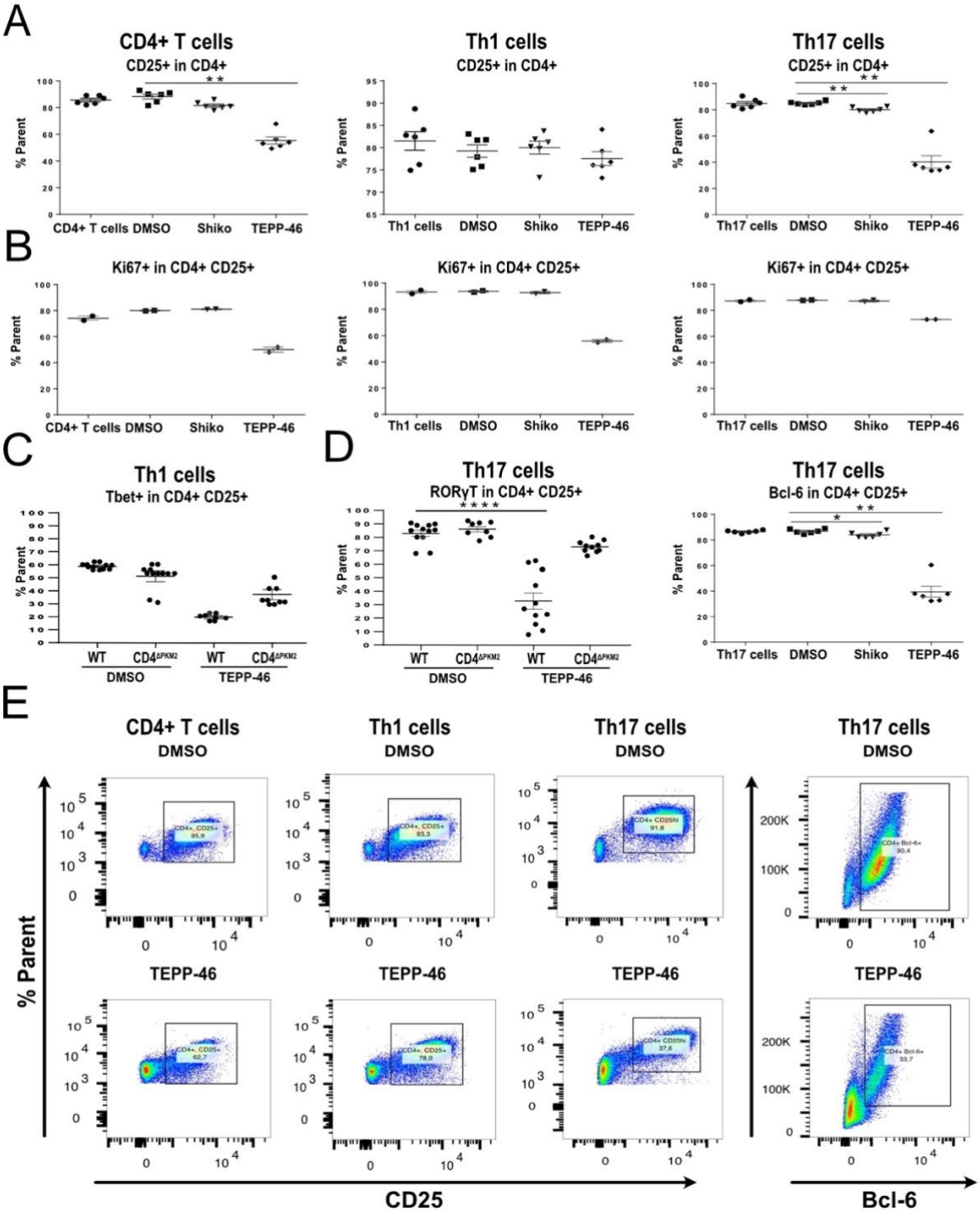

Figure 23: Proliferation of CD4^{+} T cells, Th1 and Th17 cells under the influence of Tepp 46 and Shikonin. (A) Expression of CD25 in CD4 positive cells measured by flow cytometry. (B) Expression of Ki67 in CD4 CD25 positive cells measured by flow cytometry (C) Tbet in CD4 CD25 positive cells from in vitro Th1polarisation of WT or CD4$^{\Delta PKM2}$ under the influence of TEPP-46 and DMSO. (D) RORγT in CD4 CD25 positive cells from in vitro Th17 polarisation of WT or CD4$^{\Delta PKM2}$ under the influence of TEPP-46 and DMSO. (E) Representative dotplots of CD25 expression in CD4^{+} T cells, Th1 and Th17 cells and Bcl-6 expression in Th17 cells.

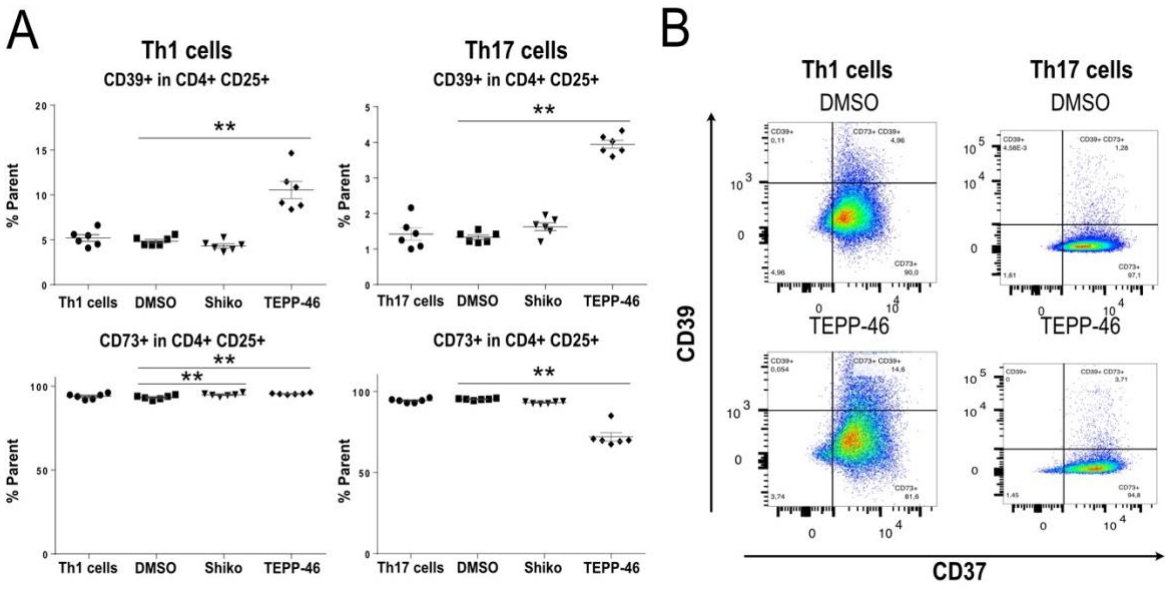

Figure 24: Ectonucleotidase expression of CD4⁺ T cells, Th1 and Th17 cells under the influence of Tepp 46 and Shikonin. (A) Frequencies of CD39 and CD73 expression in CD4⁺ Th1 and Th17 cells following in vitro differentiation. (B) Representative dot plots of flow cytometric analysis of CD39 and CD73 expression under the influence of either DMSO or TEPP-46.

3.9.2. Effects of Tepp 46 and Shikonin on cytokine production of CD4⁺ T cells

To further investigate the influence of TEPP-46 and Shikonin on the functioning of different CD4⁺ T cell subsets, ELISAs for IL-2 as well as IFNγ were performed.

In CD4⁺ T and Th1 cells TEPP-46 lead to reduced concentration of IL-2 in cell culture supernatant compared to DMSO treated cells and controls (p=0,0227 and p=0,0286). There was no significant reduction of IL-2 in culture supernatant of cells treated with Shikonin. In CD4⁺ Th17 cells TEPP-46 did not affect IL-2 production. Yet, reduced levels of IFNγ could be observed on Th17 cells treated with TEPP-46 (p=0,0225) as well as Shikonin (p=0,0173). Again, also $CD4^{\Delta PKM2}$ Th1 and Th17 cells were treated with TEPP-46 and the effects were compared to the treatment of wildtype cells. An ELISA did not show any reduction of IL-2 mediated by TEPP-46 in $CD4^{\Delta PKM2}$ Th1 cells while a reduction of IL-2 in wildtype cells could be observed. Similarly, there was no effect of TEPP-46 on IFNγ concentrations in $CD4^{\Delta PKM2}$ Th1 cell culture supernatant. FACS analysis* demonstrated a previously observed reduction of the IFNγ MFI in WT CD4⁺ Th1 (p=0,0153) and Th17 cells after restimulation. While no difference in IFNγ production was observed in in $CD4^{\Delta PKM2}$ Th17 cells treated with TEPP-46, a small yet insignificant reduction in $CD4^{\Delta PKM2}$ Th1 cells was present. In Th17 cells a significant reduction of their signature cytokine IL-17 was measured in WT cells treated with TEPP-46 (p=0,0249), which was not observed in $CD4^{\Delta PKM2}$ cells. Taken together, these data indicate that application of TEPP-46 to cell cultures of CD4⁺ T effector

* Staining and flow cytometric measurement of cytokines in restimulated cells were conducted by A. K. Horst (Institute of Experimental Immunology and Hepatology, Hamburg)

cells influences their cytokine production and thereby function and that no effect of this kind occurs in $CD4^{\Delta PKM2}$ cells (Figure 24).

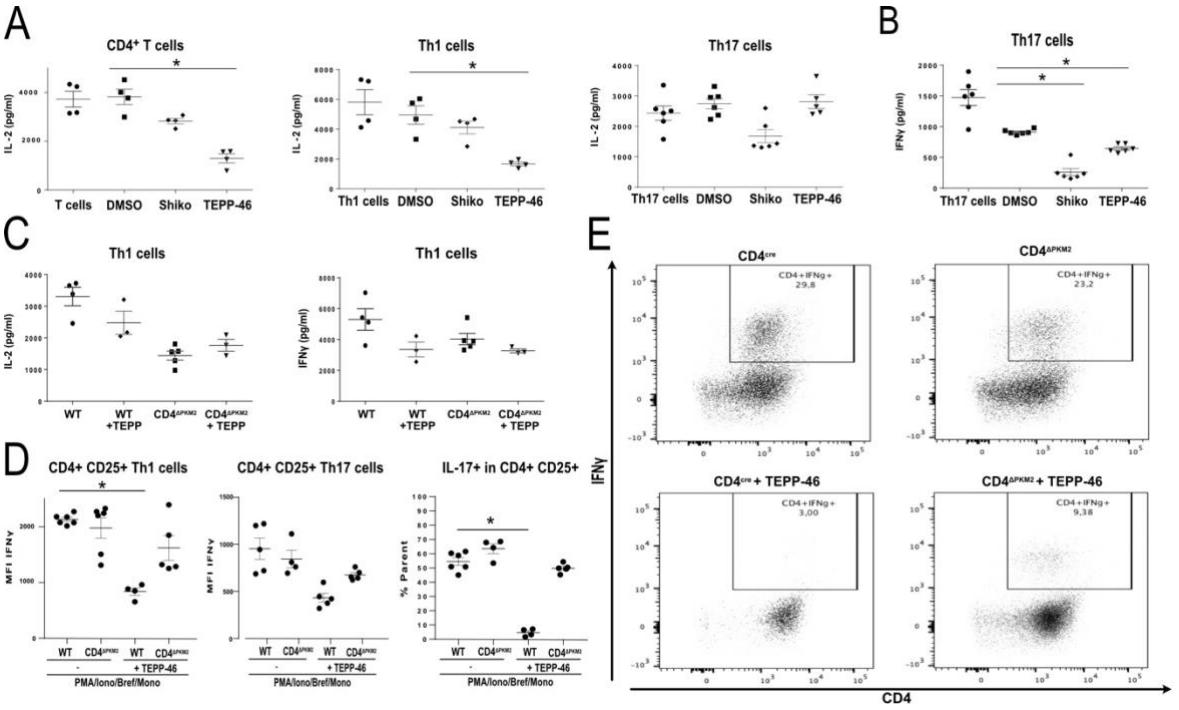

Figure 25: Cytokine production of in vitro polarised $CD4^+$ T cells, Th1 and Th17 cells under the influence of Tepp 46 and Shikonin. (A) IL-2 in cell culture supernatant determined by ELISA. (B) IFNγ in cell culture supernatant of Th17 cells determined by ELISA. (C) IL-2 and IFNγ in cell culture supernatant of WT or $CD4^{\Delta PKM2}$ Th1 cells under the influence of TEPP-46. (D) Flow cytometric analysis for IFNγ MFI in $CD4^+$ $CD25^+$ Th1 and Th17 cells and IL-17 MFI in $CD4^+$ $CD25^+$ Th17 cells. (E) Respective density plots of IFNγ positive cells in $CD4^+$ Th1 cells.

3.9.3. Effects of Tepp 46 and Shikonin on T regulatory cells induction

Finally, the effects of TEPP-46 and Shikonin on the induction of T regulatory cells were investigated by flow cytometric analysis of cells treated with both substances during T regulatory cell induction. TEPP-46 resulted in a reduced percentage of CD25 high cells among $CD4^+$ cells (p=0,05) and further less FoxP3 positive cells among $CD4^+$ CD25 high cells (p=0,05) compared to DMSO. An additional sign for impaired proliferation could be seen in a reduced amount of Ki67 positive cells in the $FoxP3^+$ subset (p=0,05). Effects of TEPP on Bcl-2 positive cells were small and non-significant. Yet, after restimulation a reduction in pSTAT5 positive cells was measured (p= 0,0475). Wildtype $CD4^+$ T regulatory cells treated with TEPP-46 still displayed high amounts of CD73 positive cells, the percentage of cell positive for CD39 was not significantly influenced either. As for effector cells, TEPP-46 was added to a culture of $CD4^{\Delta PKM2}$ regulatory cells, to examine possible

unspecific effects. Yet, no significant effects were observed on Bcl-2, pSTAT5 or ectonucleotidase expression.

These data indicate that TEPP-46 may impair T regulatory cell induction and proliferation but has no significant effect on the expression of ectonucleotidases as observed in $CD4^{\Delta PKM2}$ cells (Figure 25).

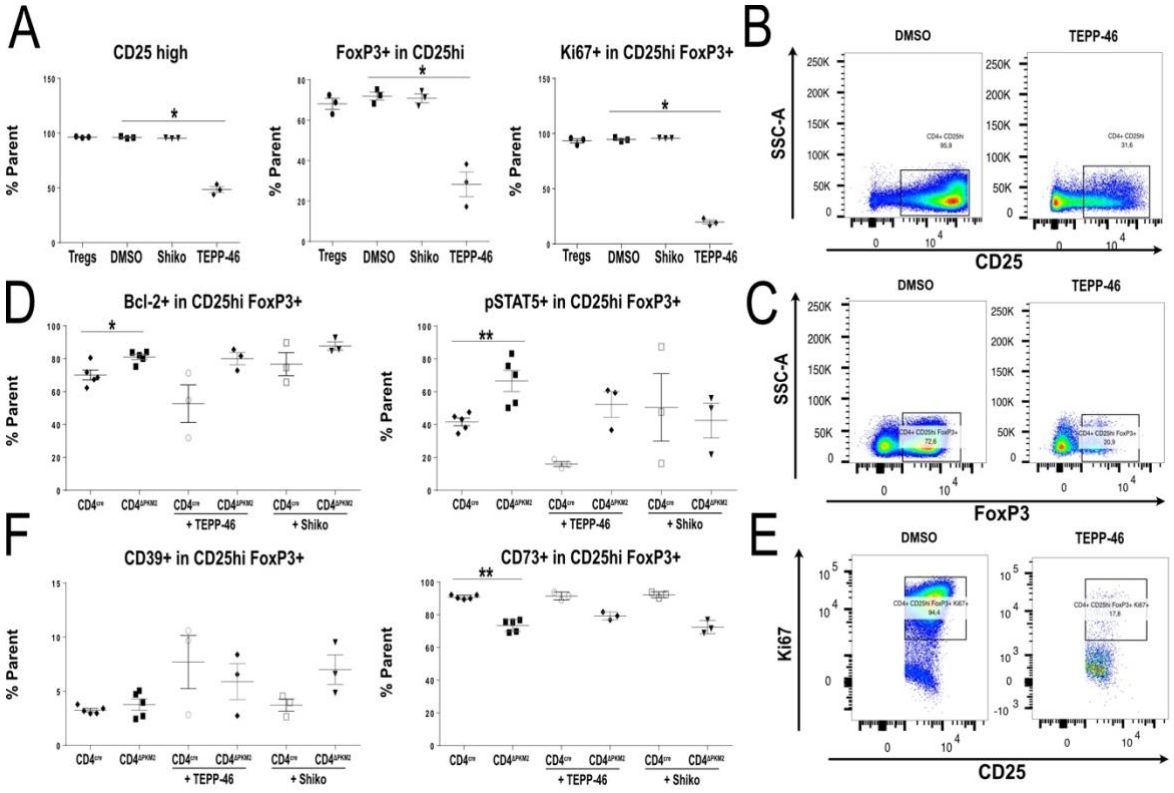

Figure 26: Proliferation of $CD4^+$ T regulatory cells under the influence of Tepp 46 and Shikonin. (A) Flow cytometric analysis of $CD25^{high}$, FoxP3 positive and Ki67 positive subsets within $CD4^+$ T cells after in vitro T regulatory cell induction. (B) Respective FACS plots for $CD25^{high}$, FoxP3 positive and Ki67 positive cells (C) Expression of Bcl-2 and pSTAT5 in CD25high FoxP3 positive T regulatory cells from either WT or $CD4^{\Delta PKM2}$ mice treated with TEPP-46 and Shikonin (D) Expression of ectonucleotidases CD39 and CD73 in $CD25^{high}$ FoxP3 positive T regulatory cells from either WT or $CD4^{\Delta PKM2}$ mice treated with TEPP-46 and Shikonin. (for both genotypes n=3)

4. Discussion

This study aimed at describing the effect of a knockout of PKM2 in mouse $CD4^+$ T cells ($CD4^{\Delta PKM2}$) regarding their metabolism and function. To investigate the effect of a complete knockout of PKM2 in $CD4^+$ T cells in vivo, $CD4^{\Delta PKM2}$ mice were challenged with 5-7mg/kg Concanavalin A. Also, $CD4^+$ T cells were isolated from mouse spleens, polarized in vitro and their characteristics were examined using different laboratory methods. In these $CD4^+$ T cells, a complete knock-out of PKM2 was achieved and confirmed by western blot analysis for PKM2 protein (see 4.1.1.). PKM2 exists in either a dimeric or tetrameric state and undergo dynamic changes of their state. As different functions are attributed to either the dimer or the tetramer, TEPP-46 was chosen as a method, to stabilize PKM2 tetramers thereby suppressing the dimers effects. Additionally, Shikonin, a PKM2 inhibitor of both the dimer and the tetramer, was tested.

4.1. The effect of Concanavalin A challenge in $CD4^{cre}$ and $CD4^{\Delta PKM2}$ mice

The Concanavalin A model induces $CD4^+$ T cell mediated acute autoimmune hepatitis by binding to LSEC and thereby activating $CD4^+$ T cells specifically in the liver (Tiegs et al. 1992). $CD4^+$ T cells are considered the immune cell subset which predominantly mediates inflammation and tissue damage in Concanavalin A hepatitis. Aerobic glycolysis is of special relevance to $CD4^+$ T effector cell activation and function and PKM2, which is considered a key enzyme in aerobic glycolysis, was shown to be upregulated upon TCR activation (Wang et al. 2011, Cao et al. 2014, Angiari et al. 2020). Therefore, it was hypothesized that the functionality of $CD4^{\Delta PKM2}$ cells may be impaired, resulting in a less severe reaction of $CD4^{\Delta PKM2}$ mice to Concanavalin A challenge.

However, $CD4^{\Delta PKM2}$ mice appeared to be hypersensitive to Concanavalin A challenge having shown an exacerbated reaction at 5mg/kg Concanavalin A and enhanced lethality at 7mg/kg Concanavalin A. Elevated liver transaminase ALT and, in some cases, a higher percentage of necrotic area in liver H.E. microscopy indicated extended liver damage compared to $CD4^{cre}$ controls. These effects weren't foreseen as doses were substantially lower than compared to previously published experiments (30mg/kg, see Tiegs et al. 1992), yet may be partly explained by higher sensitivity of C57/BL6 mice compared to NMRI mice towards ConA or variations between batches.

Despite more pronounced reactions to Concanavalin A challenge, rtPCR from whole liver tissue of $CD4^{\Delta PKM2}$ mice revealed lower concentrations of IFNγ mRNA, which may be indicative of reduced secretion by Th1 cells. Lü et al. (2018) have shown that a deletion of PKM2 in T cells reduced their IFNγ production. Similar amounts of HIF1α mRNA may be indicative of comparable metabolic conditions. Therefore, other factors were taken into consideration, which may have mediated a stronger reaction to ConA, despite a possibly impaired Th1 cell function.

Not only $CD4^+$ effector cells, but also other immune cell subsets mediate the inflammatory response to Concanavalin A. For example, monocyte derived macrophages which belong to the mononuclear phagocytic system (MPS) are stimulated by IFNγ secreting Th1 cells (Nathan et al. 1983) and in turn stimulate or suppress $CD4^+$ T cell activity in multiple ways. Additionally, Kupffer cells as liver-resident macrophages are known to interact with $CD4^+$ T cells (Shen et al. 2009). Both, monocyte-derived macrophages and Kupffer cells produce IL-18, a proinflammatory cytokine modulating innate and adaptive immunity. IL-18 appears to play a role in autoimmune diseases and hepatic inflammation (Tsutsui et al. 1997, Ikeda et al. 2014). In rtPCR from whole liver tissue 2,5 hours post Concanavalin A challenge more IL-18 mRNA was detected in $CD4^{\Delta PKM2}$ mice. Altered $CD4^+$ T cell function by PKM2 knock-out may therefore have influenced macrophage and Kupffer cell activity.

Furthermore, neutrophils play a relevant role in Concanavalin A hepatitis. It was demonstrated, that in neutrophil deprived mice, Concanavalin A fails to induce severe liver injury (Hatada et al. 2005). To investigate whether neutrophils might be involved in the strong Concanavalin A response in $CD4^{\Delta PKM2}$ mice, MPO immunohistochemistry was conducted. Yet no significant differences in neutrophil numbers were observed between genotypes.

The interpretation of these results is further limited by the small numbers (n=4 per genotype) of animals per experiment treated with Concanavalin A, as ALT as a measure for liver damage may show substantial interindividual variation.

$CD4^+$ T regulatory cells play a crucial role in finetuning the activity of other immune cells to maintain homeostasis and prevent autoimmunity. Their fueling mainly relies on oxidative phosphorylation, yet it was shown that the induction of FoxP3 also requires glycolysis (De Rosa et al. 2015). Additionally, Kupffer cells have been shown to have anti-inflammatory functions as they release anti-inflammatory IL-10 and activate T regulatory cells in the liver. Erhardt et al. (2007) have shown that levels of IL-10, produced by T regulatory cells and

Kupffer cells, do influence the severity of Concanavalin A mediated hepatitis in mice. Hence, reduced T regulatory cell function may have had an impact on disease severity by insufficiently suppressing $CD4^+$ T effector cells.

Damanesco et al. (2020) performed EAE experiments using $CD4^{crePKM2fl/fl}$ mice bred from mice carrying LoxP flanked Pkm2 specific exon 10 (Israelsen et al. 2013) and $CD4^{cre}$ mice and did not find any differences between those mice and $CD4^{cre}$ controls in general. In contrast $CD4^{\Delta PKM2}$ mice used in this work were found to have lower body weight and hints of altered liver fatty acid metabolism compared to $CD4^{cre}$ mice (data not shown). Therefore, other differences between genotypes having contributed to the hypersensitivity observed, can't be excluded fully.

Taken together the analysis of liver tissue and blood from $CD4^{\Delta PKM2}$ and $CD4^{cre}$ mice challenged with Concanavalin A indicates hypersensitivity of $CD4^{\Delta PKM2}$ mice and a dysregulated immune response which may affect other immune cell subsets such as macrophages or Kupffer cells.

4.2. The effect of PKM2 on the metabolism of Th1 and Th17 cells in vitro

$CD4^+$ T cells have specific metabolic demands that mediate lineage commitment and determine their function. While resting T cells mainly rely on OXPHOS and fatty acid oxidation for fuel, once activated, Th1 as well as Th17 cells undergo a metabolic switch towards aerobic glycolysis to ensure high proliferation rates and support effector function (Geltink et al. 2018, Pearce and Pearce 2013). Shi et al. (2011) have demonstrated how a blockage of glycolysis with 2-desoxyglucose can inhibit Th17 differentiation and ameliorate EAE in mice. PKM2 specifically, as a controlling and rate limiting enzyme in glycolysis, has been described to be upregulated upon TCR activation (Cao et al. 2014).
To assess whether a knockout of PKM2 influences glycolytic activity in $CD4^+$ T effector cells, Seahorse® glycolytic rate assay was conducted. It was hypothesized that a knockout of PKM2 would reduce $CD4^+$ T cells glycolytic capacity which would result in a reduced ECAR in the assay. While $CD4^{\Delta PKM2}$ Th17 cells appeared to be characterized by a hypoglycolytic metabolism and lower ECAR in general as well as after Rotenone/AA injection, $CD4^{\Delta PKM2}$ T cells and Th1 cells displayed a hyperglycolytic metabolism compared to $CD4^{cre}$ controls both in general and after respiratory chain blockage.

To better understand the reasons for these observations and to see whether compensatory mechanisms could explain them, a western blot for PKM1 was performed. Both, PKM1 and PKM2 originate from the PKM gene, which differs only by one exon, and are created by alternative splicing (Noguchi et al 1986, see chapter 1.3.2). It may therefore be possible that instead of PKM2 upregulation PKM1 is increasingly expressed. Polarised $CD4^{\Delta PKM2}$ cells, Th1 as well as Th17 cells expressed more PKM1 protein compared to $CD4^{cre}$ controls. This observation was supported by a rtPCR for Pkm1 with higher mRNA levels detected in $CD4^{\Delta PKM2}$ samples of T cells and Th1 cells.

To better assess glycolytic flux, a western blot for enolase was performed. Enolase is a glycolytic enzyme catalysing the dehydration of 2-phosphoglycerate to phosphoenolpyruvate (PEP), thereby being positioned just before pyruvate kinase in glycolysis. Hyperglycolytic $CD4^{\Delta PKM2}$ T and Th1 cells showed similar enolase protein expression compared to $CD4^{cre}$ cells in a western blot. A rtPCR for Enolase supported the finding of similar expression in stimulated $CD4^{+}$ T cells. Yet, in $CD4^{\Delta PKM2}$ Th1 cells a small increase in Enolase mRNA in compared to $CD4^{cre}$ Th1 cells was observed. These findings align well with the observed increased glycolytic activity and ECAR found in the Seahorse® glycolytic rate assays in $CD4^{\Delta PKM2}$ Th1 cells. The opposite effect was observed in $CD4^{\Delta PKM2}$ Th17 cells. Here, matching the lower ECAR rates compared to $CD4^{cre}$ Th17 cells, a reduced amount of Enolase protein was observed in a western blot.

The PKM2 dimer is furthermore known to influence the expression of various proteins, one of them being the glucose transporter GLUT1. Hitosugiu et al. (2019) found GLUT-1 transcription to be increased following PKM2 nuclear translocation. Therefore, a glucose uptake assay was performed, which revealed a significant reduction of 2-NBDG uptake in $CD4^{\Delta PKM2}$ T cells, Th1 cells and Th17 cells, which may be linked to the loss of the PKM2 dimer's ability to translocate to the cell's nucleus and influence gene expression.

In total, these results indicate an impaired and reduced glucose metabolism in $CD4^{\Delta PKM2}$ Th17 cells. Contrarily, Damasceno et al. (2020), who have shown that $CD4^{crePKM2fl/fl}$ T cells cultured under Th17 cell-skewing conditions did not have an altered glucose metabolism. Although they found Th17 cells to express the highest amount of Pkm2 mRNA among all examined $CD4^{+}$ T cell subsets, no significant differences in glucose uptake, consumption or lactate production occurred. Fitting these observations on Th17 metabolism, no difference in HIF1α expression was observed by Damasceno et al. (2020) which together with mTORC1 is a key regulator of Th17 metabolism (Shi et al. 2011, Delgoffe et al. 2011, Dang

et al 2011). These findings stand in contrast to the reduction glycolytic activity of $CD4^{\Delta PKM2}$ Th17 cells observed in this work (see results chapter 4.4).

Damasceno et al. (2020) found PKM1 to be upregulated in $CD4^{crePKM2fl/fl}$ Th17 cells. This indicated compensatory expression, which may in this case have compensated for PKM2 glycolytic activity as the enzymatic activity of PKM1 is about 4 times higher compared to PKM2. However, the observed reduction in enolase protein shown in this work may strengthen the assumption that overall glycolytic capacity is reduced in $CD4^{\Delta PKM2}$ Th17 cells.

Contrarily to what was hypothesized, stimulated $CD4^+$ T cells as well as Th1 cells showed a hyperglycolytic metabolism and higher ECAR, while showing reduced glucose uptake. It may therefore be possible, that elevated levels of PKM1 had compensated at least partly for PKM2 tetramer enzymatic activity in the case of $CD4^+$ T cells and Th1 cells and that the role of PKM1 in compensation for PKM2 function had been underestimated. Yet, this theory stands in contrast to the effect observed in $CD4^{\Delta PKM2}$ Th17 cells, which also showed overexpression of PKM1.

As a limitation, the assessment of glycolytic activity and capacity by ECAR may be in parts an oversimplified approach, as it doesn't take all proton producers into consideration and refers all increase in ECAR after Rot/AA application to glycolysis.

Additionally, the glycolytic enzyme phosphoglycerate mutase (PGAM) catalyzes the transformation of 3-phosphoglycerate via the intermediate 2,3-phosphoglycerate to 2-phosphoglycerate, before the latter one is catalyzed to phosphoenolpyruvate (PEP) by enolase. PGAM is primed by phosphorylation for activity, meaning that PEP increases PGAM activity in a positive feedback loop. To allow for pyruvate production in the absence of PKM, two mechanisms are described by Vander Heiden (2011). Cells appear to have a phosphatase converting the 2,3-phosphoglycerate to 2-phosphoglycerate. Also PEP dependent phosphorylation of PGAM may release phosphate from PEP, thereby creating pyruvate in the absence of pyruvate kinase. Vander Heiden et al. (2010) have shown this mechanism to be active in PKM2 expressing cells with low pyruvate kinase activity thereby bypassing PKM2.

In conclusion, all $CD4^+$ T cell subsets examined showed reduced uptake of glucose, while overexpressing PKM1. While TH1 cells displayed a hyperglycolytic metabolism, Th17 cells

may have reacted with hypoglycolysis due to the importance of HIF1α in regulating their metabolic profile, which distinguishes them from Th1 cells.

4.3. The effect of PKM2 on the expansion and function of Th1 and Th17 cells in vitro

Metabolism, expansion, and function of $CD4^+$ T cells are tightly intertwined and share the same regulatory mechanisms and transcription factors, among them the HIF1α-mTorC1 signaling axis, which is also known to upregulate PKM2 in tumor cells (Sun et al. 2011). It's impairment by mTorC1 deletion was shown to impair Th17 differentiation. (Dang et al. 2011, Delgoffe et al. 2011). Upon activation, the glycolytic switch enables biosynthesis, proliferation, and cytokine production. Highlighting the relevance of glycolysis, Shi et al. (2011) have shown that blockage of glycolysis using 2-desoxyglucose can inhibit Th17 cell differentiation and thereby ameliorate EAE. Additionally, glycolytic enzymes act as transcription factors and have additional roles to their function of catalyzing metabolism. PKM2 specifically acts as a transcriptional regulator of HIF1α (Luo et al. 2011). It was therefore hypothesized, that a knockout of PKM2 would not only influence $CD4^+$ T cells metabolism but also their function.

First, cytokine production was assessed. Activated $CD4^+$ T cells, Th1 and Th17 cells produce IL-2 as well as INFγ. IL-2 itself activated other $CD4^+$ T effector cells, but also T regulatory cells. IFNγ is a key inflammatory cytokine and of special importance to Th1 cells as their signature cytokine.

After undergoing an in vitro differentiation protocol, $CD4^{\Delta PKM2}$ T cells, Th1 cells and Th17 cells showed a less inflammatory phenotype compared to $CD4^{cre}$ controls. They all expressed both significantly less IL-2 and IFNγ. These cytokines are especially important regarding Th1 cell function, yet IFNγ may be co-produced by Th17 cells in smaller amounts (Stadhouders et al. 2018) and IL-2 production might be influenced by an overall less inflammatory milieu in the culture.

The results in Th17 cells align very well with the finding that $CD4^{\Delta PKM2}$ Th17 cells are also hypoglycolytic. Lü et al. (2018) have already linked glycolytic metabolism, IFNγ expression and PKM2 expression in experiments using homocysteine stimulated T cells.

Chang and colleagues (2013) discovered that the glycolytic enzyme GAPDH can act as modulator of IFNγ translation by binding its mRNA at the ribosome and thereby inhibiting translation, if not used in glycolysis. Therefore, in $CD4^{\Delta PKM2}$ Th17 cells this may be an

additional explanation for a connection between reduced glycolytic activity and reduced IFNγ production. Yet, Argus (2013) mentioned, that it is not clear whether there will ever be insufficient glycolysis to free up sufficient GAPDH to block IFNγ translation in a relevant manner, especially in vivo.
It may also be possible, that no such connection exists in $CD4^{\Delta PKM2}$ Th1 cells as they display a reduction in IFNγ, and IL-2 production yet appear hyperglycolytic in glycolytic rate assays and show elevated Enolase and Pkm1 expression and protein production. Still, the findings in supernatant from Th1 polarisation experiments align with the reduction of IFNγ mRNA found in Concanavalin A challenged $CD4^{\Delta PKM2}$ mice (see 5.1).

PKM2, especially it's dimer, may translocate to the nucleus and is tightly linked to cell proliferation (Yang et al. 2011, Gao et al. 2012). It was therefore hypothesized that a knockout of PKM2 would impair effector cell proliferation and possibly affect polarisation into Th1 and Th17 cells. To assess this, CD25 as a marker of activation of $CD4^+$ T cells was measured, as well as Tbet as a Th1 master transcription factor and RORγT as the Th17 master transcription factor.
$CD4^{\Delta PKM2}$ cells incubated with a Th1 polarisation cocktail showed reduced proliferation compared to $CD4^{cre}$ cells demonstrated by a reduced proliferating fraction of cells. Still, no significant differences in the percentage of $CD25^+$ activated $CD4^+$ T cells or $Tbet^+$ T cells were observed between genotypes. It may therefore be possible, that $CD4^{\Delta PKM2}$ T cells ability to uphold a glycolytic metabolism or to be hyperglycolytic has compensated for the loss of PKM2 function in upholding cell proliferation. The fact that these cells showed no significant difference in PD-1 or Gal-9 expression compared to $CD4^{cre}$ cells aligns well with the findings regarding proliferation and Th1 polarisation.
While these results showing only slight impairment of proliferation stand in contrast to the reduced cytokine production, the loss of PKM2 could have only affected Th1 function and not their ability to proliferate. Damanesco et al. (2020) observed no effect at all in Th1 and T regulatory cells other than Pkm1 upregulation. The authors therefore concluded that PKM2 is only relevant to Th17 cell function.

Damasceno et al. (2020) previously showed impaired Th17 differentiation of $CD4^{crePKM2fl/fl}$ cells, mediated by a reduced nuclear Stat3 phosphorylation. Stat3 phosphorylation had previously been demonstrated to be crucial to Th17 differentiation and activation. Nuclear PKM2 may act as a protein kinase to phosphorylate Stat3 in tumor cells (Renner et al 2008, Gao et al. 2012).

While Damanesco et al. (2020) did not find proliferative capacity of $CD4^{crePKM2fl/fl}$ Th17 cells be impaired compared to $CD4^{cre}$ Th17 cells, the expression of IL-17 and other Th17 related genes was reduced. Fitting these observations, $CD4^{crePKM2fl/fl}$ mice showed reduced incidence and clinical severity of EAE. An amelioration of EAE achieved by blockage of glycolysis with 2-DG had previously been demonstrated by Shi et al. (2011).

Here, among $CD4^{\Delta PKM2}$ Th17 cells the proliferating fraction of cell was smaller compared to $CD4^{cre}$ Th17 cells. Among activated $CD25^{+}$ $CD4^{+}$ T cells which underwent in vitro Th17 polarisation, the amount of RORγT positive cells was significantly smaller, indicating impaired Th17 induction. Furthermore, cells were analysed for PD-1 and galectin-9, which both play a role in regulating apoptosis. It was found that Galectin 9 may further suppress Th17 differentiation in an IL-2 dependent manner (Oomizu et al. 2012). While no significant differences occurred regarding galectin-9 expression, in $CD4^{\Delta PKM2}$ Th17 cells a significant reduction of PD-1 positive cells was observed. Generally, PD-1 acts as an inhibitory regulator, contributing to anti-inflammatory environments. Paradoxically, in Th17 cells, PD-1 engagement it is also associated with enhanced Stat3 activity and therefore Th17 transcriptional programs (Celada et al. 2018). It is therefore difficult to say whether a reduction in PD-1 positive Th17 $CD4^{\Delta PKM2}$ cells is also associated with other inhibitory effects of a PKM2 knockout or does indeed show reduced inhibition of Th17 activity. These effects stand in contrast to the previous observations that a PKM2 knockout does not impair Th17 proliferation (Damanesco et al. 2020) and may hint at a broader effect of PKM2 knock-out.

Whether the effects observed are due to a general reduction in glycolytic activity in $CD4^{\Delta PKM2}$ Th17 cells (see 5.2.) or to a loss of only the dimers potential effects on T cells activation and cell proliferation, remains unclear, as $CD4^{\Delta PKM2}$ cells lack both, the PKM2 dimer and tetramer. Yet, a knockout of the dimer appears to be at least partially responsible, as it can translocate to the nucleus to influence transcriptional regulators (Yang et al. 2011 Gao et al. 2012). Additionally, tetramerisation achieved by treatment with TEPP-46 has been shown to impair Th17 differentiation as well (see 4.7, Damanesco et al. 2020, Angiari et al. 2020).

Summarized, $CD4^{\Delta PKM2}$ T cells, Th1 and Th17 cells show impaired IL-2 as well as IFNγ production. Especially Th17 cells appear to be affected in their polarisation and proliferation, while in activated $CD4^{+}$ T cells and Th1 cells no significant effects were observed apart from a small reduction of the proliferating fraction.

These findings stand somewhat in contrast with the observation that $CD4^{\Delta PKM2}$ mice were hypersensitive towards Concanavalin A challenge. It may be possible, that altering cellular metabolism affects $CD4^+$ T cell function differently in vitro and in vivo.

A possible explanation, which may further explain the hyperglycolytic metabolism of Th1 cells, may be that PKM2 function was bypassed. Vander Heiden et al. (2010) and Christofk et al. (2008) described how cells can metabolise PEP to pyruvate in the absence of pyruvate kinase and uphold their ability to proliferate despite expressing the PKM2 dimer, which has only little enzymatic activity. As no ATP is produced in this reaction, it may also display a way to prevent the inhibition of a glycolytic metabolism by high ATP/AMP ratios.

Yet, especially in the in vivo setting, the relationship between PKM2 function and disease severity may also be questionable. To illustrate, Franchi et al. (2017) have shown that inhibition of OXPHOS inhibits Th17 response in murine colitis as well. This stands in contrast to the observations in this work and observations of Damanesco et al. (2020), that especially Th17 cells strongly rely on glycolysis, as well as to the hypothesis that this dependency on glycolysis may be part of a Th17 specific HIF1α signature.

4.4. The effect of PKM2 on the expression of ectonucleotidases by Th1 and Th17 cells in vitro

In inflammatory environments ATP is released in multiple ways such as cell lysis, exocytosis or by immune cells themselves through Pannexin 1 channels (Antonioli et al. 2013, Schenk et al. 2008). It then induces clearance from damaged cells and a proinflammatory response mediated through purinergic P2X receptors expressed by immune cells. (Bono et al. 2015). CD39 and CD73 are both ectonucleotidases, expressed by a variety of T cells and other immune cells. While CD39 catalyzes the conversion of ATP to AMP, CD73 phosphorylases AMP to adenosine (Robson et al. 2006, Regateiro et al. 2013). Adenosine for example binds to A2A receptors of T cells and prevents their proliferation and function, thereby contributing to an immunosuppressive environment (Sitkovski et al. 2004, Antonioli et al. 2013).

Besides their immunoregulatory function, both, CD39 and CD73, can be considered activation markers of T cells. Ectonucleotidase expression has so far been shown to be HIF-1α and Stat-3 regulated (Synnestvedt et al. 2002, Chalmin et al. 2012). It was therefore hypothesized, that their expression may be influenced by PKM2 activity as PKM2 expression and activity is tightly intertwined with HIF1α and Stat-3 signaling (Yang et al. 2011, Yang et al. 2012a, Luo et al. 2011, Damanesco et al. 2020).

CD39 and CD73 expression has been shown to be upregulated in the presence of IL-6, IL-1β and TGFβ, all used for in vitro Th17 polarisation protocols (Chalmin et al. 2012, Regateiro et al. 2011). In this study, $CD4^+$ Th17 cells show a substantially higher rate of ectonucleotidase expression compared to stimulated $CD4^+$ T cells and $CD4^+$ T cells which underwent Th1 polarisation protocols. These findings generally align with the special relevance of HIF1α to the Th17 signature (Dolgoff et al. 2011, Kurebayashi et al. 2012, Shi et al. 2011, Dang et al. 2011).

Fitting these observations, $CD4^{\Delta PKM2}$ Th17 cells a show significantly reduced expression of CD73 and CD39 compared to $CD4^{cre}$ cells. The effect may be mediated by a downregulation of the HIF1α due to the PKM2 knockout.

PKM2 deficient Th17 cells have been shown to express lower pStat3 (Damanesco et al. 2020). In addition, Stat3 is known to control the expression of CD39 and thereby Th17 immunosuppressive abilities (Chalmin et al. 2012). The possibility of Th17 cells undergoing a switch towards a more regulatory phenotype has been reported multiple times (Yang et al. 2008, Gagliani et al. 2015). It may therefore be possible, that $CD4^{\Delta PKM2}$ Th17 cells due to their altered glycolytic metabolism also show limitations regarding their suppressive function.

To date no connection between either PKM2 activity or it's knockout and ectonucleotidase expression has been described in $CD4^+$ T cells. The results from this work indicate that PKM2 may directly through intracellular pathways or indirectly by influencing the cells metabolism and thereby modifying the extracellular environment influence ectonucleotidase expression in $CD4^+$ T effector cells. Yet, it is difficult to say how this change may influence the concentrations of eATP and extracellular adenosine, as they have not been measured in this study.

4.5. The role of PKM2 on the function of T regulatory cells in vitro

Contrary to Th1 and Th17 $CD4^+$ T cells, $CD4^+$ T regulatory cells display a more naïve like metabolic phenotype, as they rely on OXPHOS for energy supply (Geltink et al. 2018). Yet although they thrive on OXPHOS, they may use glycolysis for initial induction (De Rosa et al. 2015). It is established that T regulatory cells suppress liver inflammatory disease amongst other inflammatory and autoimmune diseases (Dejaco, 2006). Specifically, within the liver, hepatocytes may interact with $CD4^+$ T regulatory cells. Burghardt et al. (2013) have demonstrated, that hepatocytes can induce hepatic T regulatory cells in vitro, a phenomenon

mediated by Notch signaling. These induced HC-iTregs have further been shown to have suppressive ability, thereby being an important mechanism for the mediation of immune tolerance and limiting inflammatory processes in the liver. For example, antigen specific GMP-Treg therapy has previously been examined for its' potential to treat autoimmune disease or to be used in the setting of organ transplantation (Wawman et al. 2018).

We asked whether PKM2 would influence the hepatocyte mediated induction of Tregs and performed co-cultures of T cells and hepatocytes from either $CD4^{\Delta PKM2}$ or $CD4^{cre}$ mice. The previously described hypersensitivity of $CD4^{\Delta PKM2}$ mice towards Concanavalin A challenge led to the hypothesis that T regulatory cell induction may be impaired in these mice. In contrast to what was hypothesized, co-cultures with $CD4^{\Delta PKM2}$ T cells showed augmented Treg induction and a higher amount of FoxP3 positive cells.
Using standard in vitro T regulatory cell induction protocols, no difference of FoxP3 positive cells could be shown between genotypes. Yet, $CD4^{\Delta PKM2}$ T regulatory cells expressed higher Bcl-2, higher pStat5 and lower PD-1, indicating for better survival and T regulatory cells ability to sustain their immunosuppressive function. It was demonstrated by Wang et al. (2012) that expression of anti-apoptotic Bcl-2 in T regulatory cells is of importance in the context of autoimmunity as it promotes survival and maintains homeostasis in T regulatory cells. pStat5 is known to promote T regulatory cell lineage commitment and improve the production of immunomodulatory IL-10 and TGFβ in T regulatory cells (Tsuji-Takayama et al. 2008).
The possibly enhanced Treg induction led us to examine Treg suppressive ability in an experiment with CD90.1 cells as well as one with CSFE labeled $CD4^+$ T cells. Yet, a suppression assay revealed only a small effect in a 1:1 ratio of T regulatory and labeled effector cells in favor of $CD4^{\Delta PKM2}$ T regulatory cells suppressive function.

Taken together, these results indicate that there might be improved T regulatory cell survival or formation in $CD4^{\Delta PKM2}$ T regulatory cells. Prior, an association between $FoxP3^+$ T regulatory cells and $ROR\gamma T^+$ Th17 cells was shown (Yang et al. 2007). It may be possible that through inhibition of HIF1α not only an impaired Th17 polarisation but also enhanced T regulatory cell formation is induced (Feldhoff et al. 2017). However, the role of PKM2 in this context needs to be further elucidated.

Tregs generated using in vitro protocols appear to favor oxidative phosphorylation for energy production. Still, T regulatory cells isolated ex vivo may well be glycolytic (Procaccini et al. 2016). Therefore, it remains difficult to explain the effects observed in Concanavalin A hepatitis based on data from in vitro T regulatory cell induction and further examination of T regulatory cells metabolic behavior are necessary, such as seahorse metabolic rate assay from in vitro polarised T regulatory cells compared to cells isolated from blood directly by FACS sorting.

4.6. The effect of PKM2 on the expression of ectonucleotidases by T regulatory cells in vitro

As described in chapter 1.1.3 CD39 and CD73 are ectonucleotidases catalyzing the conversion of extracellular, proinflammatory ATP to adenosine, which by binding the A2A receptors has anti-inflammatory effects (Kobie et al. 2006, Deaglio et al. 2007). Both ectonucleotidases are known to be expressed by murine $CD4^+$ $FoxP3^+$ T regulatory cells and – due to their special relevance to suppressive ability – have been frequently used as their activation markers (Deaglio 2007). Regateiro et al. (2011) have demonstrated that TGFβ upregulates ectonucleotidase expression in T regulatory cells.
Lukashev et al. (2004) revealed a protective role of adenosine in Concanavalin A mediated hepatitis in mice by treating them with adenosine agonists and antagonists. Therefore, it was hypothesized that altered ectonucleotidase expression in T regulatory cells and thereby a reduced suppressive function, may have played a role in the exacerbated Concanavalin A response of $CD4^{\Delta PKM2}$ mice (see 4.1).

$CD4^{\Delta PKM2}$ T regulatory cells appeared to express lower levels of ectonucleotidases, both CD39 and CD73. A similar effect of a CD4+ specific knockout of PKM2 was already observed strongly pronounced in Th17 $CD4^+$ T cells. It may therefore be possible that PKM2 influences ectonucleotidase expression.
Data from a suppression assay indicate if at all, only slightly enhanced suppressive function of $CD4^{\Delta PKM2}$ T regulatory cells. Therefore, T regulatory cell development may be improved, yet a gain in function may be limited by reduced ectonucleotidase expression, which could have contributed to only a small overall suppressive advantage of $CD4^{\Delta PKM2}$ T regulatory cells in a suppression assay.

Again, the concentrations of eATP or extracellular adenosine have not been measured, therefore it cannot be said how altered ectonucleotidase expression in T regulatory cells affected the cellular environment.

4.7. The effects of TEPP-46 and Shikonin on $CD4^+$ T cell expansion and function in vitro

Due to its' relevance to $CD4^+$ T cell function, modulating glycolytic metabolism may be an interesting therapeutic target in inflammation (O'Neill et al. 2016, Bettencourt and Powell, 2017). PKM2 exists in dynamic balance of its monomeric, dimeric, and tetrameric form. While the monomer has no enzymatic activity, the dimer is a bit and the tetramer highly active (Morgan et al 2013). The dimers limited function as a glycolytic enzyme together with its non-glycolytic effects allow for optimized cell proliferation by diverting glycolytic intermediates into other pathways or influencing the expression of glycolytic genes (Lunt et al. 2015). It has been shown that upon T cell activation, especially the dimer is upregulated, and that this upregulation is accompanied by serine 37 phosphorylation, allowing for nuclear translocation in $CD4^+$ T cells (Prakasam et al. 2018, Angiari et al. 2020)
Several substances have been discovered to either stabilize the PKM2 tetramer or inhibit PKM2 altogether, thereby also inhibiting the effects of the dimer.

TEPP-46 is an activator of PKM2 enzymatic function as it induces and stabilizes its tetrameric form in T cells at doses of 50 and 100 mM (Angiari et al. 2020). Thereby it may reduce effects associated with the dimer, such as the use of glycolytic intermediates for proliferation processes and effects associated with nuclear translocation. Damanesco et al. (2020) have demonstrated that TEPP-46 disrupted nuclear translocation of PKM2 fully in Th1 as well as Th17 $CD4^+$ T cells.
Palsson-McDermott et al. (2015) previously showed an inhibitory effect of TEPP-46 on macrophages. It was hypothesized, that TEPP-46 would inhibit $CD4^+$ T effector proliferation and function in vitro, as these cells rely on aerobic glycolysis, and that it may not harm or even benefit $CD4^+$ T regulatory cells, which are known to thrive on oxidative phosphorylation (Gerrits et al. 2015, Michalek et al. 2011).
$CD4^+$ T cells were isolated from spleens of wildtype mice and cultured to induce expansion or Th1 and Th17 polarisation while being treated with TEPP-46. TEPP-46 reduced activation measured as $CD25^+$ cells in $CD4^+$ T cells and Th17 cells significantly. All $CD4^+$ T cell subsets examined showed a reduction in Ki67 positive cells, indicating impaired cellular

proliferation. Th1 cells treated with TEPP did not show significant differences in Tbet positive cells. Contrarily, in Th17 cells a significant reduction of RORγT positive cells was observed, indicating impaired Th17 polarisation. Additionally, in Th17 cells TEPP-46 application resulted in a significant reduction of Bcl-6 positive cells. Bcl-6 is known to be an important regulator of Th17 differentiation by downregulating Th17 fate suppressors (Kotov et al. 2019). Reduction of Bcl-6 positive cells within the TEPP-46 treated cultures therefore indicates impaired Th17 differentiation, fitting the observation that Th17 cells appear to be strongly affected by interference with PKM2 metabolism.

TEPP-46 treatment further resulted in reduced production of cytokines. Stimulated $CD4^+$ T cells and Th1 cells reacted with significantly reduced IL-2 secretion compared to DMSO treatment. In Th17 cells no significant difference in IL-2 secretion was observed. Contrarily, Th17 cells showed a significant reduction in IFNγ production, while reduction in Th1 cells was only significantly impaired after restimulation. Th17 cells treated with TEPP-46 additionally showed a strong reduction of their signature cytokine IL-17 indicating impaired function with a focus on Th17 cells.

These results are in line with those published by Angiari et al. (2020), who have shown that TEPP-46 inhibits $CD4^+$ Th1 and Th17 effector cell proliferation and production of IL-2 and TNFα at mRNA and protein level in a dose dependent manner in vitro and ameliorated EAE in vivo by blocking nuclear translocation of the PKM2 dimer.

Angiari et al. (2020) have shown TEPP-46 to reduce glycolytic activity and the induction of different glycolytic genes, such as Glut 1, fitting the observed differences in Th17 metabolism and glucose uptake in PKM2 knockouts observed in this study. By modulating PKM2 dimeric activity and its' nuclear HIF1α stabilizing activity, TEPP-46 reduces aerobic glycolysis and thereby activation of effector cells. HIF1α, Myc and mTORC1 activity are all necessary for the generation of pro-inflammatory T cells, especially Th17 cells (Geltink et al. 2018).
Additionally, Damanesco et al. (2020) have shown that treatment with TEPP reduced pStat3 levels as well as Th17 polarisation in a similar level compared to knockouts. Yet, no effect on Th1 polarisation was observed, which is in line with previous assumption, that PKM2 is of special relevance to Th17 cells. Yet, these observations stand partially in contrast to the observed effects on Th1 cells in this study as well as data from Angiari et al. (2020).

In this study TEPP- 46 also affected T regulatory cells. $CD4^+$ T cells treated with TEPP-46 under Treg polarizing conditions showed reduced amounts of CD25hi and $FoxP3^+$ cells. These T regulatory cells furthermore showed a reduction in Ki67 indicating impaired T regulatory cell induction. To further assess the characteristics of these cells Bcl-2 and pTat5 were measured, yet no significant effects were observed.
Although Angiari et al. (2020) found TEPP-46 to favor T regulatory cell development and increase $FoxP3^+CD25^+$ cells under non-polarizing conditions, TEPP-46 inhibited TGFβ induced Treg generation and no increase in $FoxP3^+$ $CD25^+$ T cells was found in the CNS of TEPP-46 treated mice in EAE. These findings highlight a potential lack of comparison of experimental setting, especially when it comes to comparing in vitro induction protocols with in vivo data. A favorable effect under non-polarizing conditions may well be plausible as T regulatory cells rely mainly on OXPHOS for fueling and limiting the translocation of the dimer to the nucleus might favor a transcriptional program favoring T regulatory over T effector cells. Also, the effects of TEPP-46 found in this work contrast previous results from knockout experiments, where a favorable effect towards T regulatory cell induction was observed.

Due to the strongly pronounced effects of TEPP-46 on the T cell subsets investigated, possible cytotoxic effects were considered as an explanation. To address the question of toxicity, $CD4^{\Delta PKM2}$ cells were used as off target controls. No significant effects were observed on Th1 or Th17 polarisation and Treg induction using TEPP-46 in $CD4^{\Delta PKM}$ cultures. Additionally, TEPP-46 did not affect cytokine production of $CD4^{\Delta PKM2}$ significantly. These data indicate that the effects of TEPP-46 treatment are specific to its interaction with the PKM2 protein. These findings align with results published by Angiari et al. (2020) who similarly found no cytotoxic effects of TEPP-46.

It can therefore be concluded that TEPP-46 impairs T effector cells proliferation and function in vitro, as well as the induction of T regulatory cells in vitro. Yet, further investigations into the amount of PKM2 existing in the form of either dimer or tetramer after TEPP-46 application would have been necessary to clearly associate the effects observed in this study with PKM2 tetramerisation.

Shikonin, a plant-derived naphthoquinone, is a general inhibitor of PKM2 activity (Chen et al. 2012). Here, no significant effects of Shikonin were observed on polarisation of $CD4^+$ T

cells or cytokine production. These results stand in contrast to previously published literature on the effects of Shikonin on $CD4^+$ T cell polarisation. Kono et al. (2019) showed that PKM2 was relevant for Th1 and Th17 cell differentiation by using Shikonin to inhibit PKM2 in a model of EAE in B6 mice. Shikonin reduced ECAR and therefore glycolytic activity in Th1 and Th17 cells, yet not in T regulatory cells. Further, a reduction of IFNγ and IL17 expression could be demonstrated in a dose dependent manner (Kono et al. 2019). These results were supported by a reduced clinical and histological score in mice subjected to EAE (Kono et al. 2019). In line with the results of this work, Shikonin did not reduce the percentage of Ki67 positive cells, thereby likely not influencing proliferation in general. One reason for the discrepancy of the effects observed in this work may be a too small dose of Shikonin used in experiments. Furthermore, there might have been differences in Shikonin quality.

In summary, TEPP-46 reduced $CD4^+$ T effector cell function. Shikonin appeared to have no relevant effect on $CD4^+$ T cell function. For further investigations, FBP as a natural mediator of PKM2 tetramerisation could be tested as a possible positive control and comparison (Ashizawa et al. 1991).

4.8. The effect of TEPP-46 and Shikonin on the expression of ectonucleotidases in vitro

A knockout of PKM2 in $CD4^+$ T effector cells reduced the expression of the ectonucleotidase CD39 and CD73 in Th17 cells and T regulatory cells (see chapter 5.4 and 5.6). While it is not sure how these alterations in ectonucleotidase expression influence the extracellular concentrations of ATP and adenosine and therefore affect immune regulation, an influence of PKM2 by modulating cellular metabolism appears likely. It was therefore hypothesized that treatment with TEPP-46 or Shikonin would affect the expression of CD39 and CD73.
Neither Th1, Th17 or T regulatory cells reacted significantly towards Shikonin treatment. TEPP-46 lead to a small reduction of CD73 expression in Th1 cells, while Th17 cells treated with TEPP-46 showed a more pronounced reduction of cells positive for CD73. These results fit the previous observations that PKM2 is of special importance to Th17 cells, as seen in the effect size on ectonucleotidase alterations in the knockout experiment. Both, Th1 and Th17 cells expressed significantly more CD39 after being treated with TEPP-46. It is important to note, that CD39 and CD73 expression don't necessarily go together and therefore should not be viewed as regulated and controlled by the same mechanisms. In T regulatory cells no significant effects of TEPP-46 on ectonucleotidase expression were observed. No results are

published so far on the effect on ectonucleotidase expression by Th1 or Th17 cells under the influence of TEPP-46.

It can be concluded, that PKM2 is a regulator of $CD4^+$ T cells metabolism and influences both T effector cell and T regulatory cell proliferation and function. It may further be a therapeutic target, as TEPP-46 induced tetramerisation alters T effector cell polarisation and function.

4.9. Outlook

This study aimed at understanding the effect of a $CD4^+$ T cell specific knockout of PKM2 on T cell polarisation and function in vivo and primarily in vitro. It may serve as an observational groundwork, as it is one of the few studies examining the effect of a PKM2 knockout in $CD4^+$ Th1 and Th17 cells and the only study examining a knockout in T regulatory cells. A connection between $CD4^+$ T cell metabolism and especially PKM2 and a variety of immune cell functions, proliferation, cytokine production but also regulatory aspects such as ectonucleotidase expression was demonstrated.

Its main limitations lay in is methodical depth and the limited in vivo data. In vivo versus in vitro immune metabolism may differ and circulating T cells may have a different metabolic signature compared to those at the site of inflammation, which is why in vivo data is of special importance to further investigate the implications of a PKM2 knockout in CD4+ T cells. Experiments on Concanavalin A hepatitis would need to be repeated with higher numbers of animals or replaced by a model that better addresses Th17 cell response such as the DCC colitis model.

Some findings, such as the effect of a PKM2 knockout on altered ectonucleotidase expression and the suppressive function of $CD4^{\Delta PKM2}$ Tregs, need to be confirmed and their implications to be further investigated. Also, regarding the effects of TEPP-46, the extend of induced tetramerisation upon TEPP-46 application and comparisons to FBP could contribute to a more conclusive understanding of its effects.

Abstract

Background: Autoimmune diseases, such as autoimmune hepatitis, are driven by a functional imbalance between effector T cells and T regulatory cells. Therapeutic options in many cases still lack specificity and employ general immune suppression with glucocorticoids or purine analogs.
When activated in the course of autoimmune disease, $CD4^+$ T cells switch to a pro-proliferative metabolism characterized by aerobic glycolysis – a process also known as Warburg effect. Pyruvate kinase M2, which is expressed in proliferative tissue, plays a key role in this glycolytic switch as it catalyzed the last and rate limiting step of glycolysis. It changes from a catalytically active tetramer toward a less active dimer amplifying glycolysis and acting as a transcription factor for glycolytic enzymes as well as inflammatory cytokines. By diverging intermediates from glycolysis into biosynthetic pathways for lipid, nucleotide and amino acid synthesis, this change provides substrates for cell growth, proliferation, and cytokine production. To the contrary, T regulatory cells are believed to rely on oxidative phosphorylation for fueling.

Methods: $CD4^+$ T cells with a cre-mediated PKM2 knockout were isolated from mouse spleens and polarised into Th1 and Th17 $CD4^+$ T cells as well as T regulatory cells. Using seahorse metabolic rate assay, restimulation and suppression assay these cells were characterized regarding their glycolytic metabolism, proliferation and function and compared with regular $CD4^+$ T cells. Additionally, the effects of a small molecule activator of PKM2 (TEPP-46) were tested regarding its influence on proliferation and cytokine production.

Results: Here we show that a knockout of PKM2 in $CD4^+$ T cells results in altered glycolytic metabolism despite compensatory overexpression of PKM1. Subsequently, reduced production of IL-2 as well as IFNγ could be measured. In Th17 cells particularly, a strongly pronounced reduction of glycolytic activity was observed. Th17 proliferation and polarisation were affected with a reduced expression of RORγT and an altered expression of the ectonucleotidases CD39 and CD73. Contrarily to what was observed in the effector T cells, T regulatory cells showed enhanced expression of their signature transcription factor FoxP3 upon PKM2 knock out.
Treatment of cultured $CD4^+$ T cells with the small molecule activator TEPP-46 resulted in impairment of activation and proliferation, again with the most pronounced effect in the Th17 cell subset. Upon TEPP-46 application, IL-2 production was reduced in Th1 cells as was IL-17 expression in Th17 cells.
Yet, in vitro results may differ from in vivo effects of a PKM2 knockout as liver damage in a Concanavalin A model of autoimmune hepatitis persisted in mice with a $CD4^+$ T cells specific PKM2 knockout.

Conclusion: This work demonstrated the relevance of PKM2 to $CD4^+$ T cell proliferation and function in vitro. A strongly pronounced effect was observed in Th17 $CD4^+$ T cells, possibly explained by the relevance of the HIF1α signature to their metabolic and inflammatory profile. In vivo effects of a knockout of PKM2 in Th17 cells in organ inflammation still remain to be better examined in different disease models.

Zusammenfassung

Hintergrund: Autoimmunerkrankungen, wie beispielweise die Autoimmune Hepatitis, werden durch ein funktionelles Ungleichgewicht zwischen entzündundsfördernder und entzündungsregulierender Immunantwort hervorgerufen. In vielen Fällen beruht die Behandlung primär auf einer allgemeinen Immunsupression durch Glukokortikoide oder Purinanaloga, welche kaum spezifisch und nebenwirkungsreich sind.
Wenn $CD4^+$ T Zellen im Rahmen einer Autoimmunerkrankung aktiviert werden, untergehen sie einem Wechsel hin zu einem pro-proliferativem Stoffwechsel, welcher durch aerobe Glykolyse charakterisiert wird. Diesen Effekt nennt man Warburg Effekt. Die Pyruvatkinase M2, welche in Gewebe exprimiert wird, welches schnell proliferiert, spielt hierbei eine Schlüsselrolle, da sie den letzten und geschwindigkeitsbestimmenden Schritt der Glykolyse einnimmt. Sie wechselt von einem katalytisch aktiven Tetramer zu einem Dimer, wodurch die Glykolytische Aktivität insgesamt verstärkt wird. Weiterhin bewirkt der Wechsel die Transkription glykolytischer Enzyme sowie inflammatorischer Zytokine. Durch die Umleitung glykolytischer Zwischenprodukte in Biosynthesewege zur Lipid-, Nukleotid- und Aminosäuresynthese entstehen Substrate für Zellwachstum, Proliferation und Zytokinproduktion. Im Gegensatz zu Effektor T Zellen nutzen regulatorische T Zellen primär oxidative Phosphorylierung zur Energiegewinnung.

Methoden: $CD4^+$ T Zellen mit einem cre-vermittelten PKM2 Knockout wurden aus Milzen von Mäusen isoliert und in Th1, Th17 sowie regulatorische T Zellen polarisiert und hinsichtlich verschiedener Aktivitätsmarker analysiert. Mittels Seahorse Metabolic Rate Assay, Restimulations- und Suppressionsanalysen wurden der Stoffwechsel sowie die Funktionalität bewertet und jeweils mit regulären $CD4^+$ T Zellen verglichen. Zusätzlich wurden die Effekte eines Small Molecule Ativators (TEPP-46) hinsichtlich der Proliferation und Zytokinproduktion von $CD4^+$ T Zellen analysiert.

Ergebnisse: Diese Arbeit zeigt, dass ein Knockout von PKM2 in $CD4^+$ T Zellen trotz kompensatorischer Überexpression von PKM1 in einem veränderten glykolytischem Stoffwechsel mündet. In der Folge konnte eine verminderte Produktion von IL-2 sowie IFNγ festgestellt werden. Insbesondere Th17 Zellen zeigten eine starke Reduktion der glykolytischen Aktivität, reduzierte Proliferation und eingeschränkte Polarisierung, was sich in reduzierten RORγT Messwerten zeigte. Weiterhin zeigte sich eine veränderte Expression der Ektonukleotidasen CD39 und CD73 in $CD4^+$ T Zellen mit einem Knockout von PKM2. Im Gegensatz zu T Effektorzellen zeigten regulatorische T Zellen in der Folge des PKM2 Knockouts eine verstärkte Expression von FoxP3.
Die Behandlung von $CD4^+$ T Zellen mit dem Small Molecule Activator TEPP-46 resultierte in einer beeinträchtigten Proliferation und Aktivierung der Zellen, wobei sich erneut der stärkste Effekt in Th17 Zellen zeigte. In Th17 Zellen war die Expression von IL.17 reduziert, während in Th1 Zellen die IL-2 Produktion sankt.
Die in vitro beobachteten Verhältnisse zeigten sich jedoch nicht in vergleichbarer Form in vivo. Im Concanavalin A Modell für Autoimmune Hepatitis resultierte ein $CD4^+$-spezifischer Knockout von PKM2 in persistierenden Lebergewebeschäden.

Schlussfolgerung: Diese Arbeit demonstriert die Relevanz der Pyruvatkinase M2 für die Proliferation und Funktion von $CD4^+$ T Zellen in vitro. Ein besonders ausgeprägter Effekt konnte in Th17 Zellen festgestellt werden. Dieser lässt sich möglicherweise durch die Relevanz der HIF1α Signatur für deren metabolisches und inflammatorisches Profil erklären. Die in vivo Effekte eines PKM2 Knockouts insbesondere in Th17 Zellen und deren Konsequenzen für Autoimmunerkrankungen müssen jedoch noch im Detail für unterschiedliche Krankheitsmodelle erforscht werden.

References

Alla, V., Abraham, J., Siddiqui, J., Raina, D., Wu, G. Y., Chalasani, N. P., & Bonkovsky, H. L. (2006). Autoimmune Hepatitis Triggered by Statins. Journal of Clinical Gastroenterology, 40(8), 757–761. https://doi.org/10.1097/00004836-200609000-00018

Anastasiou D, Yu Y, Israelsen WJ, Jiang JK, Boxer MB, Hong BS, Tempel W, Dimov S, Shen M, Jha A, Yang H, Mattaini KR, Metallo CM, Fiske BP, Courtney KD, Malstrom S, Khan TM, Kung C, Skoumbourdis AP, Veith H, Southall N, Walsh MJ, Brimacombe KR, Leister W, Lunt SY, Johnson ZR, Yen KE, Kunii K, Davidson SM, Christofk HR, Austin CP, Inglese J, Harris MH, Asara JM, Stephanopoulos G, Salituro FG, Jin S, Dang L, Auld DS, Park HW, Cantley LC, Thomas CJ, Vander Heiden MG. Pyruvate kinase M2 activators promote tetramer formation and suppress tumorigenesis. Nat Chem Biol. 2012 Oct;8(10):839-47. doi: 10.1038/nchembio.1060.

Angelin A, Gil-de-Gómez L, Dahiya S, Jiao J, Guo L, Levine MH, Wang Z, Quinn WJ 3rd, Kopinski PK, Wang L, Akimova T, Liu Y, Bhatti TR, Han R, Laskin BL, Baur JA, Blair IA, Wallace DC, Hancock WW, Beier UH. Foxp3 Reprograms T Cell Metabolism to Function in Low-Glucose, High-Lactate Environments. Cell Metab. 2017 Jun 6;25(6):1282-1293.e7. doi: 10.1016/j.cmet.2016.12.018.

Angiari S, Runtsch MC, Sutton CE, Palsson-McDermott EM, Kelly B, Rana N, Kane H, Papadopoulou G, Pearce EL, Mills KHG, O'Neill LAJ. Pharmacological Activation of Pyruvate Kinase M2 Inhibits CD4$^+$ T Cell Pathogenicity and Suppresses Autoimmunity. Cell Metab. 2020 Feb 4;31(2):391-405.e8. doi: 10.1016/j.cmet.2019.10.015.

Antonioli L, Pacher P, Vizi ES, Haskó G. CD39 and CD73 in immunity and inflammation. Trends Mol Med. 2013 Jun;19(6):355-67. doi: 10.1016/j.molmed.2013.03.005.

Argus JP, Bensinger SJ. Immunology. Fueling function over expansion in T cells. Science. 2013 Jul 5;341(6141):37-8. doi: 10.1126/science.1242100.

Ashizawa, K., Willingham, M., Liang, C., & Cheng, S. (1991). In vivo regulation of monomer tetramer conversion of pyruvate kinase subtype M2 by glucose is mediated via fructose 1,6-bisphosphate. Journal of Biological Chemistry, 266(25), 16842–16846. https://doi.org/10.1016/S0021-9258(18)55378-3

Asseman C, Mauze S, Leach MW, Coffman RL, Powrie F. An essential role for interleukin 10 in the function of regulatory T cells that inhibit intestinal inflammation. J Exp Med. 1999 Oct 4;190(7):995-1004. doi: 10.1084/jem.190.7.995.

Aswad F, Kawamura H, Dennert G. High sensitivity of CD4+CD25+ regulatory T cells to extracellular metabolites nicotinamide adenine dinucleotide and ATP: a role for P2X7 receptors. J Immunol. 2005 Sep 1;175(5):3075-83. doi: 10.4049/jimmunol.175.5.3075.

Aujla SJ, Chan YR, Zheng M, Fei M, Askew DJ, Pociask DA, Reinhart TA, McAllister F, Edeal J, Gaus K, Husain S, Kreindler JL, Dubin PJ, Pilewski JM, Myerburg MM, Mason CA, Iwakura Y, Kolls JK. IL-22 mediates mucosal host defense against Gram-negative bacterial pneumonia. Nat Med. 2008 Mar;14(3):275-81. doi: 10.1038/nm1710.

Bakker, A. (1927). Einige U¨ bereinstimmungen im Stoffwechsel der Carcinomzellen und Exsudatleukocyten. Klinische Wochenschrift, 6(6), 252–254. https://doi.org/10.1007/BF01710710

Bantug GR, Galluzzi L, Kroemer G, Hess C. The spectrum of T cell metabolism in health and disease. Nat Rev Immunol. 2018 Jan;18(1):19-34. doi: 10.1038/nri.2017.99.

Bettelli E, Carrier Y, Gao W, Korn T, Strom TB, Oukka M, Weiner HL, Kuchroo VK. Reciprocal developmental pathways for the generation of pathogenic effector TH17 and regulatory T cells. Nature. 2006 May 11;441(7090):235-8. doi: 10.1038/nature04753

Bettencourt IA, Powell JD. Targeting Metabolism as a Novel Therapeutic Approach to Autoimmunity, Inflammation, and Transplantation. J Immunol. 2017 Feb 1;198(3):999-1005. doi: 10.4049/jimmunol.1601318.

Blume C, Felix A, Shushakova N, Gueler F, Falk CS, Haller H, Schrader J. Autoimmunity in CD73/Ecto-5'-nucleotidase deficient mice induces renal injury. PLoS One. 2012;7(5):e37100. doi: 10.1371/journal.pone.0037100

Bluemlein, K., Gr¨uning, N.-M., Feichtinger, R. G., Lehrach, H., Kofler, B., & Ralser, M. (2011). No evidence for a shift in pyruvate kinase PKM1 to PKM2 expression during tumorigenesis. Oncotarget, 2(5), 393–400. doi: 10.18632/oncotarget.278

Bono MR, Fernández D, Flores-Santibáñez F, Rosemblatt M, Sauma D. CD73 and CD39 ectonucleotidases in T cell differentiation: Beyond immunosuppression. FEBS Lett. 2015 Nov 14;589(22):3454-60. doi: 10.1016/j.febslet.2015.07.027.

Borsellino G, Kleinewietfeld M, Di Mitri D, Sternjak A, Diamantini A, Giometto R, Höpner S, Centonze D, Bernardi G, Dell'Acqua ML, Rossini PM, Battistini L, Rötzschke O, Falk K. Expression of ectonucleotidase CD39 by Foxp3+ Treg cells: hydrolysis of extracellular ATP and immune suppression. Blood. 2007 Aug 15;110(4):1225-32. doi: 10.1182/blood-2006-12-064527.

Burchill MA, Yang J, Vogtenhuber C, Blazar BR, Farrar MA. IL-2 receptor beta-dependent STAT5 activation is required for the development of Foxp3+ regulatory T cells. J Immunol. 2007 Jan 1;178(1):280-90. doi: 10.4049/jimmunol.178.1.280.

Burghardt S, Erhardt A, Claass B, Huber S, Adler G, Jacobs T, Chalaris A, Schmidt-Arras D, Rose-John S, Karimi K, Tiegs G. Hepatocytes contribute to immune regulation in the liver by activation of the Notch signaling pathway in T cells. J Immunol. 2013 Dec 1;191(11):5574-82. doi: 10.4049/jimmunol.1300826.

Calcinotto A, Filipazzi P, Grioni M, Iero M, De Milito A, Ricupito A, Cova A, Canese R, Jachetti E, Rossetti M, Huber V, Parmiani G, Generoso L, Santinami M, Borghi M, Fais S, Bellone M, Rivoltini L. Modulation of microenvironment acidity reverses anergy in human and murine tumor-infiltrating T lymphocytes. Cancer Res. 2012 Jun 1;72(11):2746-56. doi: 10.1158/0008-5472.CAN-11-1272.

Cao Y, Rathmell JC, Macintyre AN. Metabolic reprogramming towards aerobic glycolysis correlates with greater proliferative ability and resistance to metabolic inhibition in CD8 versus CD4 T cells. PLoS One. 2014 Aug 4;9(8):e104104. doi: 10.1371/journal.pone.0104104.

Cekic C, Linden J. Purinergic regulation of the immune system. Nat Rev Immunol. 2016 Mar;16(3):177-92. doi: 10.1038/nri.2016.4.

Celada LJ, Kropski JA, Herazo-Maya JD, Luo W, Creecy A, Abad AT, Chioma OS, Lee G, Hassell NE, Shaginurova GI, Wang Y, Johnson JE, Kerrigan A, Mason WR, Baughman RP, Ayers GD, Bernard GR, Culver DA, Montgomery CG, Maher TM, Molyneaux PL, Noth I, Mutsaers SE, Prele CM, Peebles RS Jr, Newcomb DC, Kaminski N, Blackwell TS, Van Kaer L, Drake WP. PD-1 up-regulation on $CD4^+$ T cells promotes pulmonary fibrosis through STAT3-mediated IL-17A and TGF-β1 production. Sci Transl Med. 2018 Sep 26;10(460):eaar8356. doi: 10.1126/scitranslmed.aar8356.

Boxer, M. B., Jiang, J., Vander Heiden, M. G., Shen, M., Skoumbourdis, A. P., Southall, N., Veith, H., Leister, W., Austin, C. P., Park, H. W., Inglese, J., Cantley, L. C., Auld, D. S., & Thomas, C. J. (2010). Evaluation of Substituted N,N'-Diarylsulfonamides as Activators of the Tumor Cell Specific

M2 Isoform of Pyruvate Kinase. Journal of Medicinal Chemistry, 53(3), 1048–1055. https://doi.org/10.1021/jm901577g

Chalmin F, Mignot G, Bruchard M, Chevriaux A, Végran F, Hichami A, Ladoire S, Derangère V, Vincent J, Masson D, Robson SC, Eberl G, Pallandre JR, Borg C, Ryffel B, Apetoh L, Rébé C, Ghiringhelli F. Stat3 and Gfi-1 transcription factors control Th17 cell immunosuppressive activity via the regulation of ectonucleotidase expression. Immunity. 2012 Mar 23;36(3):362-73. doi: 10.1016/j.immuni.2011.12.019.

Chaneton B, Hillmann P, Zheng L, Martin ACL, Maddocks ODK, Chokkathukalam A, Coyle JE, Jankevics A, Holding FP, Vousden KH, Frezza C, O'Reilly M, Gottlieb E. Serine is a natural ligand and allosteric activator of pyruvate kinase M2. Nature. 2012 Nov 15;491(7424):458-462. doi: 10.1038/nature11540.

Chang CH, Curtis JD, Maggi LB Jr, Faubert B, Villarino AV, O'Sullivan D, Huang SC, van der Windt GJ, Blagih J, Qiu J, Weber JD, Pearce EJ, Jones RG, Pearce EL. Posttranscriptional control of T cell effector function by aerobic glycolysis. Cell. 2013 Jun 6;153(6):1239-51. doi: 10.1016/j.cell.2013.05.016.

Chen W, Jin W, Hardegen N, Lei KJ, Li L, Marinos N, McGrady G, Wahl SM. Conversion of peripheral CD4+CD25- naive T cells to CD4+CD25+ regulatory T cells by TGF-beta induction of transcription factor Foxp3. J Exp Med. 2003 Dec 15;198(12):1875-86. doi: 10.1084/jem.20030152.

Chen J, Xie J, Jiang Z, Wang B, Wang Y, Hu X. Shikonin and its analogs inhibit cancer cell glycolysis by targeting tumor pyruvate kinase-M2. Oncogene. 2011 Oct 20;30(42):4297-306. doi: 10.1038/onc.2011.137.

Chiang EY, Kolumam GA, Yu X, Francesco M, Ivelja S, Peng I, Gribling P, Shu J, Lee WP, Refino CJ, Balazs M, Paler-Martinez A, Nguyen A, Young J, Barck KH, Carano RA, Ferrando R, Diehl L, Chatterjea D, Grogan JL. Targeted depletion of lymphotoxin-alpha-expressing TH1 and TH17 cells inhibits autoimmune disease. Nat Med. 2009 Jul;15(7):766-73. doi: 10.1038/nm.1984.

Christofk HR, Vander Heiden MG, Harris MH, Ramanathan A, Gerszten RE, Wei R, Fleming MD, Schreiber SL, Cantley LC. The M2 splice isoform of pyruvate kinase is important for cancer metabolism and tumour growth. Nature. 2008 Mar 13;452(7184):230-3. doi: 10.1038/nature06734.

Cori CF and Cori GT (1946) Carbohydrate Metabolism. Annual Review of Biochemistry 15:193-218.

Clower, C. V., Chatterjee, D., Wang, Z., Cantley, L. C., Vander Heiden, M. G., & Krainer, A. R. (2010). The alternative splicing repressors hnRNP A1/A2 and PTB influence pyruvate kinase isoform expression and cell metabolism. Proceedings of the National Academy of Sciences, 107(5), 1894–1899. doi: 10.1073/pnas.0914845107

Csóka B, Himer L, Selmeczy Z, Vizi ES, Pacher P, Ledent C, Deitch EA, Spolarics Z, Németh ZH, Haskó G. Adenosine A2A receptor activation inhibits T helper 1 and T helper 2 cell development and effector function. FASEB J. 2008 Oct;22(10):3491-9. doi: 10.1096/fj.08-107458.

Czaja, A. J. (2019). Examining pathogenic concepts of autoimmune hepatitis for cues to future investigations and interventions. World Journal of Gastroenterology, 25(45), 6579–6606. Doi: 10.3748/wjg.v25.i45.6579

Dejaco C, Duftner C, Grubeck-Loebenstein B, Schirmer M. Imbalance of regulatory T cells in human autoimmune diseases. Immunology. 2006 Mar;117(3):289-300. doi: 10.1111/j.1365-2567.2005.02317.x.

Damasceno LEA, Prado DS, Veras FP, Fonseca MM, Toller-Kawahisa JE, Rosa MH, Públio GA, Martins TV, Ramalho FS, Waisman A, Cunha FQ, Cunha TM, Alves-Filho JC. PKM2 promotes Th17 cell differentiation and autoimmune inflammation by fine-tuning STAT3 activation. J Exp Med. 2020 Oct 5;217(10):e20190613. doi: 10.1084/jem.20190613.

Dang EV, Barbi J, Yang HY, Jinasena D, Yu H, Zheng Y, Bordman Z, Fu J, Kim Y, Yen HR, Luo W, Zeller K, Shimoda L, Topalian SL, Semenza GL, Dang CV, Pardoll DM, Pan F. Control of T(H)17/T(reg) balance by hypoxia-inducible factor 1. Cell. 2011 Sep 2;146(5):772-84. doi: 10.1016/j.cell.2011.07.033.

Davidson TS, DiPaolo RJ, Andersson J, Shevach EM. Cutting Edge: IL-2 is essential for TGF-beta-mediated induction of Foxp3+ T regulatory cells. J Immunol. 2007 Apr 1;178(7):4022-6. doi: 10.4049/jimmunol.178.7.4022.

Dayton TL, Jacks T, Vander Heiden MG. PKM2, cancer metabolism, and the road ahead. EMBO Rep. 2016 Dec;17(12):1721-1730. doi: 10.15252/embr.201643300.

Deaglio S, Dwyer KM, Gao W, Friedman D, Usheva A, Erat A, Chen JF, Enjyoji K, Linden J, Oukka M, Kuchroo VK, Strom TB, Robson SC. Adenosine generation catalyzed by CD39 and CD73 expressed on regulatory T cells mediates immune suppression. J Exp Med. 2007 Jun 11;204(6):1257-65. doi: 10.1084/jem.20062512.

Delgoffe GM, Kole TP, Zheng Y, Zarek PE, Matthews KL, Xiao B, Worley PF, Kozma SC, Powell JD. The mTOR kinase differentially regulates effector and regulatory T cell lineage commitment. Immunity. 2009 Jun 19;30(6):832-44. doi: 10.1016/j.immuni.2009.04.014.

De Rosa V, Galgani M, Porcellini A, Colamatteo A, Santopaolo M, Zuchegna C, Romano A, De Simone S, Procaccini C, La Rocca C, Carrieri PB, Maniscalco GT, Salvetti M, Buscarinu MC, Franzese A, Mozzillo E, La Cava A, Matarese G. Glycolysis controls the induction of human regulatory T cells by modulating the expression of FOXP3 exon 2 splicing variants. Nat Immunol. 2015 Nov;16(11):1174-84. doi: 10.1038/ni.3269.

Di Cesare A, Di Meglio P, Nestle FO. The IL-23/Th17 axis in the immunopathogenesis of psoriasis. J Invest Dermatol. 2009 Jun;129(6):1339-50. doi: 10.1038/jid.2009.59.

Dombrauckas, J. D., Santarsiero, B. D., & Mesecar, A. D. (2005). Structural Basis for Tumor Pyruvate Kinase M2 Allosteric Regulation and Catalysis. Biochemistry, 44(27), 9417–9429. doi: 10.1021/bi0474923

Donaldson, P. T. (2004). Genetics of liver disease: immunogenetics and disease pathogenesis. Gut, 53(4), 599–608. Doi: 10.1136/gut.2003.031732

Erhardt A, Biburger M, Papadopoulos T, Tiegs G. IL-10, regulatory T cells, and Kupffer cells mediate tolerance in concanavalin A-induced liver injury in mice. Hepatology. 2007 Feb;45(2):475-85. doi: 10.1002/hep.21498.

Elliott MR, Chekeni FB, Trampont PC, Lazarowski ER, Kadl A, Walk SF, Park D, Woodson RI, Ostankovich M, Sharma P, Lysiak JJ, Harden TK, Leitinger N, Ravichandran KS. Nucleotides released by apoptotic cells act as a find-me signal to promote phagocytic clearance. Nature. 2009 Sep 10;461(7261):282-6. doi: 10.1038/nature08296.

Feldhoff LM, Rueda CM, Moreno-Fernandez ME, Sauer J, Jackson CM, Chougnet CA, Rupp J. IL-1β induced HIF-1α inhibits the differentiation of human FOXP3^{+} T cells. Sci Rep. 2017 Mar 28;7(1):465. doi: 10.1038/s41598-017-00508-x

Feo S, Arcuri D, Piddini E, Passantino R, Giallongo A. ENO1 gene product binds to the c-myc promoter and acts as a transcriptional repressor: relationship with Myc promoter-binding protein 1 (MBP-1). FEBS Lett. 2000 May 4;473(1):47-52. doi: 10.1016/s0014-5793(00)01494-0.

Fontenot JD, Gavin MA, Rudensky AY. Foxp3 programs the development and function of CD4+CD25+ regulatory T cells. Nat Immunol. 2003 Apr;4(4):330-6. doi: 10.1038/ni904.

Fischer K, Hoffmann P, Voelkl S, Meidenbauer N, Ammer J, Edinger M, Gottfried E, Schwarz S, Rothe G, Hoves S, Renner K, Timischl B, Mackensen A, Kunz-Schughart L, Andreesen R, Krause SW, Kreutz M. Inhibitory effect of tumor cell-derived lactic acid on human T cells. Blood. 2007 May 1;109(9):3812-9. doi: 10.1182/blood-2006-07-035972.

Franchi L, Monteleone I, Hao LY, Spahr MA, Zhao W, Liu X, Demock K, Kulkarni A, Lesch CA, Sanchez B, Carter L, Marafini I, Hu X, Mashadova O, Yuan M, Asara JM, Singh H, Lyssiotis CA, Monteleone G, Opipari AW, Glick GD. Inhibiting Oxidative Phosphorylation In Vivo Restrains Th17 Effector Responses and Ameliorates Murine Colitis. J Immunol. 2017 Apr 1;198(7):2735-2746. doi: 10.4049/jimmunol.1600810.

Friedman DJ, Künzli BM, A-Rahim YI, Sevigny J, Berberat PO, Enjyoji K, Csizmadia E, Friess H, Robson SC. From the Cover: CD39 deletion exacerbates experimental murine colitis and human polymorphisms increase susceptibility to inflammatory bowel disease. Proc Natl Acad Sci U S A. 2009 Sep 29;106(39):16788-93. doi: 10.1073/pnas.0902869106.

Gagliani N, Amezcua Vesely MC, Iseppon A, Brockmann L, Xu H, Palm NW, de Zoete MR, Licona-Limón P, Paiva RS, Ching T, Weaver C, Zi X, Pan X, Fan R, Garmire LX, Cotton MJ, Drier Y, Bernstein B, Geginat J, Stockinger B, Esplugues E, Huber S, Flavell RA. Th17 cells transdifferentiate into regulatory T cells during resolution of inflammation. Nature. 2015 Jul 9;523(7559):221-5. doi: 10.1038/nature14452.

Gantner F, Leist M, Lohse AW, Germann PG, Tiegs G. Concanavalin A-induced T-cell-mediated hepatic injury in mice: the role of tumor necrosis factor. Hepatology. 1995 Jan;21(1):190-8. doi: 10.1016/0270-9139(95)90428-x.

Gao X, Wang H, Yang JJ, Liu X, Liu ZR. Pyruvate kinase M2 regulates gene transcription by acting as a protein kinase. Mol Cell. 2012 Mar 9;45(5):598-609. doi: 10.1016/j.molcel.2012.01.001.

Germain RN. T-cell development and the CD4-CD8 lineage decision. Nat Rev Immunol. 2002 May;2(5):309-22. doi: 10.1038/nri798.

Geltink RIK, Kyle RL, Pearce EL. Unraveling the Complex Interplay Between T Cell Metabolism and Function. Annu Rev Immunol. 2018 Apr 26;36:461-488. doi: 10.1146/annurev-immunol-042617-053019.

Gerriets VA, Kishton RJ, Nichols AG, Macintyre AN, Inoue M, Ilkayeva O, Winter PS, Liu X, Priyadharshini B, Slawinska ME, Haeberli L, Huck C, Turka LA, Wood KC, Hale LP, Smith PA, Schneider MA, MacIver NJ, Locasale JW, Newgard CB, Shinohara ML, Rathmell JC. Metabolic programming and PDHK1 control CD4+ T cell subsets and inflammation. J Clin Invest. 2015 Jan;125(1):194-207. doi: 10.1172/JCI76012.

Ghoreschi K, Laurence A, Yang XP, Tato CM, McGeachy MJ, Konkel JE, Ramos HL, Wei L, Davidson TS, Bouladoux N, Grainger JR, Chen Q, Kanno Y, Watford WT, Sun HW, Eberl G, Shevach EM, Belkaid Y, Cua DJ, Chen W, O'Shea JJ. Generation of pathogenic T(H)17 cells in the absence of TGF-β signalling. Nature. 2010 Oct 21;467(7318):967-71. doi: 10.1038/nature09447.

Han W, Li L, Qiu S, Lu Q, Pan Q, Gu Y, Luo J, Hu X. Shikonin circumvents cancer drug resistance by induction of a necroptotic death. Mol Cancer Ther. 2007 May;6(5):1641-9. doi: 10.1158/1535-7163.MCT-06-0511.

Hatada S, Ohta T, Shiratsuchi Y, Hatano M, Kobayashi Y. A novel accessory role of neutrophils in concanavalin A-induced hepatitis. Cell Immunol. 2005 Jan;233(1):23-9. doi: 10.1016/j.cellimm.2005.03.003.

Hernandez-Mir G, McGeachy MJ. CD73 is expressed by inflammatory Th17 cells in experimental autoimmune encephalomyelitis but does not limit differentiation or pathogenesis. PLoS One. 2017 Mar 13;12(3):e0173655. doi: 10.1371/journal.pone.0173655.

Hitosugi T, Kang S, Vander Heiden MG, Chung TW, Elf S, Lythgoe K, Dong S, Lonial S, Wang X, Chen GZ, Xie J, Gu TL, Polakiewicz RD, Roesel JL, Boggon TJ, Khuri FR, Gilliland DG, Cantley LC, Kaufman J, Chen J. Tyrosine phosphorylation inhibits PKM2 to promote the Warburg effect and tumor growth. Sci Signal. 2009 Nov 17;2(97):ra73. doi: 10.1126/scisignal.2000431.

Horst, A. K., Kumashie, K. G., Neumann, K., Diehl, L., & Tiegs, G. (2021). Antigen presentation, autoantibody production, and therapeutic targets in autoimmune liver disease. Cellular and Molecular Immunology, 18(1), 92–111. doi: 10.1038/s41423-020-00568-6

Ikeda A, Aoki N, Kido M, Iwamoto S, Nishiura H, Maruoka R, Chiba T, Watanabe N. Progression of autoimmune hepatitis is mediated by IL-18-producing dendritic cells and hepatic CXCL9 expression in mice. Hepatology. 2014 Jul;60(1):224-36. doi: 10.1002/hep.27087.

Imamura, K., & Tanaka, T. (1972). Multimolecular Forms of Pyruvate Kinase from Rat and Other Mammalian Tissues. The Journal of Biochemistry, 71(6), 1043–1051. doi: 10.1093/oxfordjournals.jbchem.a129852

Israelsen WJ, Dayton TL, Davidson SM, Fiske BP, Hosios AM, Bellinger G, Li J, Yu Y, Sasaki M, Horner JW, Burga LN, Xie J, Jurczak MJ, DePinho RA, Clish CB, Jacks T, Kibbey RG, Wulf GM, Di Vizio D, Mills GB, Cantley LC, Vander Heiden MG. PKM2 isoform-specific deletion reveals a differential requirement for pyruvate kinase in tumor cells. Cell. 2013 Oct 10;155(2):397-409. doi: 10.1016/j.cell.2013.09.025.

Jiang JK, Walsh MJ, Brimacombe KR, Anastasiou D, Yu Y, Israelsen WJ, Hong BS, Tempel W, Dimov S, Veith H, Yang H, Kung C, Yen KE, Dang L, Salituro F, Auld DS, Park HW, Vander Heiden MG, Thomas CJ, Shen M, Boxer MB. ML265: A potent PKM2 activator induces tetramerization and reduces tumor formation and size in a mouse xenograft model. 2012 Mar 16 [updated 2013 May 8]. In: Probe Reports from the NIH Molecular Libraries Program

Jurica, M. S., Mesecar, A., Heath, P. J., Shi, W., Nowak, T., & Stoddard, B. L. (1998). The allosteric regulation of pyruvate kinase by fructose-1,6-bisphosphate. Structure, 6(2), 195–210. doi: 10.1016/S0969-2126(98)00021-5

Keller, K. E., Tan, I. S., & Lee, Y.-S. (2012). SAICAR Stimulates Pyruvate Kinase Isoform M2 and Promotes Cancer Cell Survival in Glucose-Limited Conditions. Science, 338(6110), 1069–1072. doi: 10.1126/science.1224409

Kobie JJ, Shah PR, Yang L, Rebhahn JA, Fowell DJ, Mosmann TR. T regulatory and primed uncommitted CD4 T cells express CD73, which suppresses effector CD4 T cells by converting 5'-adenosine monophosphate to adenosine. J Immunol. 2006 Nov 15;177(10):6780-6. doi: 10.4049/jimmunol.177.10.6780.

Kohu K, Ohmori H, Wong WF, Onda D, Wakoh T, Kon S, Yamashita M, Nakayama T, Kubo M, Satake M. The Runx3 transcription factor augments Th1 and down-modulates Th2 phenotypes by

interacting with and attenuating GATA3. J Immunol. 2009 Dec 15;183(12):7817-24. doi: 10.4049/jimmunol.0802527.

Kono M, Maeda K, Stocton-Gavanescu I, Pan W, Umeda M, Katsuyama E, Burbano C, Orite SYK, Vukelic M, Tsokos MG, Yoshida N, Tsokos GC. Pyruvate kinase M2 is requisite for Th1 and Th17 differentiation. JCI Insight. 2019 Jun 20;4(12):e127395. doi: 10.1172/jci.insight.127395.

Korn T, Bettelli E, Oukka M, Kuchroo VK. IL-17 and Th17 Cells. Annu Rev Immunol. 2009; 27:485-517. doi: 10.1146/annurev.immunol.021908.132710.

Kotov JA, Kotov DI, Linehan JL, Bardwell VJ, Gearhart MD, Jenkins MK. BCL6 corepressor contributes to Th17 cell formation by inhibiting Th17 fate suppressors. J Exp Med. 2019 Jun 3;216(6):1450-1464. doi: 10.1084/jem.20182376.

Kurebayashi Y, Nagai S, Ikejiri A, Ohtani M, Ichiyama K, Baba Y, Yamada T, Egami S, Hoshii T, Hirao A, Matsuda S, Koyasu S. PI3K-Akt-mTORC1-S6K1/2 axis controls Th17 differentiation by regulating Gfi1 expression and nuclear translocation of RORγ. Cell Rep. 2012 Apr 19;1(4):360-73. doi: 10.1016/j.celrep.2012.02.007.

Lazarevic V, Chen X, Shim JH, Hwang ES, Jang E, Bolm AN, Oukka M, Kuchroo VK, Glimcher LH. T-bet represses T(H)17 differentiation by preventing Runx1-mediated activation of the gene encoding RORγt. Nat Immunol. 2011 Jan;12(1):96-104. doi: 10.1038/ni.1969.

Leonard WJ, Spolski R. Interleukin-21: a modulator of lymphoid proliferation, apoptosis and differentiation. Nat Rev Immunol. 2005 Sep;5(9):688-98. doi: 10.1038/nri1688.

Li MO, Wan YY, Flavell RA. T cell-produced transforming growth factor-beta1 controls T cell tolerance and regulates Th1- and Th17-cell differentiation. Immunity. 2007 May;26(5):579-91. doi: 10.1016/j.immuni.2007.03.014.

Liu, V. M., Howell, A. J., Hosios, A. M., Li, Z., Israelsen, W. J., & Vander Heiden, M. G. (2020). Cancerassociated mutations in human pyruvate kinase M2 impair enzyme activity. FEBS Letters, 594(4), 646–664. doi: 10.1002/1873-3468.13648

Longhi, M. S., Hussain, M. J., Mitry, R. R., Arora, S. K., Mieli-Vergani, G., Vergani, D., & Ma, Y. (2006). Functional Study of CD4 + CD25 + Regulatory T Cells in Health and Autoimmune Hepatitis. The Journal of Immunology, 176(7), 4484–4491. doi: 10.4049/jimmunol.176.7.4484

Lukashev D, Ohta A, Apasov S, Chen JF, Sitkovsky M. Cutting edge: Physiologic attenuation of proinflammatory transcription by the Gs protein-coupled A2A adenosine receptor in vivo. J Immunol. 2004 Jul 1;173(1):21-4. doi: 10.4049/jimmunol.173.1.21.

Luckheeram RV, Zhou R, Verma AD, Xia B. $CD4^+$T cells: differentiation and functions. Clin Dev Immunol. 2012;2012:925135. doi: 10.1155/2012/925135.
Lunt SY, Vander Heiden MG. Aerobic glycolysis: meeting the metabolic requirements of cell proliferation. Annu Rev Cell Dev Biol. 2011;27:441-64. doi: 10.1146/annurev-cellbio-092910-154237.

Luo W, Hu H, Chang R, Zhong J, Knabel M, O'Meally R, Cole RN, Pandey A, Semenza GL. Pyruvate kinase M2 is a PHD3-stimulated coactivator for hypoxia-inducible factor 1. Cell. 2011 May 27;145(5):732-44. doi: 10.1016/j.cell.2011.03.054.

Lü S, Deng J, Liu H, Liu B, Yang J, Miao Y, Li J, Wang N, Jiang C, Xu Q, Wang X, Feng J. PKM2-dependent metabolic reprogramming in $CD4^+$ T cells is crucial for hyperhomocysteinemia-accelerated atherosclerosis. J Mol Med (Berl). 2018 Jun;96(6):585-600. doi: 10.1007/s00109-018-1645-6

Lv, L., Li, D., Zhao, D., Lin, R., Chu, Y., Zhang, H., Zha, Z., Liu, Y., Li, Z., Xu, Y., Wang, G., Huang, Y., Xiong, Y., Guan, K.-L., & Lei, Q.-Y. (2011). Acetylation Targets the M2 Isoform of Pyruvate Kinase for Degradation through Chaperone-Mediated Autophagy and Promotes Tumor Growth. Molecular Cell, 42(6), 719–730. doi: 10.1016/j.molcel.2011.04.025

Macintyre AN, Gerriets VA, Nichols AG, Michalek RD, Rudolph MC, Deoliveira D, Anderson SM, Abel ED, Chen BJ, Hale LP, Rathmell JC. The glucose transporter Glut1 is selectively essential for CD4 T cell activation and effector function. Cell Metab. 2014 Jul 1;20(1):61-72. doi: 10.1016/j.cmet.2014.05.004.

MacIver NJ, Michalek RD, Rathmell JC. Metabolic regulation of T lymphocytes. Annu Rev Immunol. 2013;31:259-83. doi: 10.1146/annurev-immunol-032712-095956.

Mahnke J, Schumacher V, Ahrens S, Käding N, Feldhoff LM, Huber M, Rupp J, Raczkowski F, Mittrücker HW. Interferon Regulatory Factor 4 controls T_{H1} cell effector function and metabolism. Sci Rep. 2016 Oct 20;6:35521. doi: 10.1038/srep35521.

Mangan PR, Harrington LE, O'Quinn DB, Helms WS, Bullard DC, Elson CO, Hatton RD, Wahl SM, Schoeb TR, Weaver CT. Transforming growth factor-beta induces development of the T(H)17 lineage. Nature. 2006 May 11;441(7090):231-4. doi: 10.1038/nature04754.

Manns MP. Autoimmune hepatitis: the dilemma of rare diseases. Gastroenterology. 2011 Jun;140(7):1874-6. doi: 10.1053/j.gastro.2011.04.026.

Michalek RD, Gerriets VA, Jacobs SR, Macintyre AN, MacIver NJ, Mason EF, Sullivan SA, Nichols AG, Rathmell JC. Cutting edge: distinct glycolytic and lipid oxidative metabolic programs are essential for effector and regulatory CD4+ T cell subsets. J Immunol. 2011 Mar 15;186(6):3299-303. doi: 10.4049/jimmunol.1003613.

Morgan, H. P., O'Reilly, F. J., Wear, M. A., O'Neill, J. R., Fothergill-Gilmore, L. A., Hupp, T., & Walkinshaw, M. D. (2013). M2 pyruvate kinase provides a mechanism for nutrient sensing and regulation of cell proliferation. Proceedings of the National Academy of Sciences, 110(15), 5881–5886. doi: 10.1073/pnas.1217157110

Morita, M., Sato, T., Nomura, M., Sakamoto, Y., Inoue, Y., Tanaka, R., Ito, S., Kurosawa, K., Yamaguchi, K., Sugiura, Y., Takizaki, H., Yamashita, Y., Katakura, R., Sato, I., Kawai, M., Okada, Y., Watanabe, H.,Kondoh, G., Matsumoto, S., . . . Tanuma, N. (2018). PKM1 Confers Metabolic Advantages and Promotes Cell-Autonomous Tumor Cell Growth. Cancer Cell, 33(3), 355–367.e7. doi: 10.1016/j.ccell.2018.02.004

Murray HW, Rubin BY, Carriero SM, Harris AM, Jaffee EA. Human mononuclear phagocyte antiprotozoal mechanisms: oxygen-dependent vs oxygen-independent activity against intracellular Toxoplasma gondii. J Immunol. 1985 Mar;134(3):1982-8.

Nathan, C. F., Murray, H. W., Wlebe, M. E., & Rubin, B. Y. (1983). IDENTIFICATION OF INTERFERON-y AS THE LYMPHOKINE THAT ACTIVATES HUMAN MACROPHAGE OXIDATIVE METABOLISM AND ANTIMICROBIAL ACTIVITY. Journal of Experimental Medicine, 158(September), 670–689.

Noguchi, T., Inoue, H., & Tanaka, T. (1986). The M1- and M2-type isozymes of rat pyruvate kinase are produced from the same gene by alternative RNA splicing. Journal of Biological Chemistry, 261(29), 13807–13812. doi: 10.1016/S0021-9258(18)67091-7

Oestreich KJ, Huang AC, Weinmann AS. The lineage-defining factors T-bet and Bcl-6 collaborate to regulate Th1 gene expression patterns. J Exp Med. 2011 May 9;208(5):1001-13. doi: 10.1084/jem.20102144.

Oomizu S, Arikawa T, Niki T, Kadowaki T, Ueno M, Nishi N, Yamauchi A, Hattori T, Masaki T, Hirashima M. Cell surface galectin-9 expressing Th cells regulate Th17 and Foxp3+ Treg development by galectin-9 secretion. PLoS One. 2012;7(11):e48574. doi: 10.1371/journal.pone.0048574.

O'Neill LA, Kishton RJ, Rathmell J. A guide to immunometabolism for immunologists. Nat Rev Immunol. 2016 Sep;16(9):553-65. doi: 10.1038/nri.2016.70.

Palsson-McDermott EM, Curtis AM, Goel G, Lauterbach MAR, Sheedy FJ, Gleeson LE, van den Bosch MWM, Quinn SR, Domingo-Fernandez R, Johnston DGW, Jiang JK, Israelsen WJ, Keane J, Thomas C, Clish C, Vander Heiden M, Xavier RJ, O'Neill LAJ. Pyruvate Kinase M2 Regulates Hif-1α Activity and IL-1β Induction and Is a Critical Determinant of the Warburg Effect in LPS-Activated Macrophages. Cell Metab. 2015 Feb 3;21(2):347. doi: 10.1016/j.cmet.2015.01.017.

Pandiyan P, Zheng L, Ishihara S, Reed J, Lenardo MJ. CD4+CD25+Foxp3+ regulatory T cells induce cytokine deprivation-mediated apoptosis of effector CD4+ T cells. Nat Immunol. 2007 Dec;8(12):1353-62. doi: 10.1038/ni1536.

Pearce EL, Pearce EJ. Metabolic pathways in immune cell activation and quiescence. Immunity. 2013 Apr 18;38(4):633-43. doi: 10.1016/j.immuni.2013.04.005.

Peng M, Yin N, Chhangawala S, Xu K, Leslie CS, Li MO. Aerobic glycolysis promotes T helper 1 cell differentiation through an epigenetic mechanism. Science. 2016 Oct 28;354(6311):481-484. doi: 10.1126/science.aaf6284.

Prakasam G, Iqbal MA, Bamezai RNK, Mazurek S. Posttranslational Modifications of Pyruvate Kinase M2: Tweaks that Benefit Cancer. Front Oncol. 2018 Feb 7;8:22. doi: 10.3389/fonc.2018.00022.

Procaccini C, Carbone F, Di Silvestre D, Brambilla F, De Rosa V, Galgani M, Faicchia D, Marone G, Tramontano D, Corona M, Alviggi C, Porcellini A, La Cava A, Mauri P, Matarese G. The Proteomic Landscape of Human Ex Vivo Regulatory and Conventional T Cells Reveals Specific Metabolic Requirements. Immunity. 2016 Mar 15;44(3):712. doi: 10.1016/j.immuni.2016.02.022.

Racker E. Bioenergetics and the problem of tumor growth. Am Sci. 1972 Jan-Feb;60(1):56-63.

Ray JP, Staron MM, Shyer JA, Ho PC, Marshall HD, Gray SM, Laidlaw BJ, Araki K, Ahmed R, Kaech SM, Craft J. The Interleukin-2-mTORc1 Kinase Axis Defines the Signaling, Differentiation, and Metabolism of T Helper 1 and Follicular B Helper T Cells. Immunity. 2015 Oct 20;43(4):690-702. doi: 10.1016/j.immuni.2015.08.017.

Regateiro FS, Cobbold SP, Waldmann H. CD73 and adenosine generation in the creation of regulatory microenvironments. Clin Exp Immunol. 2013 Jan;171(1):1-7. doi: 10.1111/j.1365-2249.2012.04623.x.

Renner ED, Rylaarsdam S, Anover-Sombke S, Rack AL, Reichenbach J, Carey JC, Zhu Q, Jansson AF, Barboza J, Schimke LF, Leppert MF, Getz MM, Seger RA, Hill HR, Belohradsky BH, Torgerson TR, Ochs HD. Novel signal transducer and activator of transcription 3 (STAT3) mutations, reduced T(H)17 cell numbers, and variably defective STAT3 phosphorylation in hyper-IgE syndrome. J Allergy Clin Immunol. 2008 Jul;122(1):181-7. doi: 10.1016/j.jaci.2008.04.037.

Robson SC, Sévigny J, Zimmermann H. The E-NTPDase family of ectonucleotidases: Structure function relationships and pathophysiological significance. Purinergic Signal. 2006 Jun;2(2):409-30. doi: 10.1007/s11302-006-9003-5

Rodriguez-Horche, P., Luque, J., Perez-Artes, E., Pineda, M., & Pinilla, M. (1987). Comparative kinetic behaviour and regulation by fructose-1,6-bisphosphate and ATP of pyruvate kinase from erythrocytes, reticulocytes and bone marrow cells. Comparative Biochemistry and Physiology Part B: Comparative Biochemistry, 87(3), 553–557. doi: 10.1016/0305-0491(87)90051-4

Schenk U, Westendorf AM, Radaelli E, Casati A, Ferro M, Fumagalli M, Verderio C, Buer J, Scanziani E, Grassi F. Purinergic control of T cell activation by ATP released through pannexin-1 hemichannels. Sci Signal. 2008 Sep 30;1(39):ra6. doi: 10.1126/scisignal.1160583.

Seki SM, Gaultier A. Exploring Non-Metabolic Functions of Glycolytic Enzymes in Immunity. Front Immunol. 2017 Nov 22;8:1549. doi: 10.3389/fimmu.2017.01549.

Semenza GL, Jiang BH, Leung SW, Passantino R, Concordet JP, Maire P, Giallongo A. Hypoxia response elements in the aldolase A, enolase 1, and lactate dehydrogenase A gene promoters contain essential binding sites for hypoxia-inducible factor 1. J Biol Chem. 1996 Dec 20;271(51):32529-37. doi: 10.1074/jbc.271.51.32529.

Shehade H, Acolty V, Moser M, Oldenhove G. Cutting Edge: Hypoxia-Inducible Factor 1 Negatively Regulates Th1 Function. J Immunol. 2015 Aug 15;195(4):1372-6. doi: 10.4049/jimmunol.1402552.

Shen, X., Wang, Y., Gao, F., Ren, F., Busuttil, R. W., Kupiec-Weglinski, J. W., & Zhai, Y. (2009). CD4 T cells promote tissue inflammation via CD40 signaling without de novo activation in a murine model of liver ischemia/reperfusion injury. Hepatology, 50(5), 1537–1546. doi: 10.1002/hep.23153

Shi LZ, Wang R, Huang G, Vogel P, Neale G, Green DR, Chi H. HIF1alpha-dependent glycolytic pathway orchestrates a metabolic checkpoint for the differentiation of TH17 and Treg cells. J Exp Med. 2011 Jul 4;208(7):1367-76. doi: 10.1084/jem.20110278.

Sitkovsky MV, Lukashev D, Apasov S, Kojima H, Koshiba M, Caldwell C, Ohta A, Thiel M. Physiological control of immune response and inflammatory tissue damage by hypoxia-inducible factors and adenosine A2A receptors. Annu Rev Immunol. 2004;22:657-82. doi: 10.1146/annurev.immunol.22.012703.104731.

Spellman, R., Llorian, M., & Smith, C. W. (2007). Crossregulation and Functional Redundancy between the Splicing Regulator PTB and Its Paralogs nPTB and ROD1. Molecular Cell, 27(3), 420–434. doi: 10.1016/j.molcel.2007.06.016

Stadhouders R, Lubberts E, Hendriks RW. A cellular and molecular view of T helper 17 cell plasticity in autoimmunity. J Autoimmun. 2018 Feb;87:1-15. doi: 10.1016/j.jaut.2017.12.007.

Suen WE, Bergman CM, Hjelmström P, Ruddle NH. A critical role for lymphotoxin in experimental allergic encephalomyelitis. J Exp Med. 1997 Oct 20;186(8):1233-40. doi: 10.1084/jem.186.8.1233.

Sun Q, Chen X, Ma J, Peng H, Wang F, Zha X, Wang Y, Jing Y, Yang H, Chen R, Chang L, Zhang Y, Goto J, Onda H, Chen T, Wang MR, Lu Y, You H, Kwiatkowski D, Zhang H. Mammalian target of rapamycin up-regulation of pyruvate kinase isoenzyme type M2 is critical for aerobic glycolysis and tumor growth. Proc Natl Acad Sci U S A. 2011 Mar 8;108(10):4129-34. doi: 10.1073/pnas.1014769108.

Synnestvedt K, Furuta GT, Comerford KM, Louis N, Karhausen J, Eltzschig HK, Hansen KR, Thompson LF, Colgan SP. Ecto-5'-nucleotidase (CD73) regulation by hypoxia-inducible factor-1 mediates permeability changes in intestinal epithelia. J Clin Invest. 2002 Oct;110(7):993-1002. doi: 10.1172/JCI15337.

Takimoto T, Wakabayashi Y, Sekiya T, Inoue N, Morita R, Ichiyama K, Takahashi R, Asakawa M, Muto G, Mori T, Hasegawa E, Saika S, Hara T, Nomura M, Yoshimura A. Smad2 and Smad3 are

redundantly essential for the TGF-beta-mediated regulation of regulatory T plasticity and Th1 development. J Immunol. 2010 Jul 15;185(2):842-55. doi: 10.4049/jimmunol.0904100.

Thieu VT, Yu Q, Chang HC, Yeh N, Nguyen ET, Sehra S, Kaplan MH. Signal transducer and activator of transcription 4 is required for the transcription factor T-bet to promote T helper 1 cell-fate determination. Immunity. 2008 Nov 14;29(5):679-90. doi: 10.1016/j.immuni.2008.08.017.

Tiegs G, Hentschel J, Wendel A. A T cell-dependent experimental liver injury in mice inducible by concanavalin A. J Clin Invest. 1992 Jul;90(1):196-203. doi: 10.1172/JCI115836.

Treichel, U., McFarlane, B. M., Seki, T., Krawitt, E. L., Alessi, N., Stickel, F., McFarlane, I. G., Kiyosawa, K., Furuta, S., Freni, M. A., Gerken, G., & B¨uschenfelde, K.-H. M. Z. (1994). Demographics of antiasialoglycoprotein receptor autoantibodies in autoimmune hepatitis. Gastroenterology, 107(3), 799–804. doi: 10.1016/0016-5085(94)90129-5

Tsuji-Takayama K, Suzuki M, Yamamoto M, Harashima A, Okochi A, Otani T, Inoue T, Sugimoto A, Toraya T, Takeuchi M, Yamasaki F, Nakamura S, Kibata M. The production of IL-10 by human regulatory T cells is enhanced by IL-2 through a STAT5-responsive intronic enhancer in the IL-10 locus. J Immunol. 2008 Sep 15;181(6):3897-905. doi: 10.4049/jimmunol.181.6.3897.

Tsutsui H, Matsui K, Kawada N, Hyodo Y, Hayashi N, Okamura H, Higashino K, Nakanishi K. IL-18 accounts for both TNF-alpha- and Fas ligand-mediated hepatotoxic pathways in endotoxin-induced liver injury in mice. J Immunol. 1997 Oct 15;159(8):3961-7.

Vander Heiden MG, Cantley LC, Thompson CB. Understanding the Warburg effect: the metabolic requirements of cell proliferation. Science. 2009 May 22;324(5930):1029-33. doi: 10.1126/science.1160809.

Vander Heiden MG, Lunt SY, Dayton TL, Fiske BP, Israelsen WJ, Mattaini KR, Vokes NI, Stephanopoulos G, Cantley LC, Metallo CM, Locasale JW. Metabolic pathway alterations that support cell proliferation. Cold Spring Harb Symp Quant Biol. 2011;76:325-34. doi: 10.1101/sqb.2012.76.010900.

Veldhoen M, Hocking RJ, Atkins CJ, Locksley RM, Stockinger B. TGFbeta in the context of an inflammatory cytokine milieu supports de novo differentiation of IL-17-producing T cells. Immunity. 2006 Feb;24(2):179-89. doi: 10.1016/j.immuni.2006.01.001.

Vento, S., Garofano, T., Di Perri, G., Dolci, L., Concia, E., & Bassetti, D. (1991). Identification of hepatitis A virus as a trigger for autoimmune chronic hepatitis type 1 in susceptible individuals. Lancet, 337(8751), 1183–7. doi: 10.1016/0140-6736(91)92858-y

Wang R, Dillon CP, Shi LZ, Milasta S, Carter R, Finkelstein D, McCormick LL, Fitzgerald P, Chi H, Munger J, Green DR. The transcription factor Myc controls metabolic reprogramming upon T lymphocyte activation. Immunity. 2011 Dec 23;35(6):871-82. doi: 10.1016/j.immuni.2011.09.021.

Wang, T., Liu, H., Lian, G., Zhang, S.-Y., Wang, X., & Jiang, C. (2017). HIF1 a -Induced Glycolysis Metabolism Is Essential to the Activation of Inflammatory Macrophages. Mediators of Inflammation, 2017, 1–10. doi: 10.1155/2017/9029327

Wang X, Szymczak-Workman AL, Gravano DM, Workman CJ, Green DR, Vignali DA. Preferential control of induced regulatory T cell homeostasis via a Bim/Bcl-2 axis. Cell Death Dis. 2012 Feb 9;3(2):e270. doi: 10.1038/cddis.2012.9.

Warburg, O. Über den Stoffwechsel der Carcinomzelle. Naturwissenschaften **12**, 1131–1137 (1924). doi: 10.1007/BF01504608

Wawman RE, Bartlett H, Oo YH. Regulatory T Cell Metabolism in the Hepatic Microenvironment. Front Immunol. 2018 Jan 8;8:1889. doi: 10.3389/fimmu.2017.01889.

Weiler-Normann, C., Schramm, C., Quaas, A., Wiegard, C., Glaubke, C., Pannicke, N., M¨oller, S., & Lohse, A. W. (2013). Infliximab as a rescue treatment in difficult-to-treat autoimmune hepatitis. Journal of Hepatology, 58(3), 529–534. doi: 10.1016/j.jhep.2012.11.010

Xu H, Agalioti T, Zhao J, Steglich B, Wahib R, Vesely MCA, Bielecki P, Bailis W, Jackson R, Perez D, Izbicki J, Licona-Limón P, Kaartinen V, Geginat J, Esplugues E, Tolosa E, Huber S, Flavell RA, Gagliani N. The induction and function of the anti-inflammatory fate of T_H17 cells. Nat Commun. 2020 Jul 3;11(1):3334. doi: 10.1038/s41467-020-17097-5.

Yang XO, Pappu BP, Nurieva R, Akimzhanov A, Kang HS, Chung Y, Ma L, Shah B, Panopoulos AD, Schluns KS, Watowich SS, Tian Q, Jetten AM, Dong C. T helper 17 lineage differentiation is programmed by orphan nuclear receptors ROR alpha and ROR gamma. Immunity. 2008 Jan;28(1):29-39. doi: 10.1016/j.immuni.2007.11.016.

Yang XO, Nurieva R, Martinez GJ, Kang HS, Chung Y, Pappu BP, Shah B, Chang SH, Schluns KS, Watowich SS, Feng XH, Jetten AM, Dong C. Molecular antagonism and plasticity of regulatory and inflammatory T cell programs. Immunity. 2008 Jul 18;29(1):44-56. doi: 10.1016/j.immuni.2008.05.007.

Yang W, Zheng Y, Xia Y, Ji H, Chen X, Guo F, Lyssiotis CA, Aldape K, Cantley LC, Lu Z. ERK1/2-dependent phosphorylation and nuclear translocation of PKM2 promotes the Warburg effect. Nat Cell Biol. 2012 Dec;14(12):1295-304. doi: 10.1038/ncb2629.

Yang BH, Hagemann S, Mamareli P, Lauer U, Hoffmann U, Beckstette M, Föhse L, Prinz I, Pezoldt J, Suerbaum S, Sparwasser T, Hamann A, Floess S, Huehn J, Lochner M. Foxp3(+) T cells expressing RORγt represent a stable regulatory T-cell effector lineage with enhanced suppressive capacity during intestinal inflammation. Mucosal Immunol. 2016 Mar;9(2):444-57. doi: 10.1038/mi.2015.74.

Yang W, Xia Y, Ji H, Zheng Y, Liang J, Huang W, Gao X, Aldape K, Lu Z. Nuclear PKM2 regulates β-catenin transactivation upon EGFR activation. Nature. 2011 Dec 1;480(7375):118-22. doi: 10.1038/nature10598. Erratum in: Nature. 2017 Sep 20;550(7674):142. doi: 10.1038/nature24008.

Yang XO, Panopoulos AD, Nurieva R, Chang SH, Wang D, Watowich SS, Dong C. STAT3 regulates cytokine-mediated generation of inflammatory helper T cells. J Biol Chem. 2007 Mar 30;282(13):9358-9363. doi: 10.1074/jbc.C600321200.

Zarek PE, Huang CT, Lutz ER, Kowalski J, Horton MR, Linden J, Drake CG, Powell JD. A2A receptor signaling promotes peripheral tolerance by inducing T-cell anergy and the generation of adaptive regulatory T cells. Blood. 2008 Jan 1;111(1):251-9. doi: 10.1182/blood-2007-03-081646.

Zenewicz LA, Yancopoulos GD, Valenzuela DM, Murphy AJ, Karow M, Flavell RA. Interleukin-22 but not interleukin-17 provides protection to hepatocytes during acute liver inflammation. Immunity. 2007 Oct;27(4):647-59. doi: 10.1016/j.immuni.2007.07.023.

Zeng Q, Qiu F, Chen Y, Liu C, Liu H, Liang CL, Zhang Q, Dai Z. Shikonin Prolongs Allograft Survival via Induction of $CD4^+FoxP3^+$ Regulatory T Cells. Front Immunol. 2019 Apr 1;10:652. doi: 10.3389/fimmu.2019.00652.

Zhang X, Li J, Yu Y, Lian P, Gao X, Xu Y, Geng L. Shikonin Controls the Differentiation of $CD4^+CD25^+$Regulatory T Cells by Inhibiting AKT/mTOR Pathway. Inflammation. 2019 Aug;42(4):1215-1227. doi: 10.1007/s10753-019-00982-7.

List of Figures

List of Tables

List of Abbreviations

ADP	Adenosine diphosphate
AF	AlexaFlour®
AhR	Arylhydrocarbon receptor
AIH	Autoimmune hepatitis
(c)AMP	(cyclic) Adenosine monophosphate
ALT	Alanine aminotransferase
ANOVA	Analysis of variance
APC	Antigen presenting cell
ATP	Adenosine triphosphate
Bcl-2/6	B-cell lymphoma 2/6
BSA	Bovine serum albumin
BV	Brilliant Violet®
BRC-ABL	Breakpoint Cluster Region - Abelson
CCL	C-C motif chemokine ligand
CD	Cluster of differentiation
(c)DNA	(Complementary) deoxyribonucleic acid
cMyc	Cellular myelocytomatosis oncogene
CO2	Carbon dioxide
CoA	Coenzyme A
ConA	Concanavalin A
Cre	Cyclization recombinase
CFSE	Carboxyflourescein succinimidyl ester
DPBS	Dulbecco's phosphate buffered saline
CXCL	C-X-C motif chemokine ligand
DHAP	Dihydroxyacetone phosphate
DMSO	Dimethyl sulfoxide
dNTP	Deoxynucleotide triphosphate
EAE	Experimental autoimmune encephalomyelitis
ECAR	Extracellular acidification rate
EDTA	Ethylenediaminetetraacetic acid (EDTA)
ELISA	Enzyme-linked immunosorbent ass
ETC	Electron transport chain
FACS	Fluorescence activated cell sorting
FADH	Flavin adenine dinucleotide
FASN	Fatty acid synthase
FBC	Fetal bovine serum
FBP	Fructose bisphosphate
FITC	Fluorescein isothiocyanate
fl	Floxed allele
FMO	Fluorescence minus one
FoxP3	Forkhead box protein 3
FSC	Forward scatter
GAPDH	Glyceraldehyde-3-phosphate dehydrogenase
GFE	Gravitational force equivalent
G6P	Glucose-6-phosphate
Gal1	Galectin 1
GLUT	Glucose transporter
GM-CSF	Granulocyte-Macrophage Colony-Stimulating Factor
HBSS	Hank's Balanced Salt Solution
HE	Hematoxylin & Eosin
HIF	Hypoxia inducible factor
HMGB1	High mobility group box protein 1
HLA	Human leukocyte antigen
HRP	Horseradish peroxidase
IBD	Inflammatory bowel disease
IFNγ	Interferon γ

Ig	Immune globuline
IL	Interleukin
IRF4	interferon regulatory factor 4
IU	International units
JAK	Janus kinase
kDa	Kilodalton
LDH	Lactate dehydrogenase
LSEC	Liver sinusoidal endothelial cell
MFI	Mean fluorescent intensity
MHC	Major histocompatibility complex
MPB	Myc promotor binding protein
MPO	Myeloperoxidase
mRNA	(Messenger) ribonucleic acid
mTOR	Mammalian Target of Rapamycin
MS	Multiple Sclerosis
NAD	Nicotinamide adenine dinucleotide
NADPH	Nicotinamide adenine dinucleotide phosphate
NFκB	Nuclear Factor kappa-light-chain-enhancer
NFAT	Nuclear factor of activated T cells
NK cell	Natural killer cell
NPC	Non parenchymal cells
OCR	Oxygen consumption rate
OMM	Outer mitochondrial membrane
OXPHOS	Oxidative phosphorylation
PGAM	Phosphoglycerate Mutase
PBS	Phosphate buffered saline
PD-1	Programmed death receptor 1
PDH	Pyruvate Dehydrogenase
PDK	Pyruvate Dehydrogenase Kinase
PEP	Phosphoenolpyruvate
PFA	Paraformaldehyde
PFK	Phosphofructokinase
PKM	Pyruvate kinase muscle
PKL	Pyruvate kinase liver
PPP	Pentose phosphate pathway
(q)PCR	Polymerase chain reaction/Quantitative real time
RA	Rheumatoid arthritis
RORγT	Retinoid acid receptor-related orphan receptor gamma
Rot/AA	Rotenone AA
rpm	Revolutions per minute
RPMI	Roswell Park Memorial Institute (Medium)
Runx	Runt related transcription factor
SDS	Sodium dodecyl sulfate
SLE	Systemic lupus erythematosus
SSC	Sideward scatter
STAT	Signal transducer and activator of transcription
TBS(T)	Tris-buffered saline (with Tween® 20)
TCA	Tricarboxylic acid cycle
TCR	T cell receptor
TGFβ	Transforming growth factor β
Th cell	T helper cell
TLR	Toll-like receptor
TNFα	Tumor necrosis factor α
Treg	Regulatory T cell
TRIS	Tris(hydroxymethyl)aminomethane
U	Unit
2-DG	2-desoxaglucose

Erklärung des Eigenanteils

Die in dieser Dissertation dargestellten Forschungsarbeiten wurden überwiegend eigenständig durchgeführt. Die Konzeption der Fragestellung wurde zu Anteilen von meiner Promotionsbetreuerin PD. Dr. Andrea Kristina Horst vorgenommen.

Die Planung und Durchführung der Experimente sowie die Auswertung und Interpretation der Daten wurden von mir selbst vorgenommen, wenn nicht anders in Form von Fußnoten gekennzeichnet. Sonstige Dritte, die in anderer Form, beispielsweise bei der technischen Umsetzung, unterstützt haben, sind in der Danksagung aufgelistet. Alle verwendeten Quellen und Beiträge anderer Personen wurden entsprechend zitiert.

Eidesstattliche Versicherung

Ich versichere ausdrücklich, dass ich die Arbeit selbständig und ohne fremde Hilfe, insbesondere ohne entgeltliche Hilfe von Vermittlungs- und Beratungsdiensten, verfasst, andere als die von mir angegebenen Quellen und Hilfsmittel nicht benutzt und die aus den benutzten Werken wörtlich oder inhaltlich entnommenen Stellen einzeln nach Ausgabe (Auflage und Jahr des Erscheinens), Band und Seite des benutzten Werkes kenntlich gemacht habe. Das gilt insbesondere auch für alle Informationen aus Internetquellen.
Soweit beim Verfassen der Dissertation KI-basierte Tools („Chatbots“) verwendet wurden, versichere ich ausdrücklich, den daraus generierten Anteil deutlich kenntlich gemacht zu haben. Die „Stellungnahme des Präsidiums der Deutschen Forschungsgemeinschaft (DFG) zum Einfluss generativer Modelle für die Text- und Bilderstellung auf die Wissenschaften und das Förderhandeln der DFG“ aus September 2023 wurde dabei beachtet.
Ferner versichere ich, dass ich die Dissertation bisher nicht einem Fachvertreter an einer anderen Hochschule zur Überprüfung vorgelegt oder mich anderweitig um Zulassung zur Promotion beworben habe.
Ich erkläre mich damit einverstanden, dass meine Dissertation vom Dekanat der Medizinischen Fakultät mit einer gängigen Software zur Erkennung von Plagiaten überprüft werden kann.

Hamburg, den 02.06.2025

Danksagung

Abschließend möchte ich mich für die vielfältige Unterstützung bedanken, allen voran bei meiner Doktormutter und Promotionsbetreuerin PD Dr. Andrea Kristina Host. Unter ihrer Supervision erhielt ich die Chance mich selbstständig mit einem komplexen Thema auseinanderzusetzen. Die freundliche und individuelle Betreuung, ein offenes Ohr für Probleme, unzählige konstruktive und kritische Vorschläge und ihr Humor haben die Zeit im Labor für mich zu einer wundervollen Erfahrung gemacht.
Ebenso danken möchte ich Prof. Dr. Gisa Tiegs, die in ihrer Rolle als Leiterin des Institutes für experimentelle Immunologie und Hepatologie diese Arbeit ermöglicht hat. Prof. Dr. Lutz Fischer möchte ich dafür danken, dass er mich im Rahmen des Mentoringprogramms für Studierende der Humanmedizin zu einer experimentellen Doktorarbeit ermutigt hat, und Prof. Dr. Christoph Schramm für seine wertvollen Anregungen im Rahmen der Treffen mit der Betreuungskommission.

Besonderer Dank gebührt unseren technischen Assistenten, Elena Tasika and Carsten Rothkegel, die mich nicht nur geduldig an alle Methoden herangeführt haben, sondern über den gesamten Zeitpunkt der experimentellen Arbeit und darüber hinaus offen waren für Fragen (und das ein oder andere Missgeschick toleriert haben).
Ebenso danken möchte ich den Kollegen im IEIH, ganz besonders Dr. Mareike Kellerer für wertvolle Tipps beim Erlernen von Methoden, Ratschläge zu nahezu jedem thematischen Aspekt dieser Arbeit. Dr. Jan-Phillip Weltzsch danke ich ebenso für seinen fachlichen Rat. Der gesamten Arbeitsgruppe möchte ich für die kollegiale Arbeitsatmosphäre danken. Meinen Dank ausdrücken möchte ich außerdem dem Team der Tierhaltung im Campus Forschung, der FACS Core Facility und der UKE Microscopy Imaging Facility.

Von Herzen für die vielfältige und fortwährende Unterstützung möchte ich zu guter Letzt meiner Familie - besonders meinen Eltern Sylvia Moll und Adalbert Moll, meiner Großmutter Renate Struppek und meinem Bruder Vincent Moll - sowie meinem Freund Robin Habermann danken.